12-15-2007

Physiologically-Based Toxicokinetic and Toxicodynamic (Pbtk/Td) Modeling of a Ternary Organophosphorus Insecticide Mixture in Rats: Model Development and Validation

Julian Thomas Pittman

PHYSIOLOGICALLY-BASED TOXICOKINETIC AND TOXICODYNAMIC (PBTK/TD) MODELING OF A TERNARY ORGANOPHOSPHORUS INSECTICIDE MIXTURE IN RATS: MODEL DEVELOPMENT AND VALIDATION

By

Julian Thomas Pittman

A Dissertation
Submitted to the Faculty of
Mississippi State University
in Partial Fulfillment of the Requirements
for the Degree of Doctor of Philosophy
in Environmental Toxicology
in the Department of Basic Sciences, College of Veterinary Medicine

Mississippi State, Mississippi

December 2007

PHYSIOLOGICALLY-BASED TOXICOKINETIC AND TOXICODYNAMIC (PBTK/TD) MODELING OF A TERNARY ORGANOPHOSPHORUS INSECTICIDE MIXTURE IN RATS: MODEL DEVELOPMENT AND VALIDATION

By

Julian Thomas Pittman

Approved:

Janice E. Chambers Professor Department of Basic Sciences William L. Giles Distinguished Professor (Director of Dissertation)	Matthew K. Ross Assistant Professor Department of Basic Sciences (Committee Member)
Howard W. Chambers Professor Department of Entomology and Plant Pathology (Committee Member)	Steven Pruett Professor, Department Head Department of Basic Sciences College of Veterinary Medicine (Committee Member)
Allen Crow Assistant Research Professor Department of Basic Sciences (Committee Member)	Kent H. Hoblet Dean, College of Veterinary Medicine

Name: Julian Thomas Pittman

Date of Degree: December, 2007

Institution: Mississippi State University

Major Field: Environmental Toxicology

Major Professor: Dr. Janice E. Chambers

Title of Study: PHYSIOLOGICALLY-BASED TOXICOKINETIC AND TOXICODYNAMIC (PBTK/TD) MODELING OF A TERNARY ORGANOPHOSPHORUS INSECTICIDE MIXTURE IN RATS: MODEL DEVELOPMENT AND VALIDATION

Pages in Study: 130

Candidate for Degree of Doctor of Philosophy

A physiologically-based toxicokinetic and toxicodynamic (PBTK/TD) model was developed, from the open literature, to predict the toxicokinetic disposition and toxicodynamic response (acetylcholinesterase inhibition) of a ternary organophosphorus (OP) insecticide mixture: chlorpyrifos (CP), methyl parathion (MP) and parathion (P). *In vivo* studies were conducted in adult male Sprague-Dawley rats, orally administered one of two CP/MP/P mixtures (2.5, 0.5, 0.5 mg/kg or 5, 1, 1 mg/kg) with selected tissues (blood, brain, diaphragm, liver, lung and skeletal muscle) collected at 30min, 4, 12 and 24hr postdosing. Low dosages were studied so the mixture did not result in significant disruption of cardiovascular function nor invalidate the model's underlying general physiological assumptions. The data were used to validate the model. CP and its metabolites (CP-oxon, 3,5,6-trichloro-2-pyridinol (TCP)), as well as MP, P and 4-nitrophenol, were quantified in the tissues of interest. Peak concentrations of CP were attained by 4hr in all tissues with the exception of the liver, whose peak occurred at

30min; MP, 30min in all tissues; P, 12hr in all tissues with the exception of the liver, 30min. This was supported by the model simulations. MP, P, and their respective oxons were below limits of quantitation for the lower dosage. No toxicokinetic interactions were observed in the present study. Cholinesterase inhibition in the tissues ranged from 11- 37% for the lower dosage, and 29-93% for the higher dosage group; with few exceptions, inhibition was generally additive and was also supported by the model simulations. This study demonstrates the utility of using previously developed individual PBTK/TD models and *in vitro*/*in vivo* data from the open literature to construct reliable mixture PBTK/TD models.

Key words: PBPK/PD Model; PBTK/TD Model; Mixtures; Organophosphorus Insecticides; Esterase Inhibition.

DEDICATION

This work is dedicated in loving memory of my grandfather, Julian Allen Pittman.

ACKNOWLEDGEMENTS

Many individuals contributed to the successful completion of this work. I wish to extend my sincerest appreciation to each of them.

I thank my advisor, Dr. Janice Chambers, for providing me with the opportunity to work on this research project and for her invaluable mentorship. I also wish to thank my committee members; Drs. Howard Chambers, Allen Crow, Cory Langston, and Matthew Ross for their support.

I am also grateful to Eddie Meek and Keith Davis for their technical assistance, and other graduate students and staff in the Center for Environmental Health Sciences for support.

Lastly, a special thanks to my mom and grandmother for their unwavering support of my goals in life. I would not be where I am today without their love and guidance.

TABLE OF CONTENTS

Page

Page

LIST OF TABLES

LIST OF FIGURES

Figure Page

Figure Page

CHAPTER I

GENERAL INTRODUCTION

Exposure to chemicals in the environment, such as organophosphorus (OP) insecticides, is rarely limited to a single chemical; they commonly coexist as mixtures. Multi-chemical exposure is the rule rather than the exception in both occupational and non-occupational environments. Individuals are likely to be exposed to a wide range of OP insecticides, from many different sources, in variable concentrations and routes of exposure. There are numerous public health concerns regarding chemical mixtures; however, regulatory limit values are generally set for single compounds. Research approaches and needs in this area have been well described (Teuschler et al., 2002). To protect human health, insight is needed into the combined action of chemicals, particularly OP insecticides.

We are potentially exposed to many different OP insecticides on a daily basis, albeit at very low levels, in food residues, drinking water, homes and schools. In a study by Simcox et al. (1995), azinphos-methyl, chlorpyrifos, parathion, and phosmet were found in 62% of dust samples collected from the homes of agricultural workers, demonstrating the potential for both occupational and non-occupational exposure to insecticide mixtures. Consequently, it is imperative that multiple chemical effects and interactions be considered in the risk assessment process. The mixture toxicity

problem has long challenged both toxicologists and regulators. As Haddad et al. (1999) has articulated, the mechanism that generates the toxic response and is a prime determinant of the putative human health risk cannot be examined sufficiently by only studying the individual components of the mixture. Approaching the mixture quandary with conventional toxicological studies is futile, due to the immense number of possible mixture combinations. The utilization of physiologically-based toxicokinetic/toxicodynamic (PBTK/TD) modeling is needed, as described in the present study, to address the data gaps in the risk assessment process.

The value of PBTK/TD modeling is its potential predictive power, i.e., tissue dosimetry at the toxico/pharmacokinetic and toxico/pharmacodynamic levels, minimization of animal use, amenability to cross-species scaling, and simulation of exposure scenarios that cannot be tested otherwise. Although PBTK/TD models have been developed for a variety of single chemicals, far fewer PBTK/TD models have been developed for chemical mixtures; the present study helps to fill that deficiency. One of the best-known examples of PBTK model development for concurrent exposure to a binary mixture of chemicals is that of trichloroethylene (TCE) and 1, 1-dichloroethylene (DCE). In this work, Andersen et al. (1987) linked the two single chemical models by the mass-balance equation for the liver and produced generalized liver mass-balanced equations that could be used to test for competitive, non-competitive, and uncompetitive inhibition by manipulating the values of various terms within the equations. Somewhat more recently, Tardif et al. (1995) developed a PBTK model for the interaction of toluene and xylene that was expanded into a

human PBTK model for toluene and mixed xylenes. In this study, individual PBTK models were developed for toluene and xylenes in adult male rats, then the two models were linked through a metabolism term in the liver. Subsequently, similar modeling approaches have been employed by El-Masri et al. (2004) and Timchalk et al. (2005) for binary OP mixture PBTK/TD models (chlorpyrifos/parathion and chlorpyrifos/diazinon, respectively).

Unquestionably, pesticides have greatly benefited our society by protecting our food supply, controlling harmful pests, and improving quality of life. Nevertheless, the widespread use of pesticides is not without risk for our environment and our health. OP insecticides are extensively used because of their efficacy against insect pests, rapid degradation, and lack of cross resistance in many insects as compared to the earlier organochlorine insecticides. The development of OP compounds as insecticides emerged through nerve gas research conducted in 1937 by Gerhard Schrader, Bayer Chemical Company, Germany. Schrader recognized the insecticidal significance of OP compounds and in 1944, methyl parathion and parathion were introduced as replacements for nicotine in aphid control. Subsequently, the number of OP insecticides rapidly grew during the 1950's and 60's in the United States. Presently, OP compounds are the largest family of insecticides. Although the introduction of newer compounds (i.e., synthetic pyrethroids), as well as Environmental Protection Agency (EPA) bans/restrictions, have decreased the usage of OP insecticides in recent years, they are still frequently used in agriculture.

The Food Quality Protection Act of 1996 mandates that all pesticides that act through a common mechanism of toxicity undergo cumulative risk assessments. The concern is that exposure to multiple members of a common-mechanism group might pose a health risk even if the individual components of the mixture are present at levels below their respective no-observed-adverse-effect levels. A working group of experts determined that chemicals that act via a common mechanism of toxicity must satisfy three specific points. The chemical must (1) cause the same critical effect (2) by action through the same biochemical mechanism (3) on the same molecular target or target tissue (Mileson, 1998). OP insecticides were the first class of chemicals to undergo a cumulative risk assessment (US EPA, 2002). They share a common mechanism of toxicity, the inhibition of acetylcholinesterase (AChE), resulting in accumulation of acetylcholine in cholinergic synapses and excessive stimulation of cholinergic pathways in central and peripheral nervous tissues. Gearhart et al. (1990) has suggested that PBTK/TD models capable of predicting the relationship between OP insecticide exposure and AChE inhibition are useful for evaluating the risk associated with a given exposure. The EPA is in the early stages of developing a strategy for incorporating PBTK/TD models into its cumulative risk assessments. A limited number of PBTK/TD models for OP insecticides have been published in the literature (Maxwell et al., 1988; Gearhart et al., 1990; Sultatos, 1990; Abbas & Hayton, 1997; Timchalk et al., 2002; El-Masri et al., 2004; Poet et al., 2004; Timchalk et al., 2005); at present, no models exist for ternary mixtures of OP insecticides.

Mixture Components

Although uses of OP insecticides have been greatly restricted and/or banned in the United States in recent years, they still remain a potential concern to human health due to continuing world-wide use. In addition, all three OP compounds used in the present study were on the 2003 Comprehensive Environmental Response, Compensation, and Liability Act (CERCLA) Priority List of Hazardous Substances, further highlighting the need for concern.

The nomenclature of OP insecticides is dependent on the type of atoms directly bonded to the phosphorus atom; principally oxygen and sulfur, with nitrogen and carbon present to a lesser extent. A major class of commonly used OP insecticides are the phosphorothionates, where three of the atoms surrounding the phosphorus are single bonded oxygen and the other is a coordinate covalent bonded sulfur (P=S). Chlorpyrifos, methyl parathion and parathion are phosphorothionate insecticides. Chlorpyrifos and parathion contain structural similarities (both diethyl compounds), as shown in Figure 1; however parathion is approximately 10-fold more toxic to mammals than chlorpyrifos. The oral LD_{50} for chlorpyrifos is 82-155mg/kg in rats, while the rat oral LD_{50} for parathion is 3-17mg/kg (Kidd & James, 1991). Methyl parathion (Figure 1) differs structurally (a dimethyl compound) as compared to chlorpyrifos and parathion, but is similar in acute toxicity to parathion (oral LD_{50} for methyl parathion is 14-24mg/kg in rats; Kidd & James, 1991).

Mechanism of Inhibition

AChE, the primary target for OP compounds, is responsible for the rapid hydrolysis of acetylcholine (ACh), a neurotransmitter involved in the numerous cholinergic pathways in the body; central and peripheral nervous system (somatic nervous system innervating skeletal muscles and both the sympathetic and parasympathetic divisions of the autonomic nervous system). As long as the active site of AChE is phosphorylated, it is inhibited. The phosphorylated enzyme is no longer capable of hydrolyzing ACh, which results in accumulation of ACh in cholinergic synapses and excessive stimulation of the ubiquitous cholinergic pathways (Murphy, 1986; Sultatos, 1994). Clinical manifestations of overstimulation of cholinergic pathways include hyper-salivation, lacrimation, vomiting, urination and diarrhea. Central nervous system effects include anxiety, restlessness, dizziness, confusion, ataxia and convulsion. One of the most significant consequences of AChE inhibition is depression of cardiopulmonary function. Death is generally attributed to respiratory failure resulting from a combination of central and peripheral effects; specifically bronchiolar constriction, enhanced bronchiolar secretions, paralysis of respiratory muscles, and respiratory control center shut-down in the brain. Because of the severity of these effects, the vital importance of these target systems to maintenance of life, and the rate with which many of the OP insecticides act, incapacitation and death can occur quickly. Symptoms are more-or-less severe, depending on the OP compound, dose, route, frequency and duration of exposure.

Short-term exposure to OP insecticides may also have long-term consequences, ranging from changes in behavior to prolonged or delayed peripheral neuropathy and myopathy (Savage et al., 1988; Rosenstock et al., 1991).

Structurally, AChE contains two sites, an esteratic site and an anionic site. AChE uses both sites to attach ACh with the quaternary nitrogen of ACh interacting with the negatively charged anionic site, thereby orienting the carbonyl group into the active site. Once present at the active site, AChE hydrolyzes ACh and releases choline. This hydrolysis produces an acylated enzyme which undergoes rapid hydrolysis to return to its original form. Anticholinesterases (OP insecticides) may interfere with the hydrolysis of ACh by attachment to AChE at the esteratic site. Generally, the majority of OP insecticides phosphorylate AChE at the serine group of the esteratic site. The ability of an OP compound to bind to AChE depends on the nucleophilicity of the active site. While the serine group is the primary site of phosphorylation, the imidazole of the histidine residue in the active site enhances the nucleophilicity of the active site by forming a hydrogen bond between itself and the serine hydroxyl. It is this interaction which promotes the binding of C=O of the ACh and P=O of the OP insecticide to the active site. Once the ACh is bound and choline is cleaved, the conformational changes favor the rapid release of the acyl group, hence reactivating the enzyme. However, with OP insecticides, the release of the phosphorylated group from the serine hydroxyl is quite slow, leading to long-term inhibition of the enzyme (Silver, 1972). The ability of an OP insecticide to interact with the enzyme depends on the electrophilicity of the inhibitor. The nucleophilic

attack (transesterification) of the serine hydroxyl by the phosphorus atom is dependent on the electrophilic properties of the enzyme and the inhibitor (Wallace, 1992). The OP will associate with the anionic site and this association allows the phosphorylation of the active site. Once phosphorylated, the portion of inhibitor that is associated with the anionic site is cleaved. This cleaved group is called the "leaving group". The anionic site may function to orient the inhibitor such that association with the nucleophilic active site is preferable for some inhibitors compared with others. The basis for this inhibitory preference may be either the distance between the anionic site and the esteratic site, or the electronic properties of the leaving group.

Once formed, the phosphorylated enzyme can undergo spontaneous reactivation, however this is quite slow, and in some instances depending on the groups attached to the phosphorus atom, it can be irreversibly inhibited. Reactivation involves dissociation of the enzyme-inhibitor complex, consequently breakage of a covalent bond. Although the spontaneous reactivation of cholinesterases is slow, the addition of other compounds, specifically hydroxylamine and choline, to an inhibited cholinesterase preparation can decrease the time required for reactivation to occur (Wilson, 1952). The hydroxylamine is referred to as a "reactivator", and a great deal of research has been undertaken on related compounds. The reactivators are nucleophilic compounds with a high affinity for phosphorus. The most efficient reactivators are those which possess a strong ionizable oxime group (=NOH), preferably the bis-pyridinium-aldoximes (Hobbiger and Sadler, 1959). Included among the bis-pyridinium-aldoximes are the salts of pyridine 2-aldoxime or 2-PAM,

which are used clinically. The potency of the oximes is attributed to the binding of the quaternary nitrogen to the enzyme and the positioning of the highly nucleophilic oxime moiety such that it supports the transfer of the enzyme-bound phosphate from the enzyme to the oxime (Wilson et al., 1992). Once the phosphate is removed, the cholinesterase's hydrolytic activity returns. However, not all inhibited cholinesterases are capable of being reactivated by oximes. Following the development of reactivators, it was shown that inhibited cholinesterase would remain inhibited even following removal of the excess inhibitor. The capacity to chemically reactivate the inhibited cholinesterase is lost over time. The process is termed "aging" of cholinesterase, and the mechanisms behind this phenomenon were elucidated using the potent anticholinesterase, DFP (diisopropyl fluorophosphate). Various non-cholinesterase enzymes inhibited by DFP were mildly degraded and were shown to have diisopropyl groups attached to their serine groups. However, DFP-inhibited cholinesterase yielded not only diisopropyl phosphorylated serine groups but also monoisopropyl phosphorylated serine groups, suggesting a change in the diisopropyl moiety attached to the enzyme to form a monoisopropyl moiety. The hydrolysis of the isopropyl group off the phosphorus atom attached to the enzyme converted the enzyme to a non-reactivatable form. Using enzyme inhibited with the radiolabled nerve gas, sarin, Harris et al. (1966) demonstrated that the loss of the alkyl group from the phosphorylated enzyme correlated with the amount of the enzyme that was not responsive to reactivation by an oxime. The importance of dealkylation in aging was further substantiated by Beauregard et al. (1981) using radiolabeled DFP-

inhibited AChE. This dealkylation stabilized the phosphate-enzyme complex, thus preventing both spontaneous and chemical-induced reactivation (Wilson et al., 1992).

The rate of reactivation and aging depends on the geometry of the groups attached to the phosphorus atom. This has been established using stereoisomers of sarin (Berends, 1964) in which some stereoisomers differ greatly in their rate of aging compared to others. Clothier et al. (1981) demonstrated that there are differences in the rates of reactivation and aging of AChE when the alkyl groups attached to the phosphorus differ. Dimethoxy-substituted OP compounds reactivate and age faster than those that are diethoxy-substituted. It was shown that the amount of aging increased when the oxygen atoms in the dimethoxy and diethoxy groups around the phosphorus atom were replaced with sulfur atoms (Langenburg et al., 1988). Since substitution of different groups can change the electrophilic properties of the inhibitor, aging not only can be affected but inhibitory potency also. Contribution of the anionic site to aging has also been suggested. As mentioned previously, the association of the inhibitor with the anionic site can influence the phosphorylation of the active site.

Metabolic Activation

Chlorpyrifos, methyl parathion, and parathion do not directly inhibit AChE, but must first be metabolically activated, by oxidative desulfuration (P=S to P=O) to chlorpyrifos-oxon, methyl paraoxon and paraoxon, respectively. The activation of chlorpyrifos, methyl parathion, and parathion to their oxons is mediated by

cytochromes P450, principally within the liver. However, extrahepatic metabolism has been reported in other tissues, including brain (Chambers & Chambers, 1989). All three phosphorothionates can be detoxified by P450's in a dearylation reaction to dialkyl phosphate or dialkyl phosphorothionate plus the alcohol (3,5,6-trichloro-2-pyridinol (TCP) for chlorpyrifos, 4-nitrophenol for methyl parathion and parathion). Differences in the ratio of activation to detoxication are thought to be related to the *in vivo* levels of sensitivity to OP insecticides (Ma and Chambers, 1994). Hepatic and extrahepatic A-esterases can effectively metabolize chlorpyrifos-oxon to TCP and diethylphosphate (Sultatos & Murphy, 1983). B-esterases, such as carboxylesterase (CaE) and butyrylcholinesterase (BuChE) can likewise detoxify chlorpyrifos-oxon; however the B-esterases become irreversibly phosphorylated (1:1 ratio) by chlorpyrifos-oxon and consequently become inactivated (Clement, 1984). Paraoxon also reacts irreversibly with CaE and BuChE. In contrast to paraoxon and chlorpyrifos-oxon, hepatic CaEs are not very sensitive to methyl paraoxon *in vitro*, so a large portion of methyl paraoxon generated in the liver may be able to exit the liver and reach the target sites causing AChE inhibition (Chambers et al., 1989).

Inactivation of non-critical esterases produces no known toxic effect. CaE is present in many tissues including liver, kidney, intestine, plasma and muscle (Satoh, 1987). This serine esterase catalyzes the hydrolysis of carboxylesters. BuChE occurs predominately in the plasma. The phosphorylation of the serine hydroxyl groups of CaE and BuChE by chlorpyrifos-oxon and paraoxon is important as a detoxication process, which stoichiometrically reduces the amount of both oxons available to

inhibit AChE (Maxwell, 1992). In addition to the enzymatic detoxication of OP insecticides, reactivation of the phosphorylated AChE also plays an important role in recovery of the active enzyme. As mentioned earlier, phosphorylated AChE undergoes spontaneous hydrolysis, but the rate depends on the nature of the alkyl substitutions. In the case of chlorpyrifos-oxon, methyl paraoxon and paraoxon, the rate of dephosphorylation is very slow. Dealkylation of the phosphoryl-cholinesterase complex may also occur, resulting in an aged enzyme, as stated previously, that does not readily undergo spontaneous reactivation (Berends et al., 1959). Cholinesterase lost to aging is replaced through the synthesis of new enzyme. Changes in the relative contributions of reactivation and replacement may explain the biphasic recovery of cholinesterase activity following oral administration of some OP compounds (Benke et al., 1974; Hahn et al., 1991; Chambers & Carr, 1993). Spontaneous reactivation may be more important during the initial, faster phase of recovery, whereas synthesis of new enzyme has a greater role during the later, slower phase of recovery. The balance between aging, inactivation, reactivation, and replacement determines the pattern of cholinesterase inhibition following OP compound exposure. Ultimately, these parameters are determined as much by route-of- administration/exposure as by dose.

Toxicodynamic processes alone, however, do not determine OP insecticide potency; equally important are toxicokinetic characteristics. For most OP compounds, absorption is rapid and complete, via oral or inhalation exposure, and distribution is typically quite extensive. The overall balance between metabolic generation and

elimination of more- versus less-toxic derivatives is a major factor that determines potency. For example, differences in the overall rates of detoxication contribute to the greater sensitivity of female rats to some OP compounds (chlorpyrifos, methyl parathion, parathion) as compared to male rats, and to the greater sensitivity of young animals compared to adults (Ma and Chambers, 1995; Chambers et al., 1994; Atterberry et al., 1997). In addition, differences in the overall balance between generating and eliminating more versus less toxic derivatives following oral exposures compared to inhalation exposures, due to first-pass hepatic metabolism, can contribute to differences in potency for the same compound when administered via different routes.

Chlorpyrifos

Chlorpyrifos (CP) (O,O-diethyl-O-[3,5,6-trichloro-2-pyridyl] phosphorothioate) is one of the most widely used OP insecticides. It is currently used on more than 40 different agricultural crops; its prior uses as a termiticide, residential indoor and lawn insecticide has been phased out/eliminated. CP has been registered for use in 88 countries with more than 100 indications for treating crop and urban environments and marketed under approximately 359 labels worldwide with over two dozen formulation types (Albers et al., 1999). The average daily intake of CP for humans has been reported to be 0.01mg/kg/day (Lu, 1995). CP is well absorbed orally; approximately 90% of orally administered CP is eliminated by rats in urine by 48-66 hours after dosing. The remaining 10% is eliminated in the feces. CP is

eliminated almost exclusively in the urine as TCP (3,5,6-trichloro-2-pyridinol). Elimination half-lives for liver, kidney, muscle, and fat are 10, 12, 16, and 62 hours, respectively, indicative of considerable storage in fat (Smith et al., 1967).

CP is metabolized to CP-oxon via cytochrome P450-dependent desulfuration. The oxon is rapidly hydrolyzed to TCP via microsomal esterases (including paraoxonase and CP oxonase) or via nonenzymatic processes (Sultatos et al., 1983; Costa et al., 1990). Alternatively, CP can be dearylated to form diethyl thiophosphoric acid and TCP in a reaction also catalyzed by microsomal enzymes. TCP or one of its conjugates, is almost exclusively (90%) excreted in the urine (Bakke et al., 1976), as mentioned above. CP-oxon binds to and irreversibly inhibits AChE. However, the relative affinity of CP-oxon for plasma and hepatic esterases exceeds that for AChE. Furthermore, CP-oxon causes relatively greater and longer lasting inhibition of hepatic esterases *in vivo* compared to brain AChE (Chambers and Carr, 1993). Noncatalytic binding of CP-oxon to hepatic and plasma esterases represents a significant detoxication mechanism because it prevents much of the hepatically generated CP-oxon from entering the general circulation and target tissues. High rates of hepatic dearylation and esterase binding may represent protective factors. However, CP can be activated in extrahepatic tissues, such as brain (Chambers and Chambers, 1989). Comparative difference in the rates of hepatic esterase binding and rates of dearylation have been implicated as contributors to the greater sensitivity of some tissues (i.e., brain) to CP, compared to other tissues, and to

the greater toxicity of parathion, discussed below, compared to CP (Chambers et al., 1990; Pond et al., 1995).

Methyl parathion

Methyl parathion (MP) (O,O-dimethyl O-p-nitrophenyl phosphorothioate) may only be used legally on certain agricultural crops; it is most commonly used on cotton. Other major uses include corn, peaches, wheat, barley, soybeans and rice. There has been great concern regarding the illegal indoor use of methyl parathion products in private homes and other structures. Such use posed potentially significant health risk to individuals who lived or frequented such indoor areas and has resulted in significant relocation and cleanup costs in several states. Absorption, distribution, and elimination of MP via oral exposure is rapid and extensive. For example, MP is rapidly absorbed in rats, concentrations in blood and brain are maximal in 1-3 hours, and nearly completely eliminated in urine (mostly as dimethyl phosphoric and dimethyl phosphorothioic acid) by 7 days (Miyamoto et al., 1963). In addition, following oral exposure, MP is widely distributed to blood, liver, adipose tissue, muscle and brain. Distribution coefficients are highest in adipose tissue 8 days after exposure (0.99), in liver 20 days after exposure (0.17), and in brain 16 days after exposure (0.35), but they are < 1.0, indicating no long-term accumulation of MP in tissues. Half-lives of elimination are 15 days for blood, 13 days for adipose tissue, 15 days for liver, and 15 days for brain (Garcia-Repetto et al., 1997).

MP is oxidatively desulfurated to methyl paraoxon or dearylated to dimethyl thiophosphorothioic acid and 4-nitrophenol via cytochrome P450 enzymes. MP-oxon can also be dearylated to dimethyl phosphoric acid and 4-nitrophenol and hydrolyzed to O-methyl-O-p-nitrophenyl phosphate. All of these oxidative and hydrolytic products are excreted in urine (Hollingworth et al., 1967). These metabolic conversions occur principally within the liver, but can also occur in the lung and brain. MP-oxon binds to and irreversibly inhibits AChE. Noncatalytic, stoichiometric binding to other esterases (aliesterases) in liver and plasma also occurs, however, and may represent a significant detoxication mechanism, since it can reduce the amount of MP-oxon that leaves the liver and/or blood to enter target tissues. Binding to hepatic and plasma esterase may not be as significant a detoxication mechanism for MP as it is for CP and parathion (P), however, because the affinity of MP-oxon is considerably greater for brain AChE than for hepatic esterase; the reverse is true for CP and P. Consequently, even though MP-oxon has a lower affinity for AChE than P-oxon, the relatively weaker protection afforded by the aliesterases can permit lethal levels of hepatically generated MP-oxon to reach the nervous system (Chambers and Carr, 1993).

Parathion

Parathion (P) (O,O-diethyl O-p-nitrophenyl phosphorothionate) is one of the most toxic insecticides registered with the EPA. It is used as a pre-harvest soil and foliage treatment on a wide variety of crops. In 1992 the EPA cancelled all uses of P

on fruit, nut and vegetable crops. However, P is still used on alfalfa, barley, corn, cotton, sorghum, soybeans, sunflowers and wheat. As one of the earliest and efficacious OP insecticides, P possesses a substantial database. Once absorbed, P is widely distributed regardless of the route of exposure. Distribution coefficients are highest in the liver (4.1-20.8) and adipose tissue (1.3-2.9) but also exceed 1 in the brain (1.0-1.4) and muscle (1.5-1.9) (Garcia-Repetto et al., 1995). P can be converted to P-oxon by cytochrome P450 enzymes. Alternatively, P can be dearylated to form diethyl phosphorothioic acid and 4-nitrophenol in a reaction catalyzed by microsomal enzymes. P-oxon can also be dearylated to diethyl phosphoric acid or hydrolyzed to O-ethyl-O-4-nitrophenyl phosphate. 4-nitrophenol, the primary metabolic product formed from P, is eliminated in the urine and quantifying it can provide an index of P exposure. These metabolic conversions occur principally in the liver, but also in the lung and brain. P-oxon binds to and irreversibly inhibits AChE; binding to other hepatic and plasma esterases also occurs, however, and can represent a significant detoxication mechanism since it prevents much of the hepatically generated P-oxon from entering the general circulation and target tissues.

PBTK/TD Models

Although physiological aspects of disposition of compounds by organs within the body had received attention earlier in history, it was not until 1937, with the significant work of Teorell, that an integrated approach to whole-body physiologically-based modeling of pharmacokinetics received serious consideration.

However, due to the mathematical and computational complexities and the lack of some basic physiological information at the time, whole-body PBTK/TD modeling did not come of age until the 1960's, when, with the aid of the digital computer, and modeling contributions from the chemical engineering community, interest reawakened in this area. As a means of overcoming many of the problems that plague classical compartmental models, which are basically abstract mathematical constructs, lacking actual anatomical, physiological, and biochemical relevance, Bischoff and Dedrick (1968) introduced PBTK/TD models as an alternative.

Pharmacokinetic models range from simple empirically-based models that describe observed data, to more complex PBTK/TD models that can be used to predict outcomes and extrapolate from one set of exposure conditions to another based upon an understanding of the underlying biology. PBTK/TD models for mixtures are significant tools for predicting conditions under which interactions are likely to alter assumptions of additivity and permit calculation of interaction thresholds with greater confidence. A PBTK model is a quantitative description (typically with differential equations) of the biological structures and processes that control toxicokinetic (TK) behavior in an organism (i.e., the effect of the body on the absorption, distribution, metabolism, and excretion of a chemical). PBTK modeling differs from classical compartmental PK modeling in this focus on the biological determinants of PK behavior. PBTK models simulate the events between the external dose and the internal exposure of the chemical to a target site. PBTD (toxicodynamic) models address the events from the internal dose at the target site to the response

observed (i.e., the effect(s) of the chemical on the body; inhibition of AChE in the present study). PBTK/TD models are used to establish a connection between TK behavior and the biological or toxicological effect of a chemical on the body. Thus, while classical empirical modeling is useful for interpolation between data points, a well developed PBTK/TD model can be used to simulate toxicological outcomes for a variety of different exposure conditions (different test species, exposure routes, chemical concentrations, metabolizing capacities).

Development and use of PBTK/TD models requires knowledge of organism-specific and chemical-specific biologic processes. An understanding of the parameters that govern the toxicokinetics is also essential. Proper development and use of these models often requires examination of existing data, model formulation, and testing leading to more specific data requirements, which in turn leads to model refinement. These capabilities allow PBTK/TD models to serve two different roles. First, the models can play a major role in the laboratory study of toxicokinetics and mechanism-of-action. This particular role of PBTK/TD models is especially powerful when model development and laboratory experiments are conducted in an iterative, mutually supportive manner. Models can help identify key data which are lacking, elucidate important events in the processes leading to toxicity, and also identify and quantify uncertainty. For example, PBTK/TD models may illuminate nonlinearities in high-to-low dose extrapolation, and interspecies scaling factors that perhaps would not be apparent without a quantitative, mechanistic perspective. A second important role of PBTK/TD models is in the development of risk assessments. PBTK/TD

models developed from an adequate supporting database that have been validated, demonstrate reasonable ability to predict the behavior of data sets NOT used during model development, can be used for partial or complete replacement of the default assumptions used in risk assessment (i.e. intra- and inter-species extrapolation factors or route-to-route extrapolation). Once a PBTK/TD model is defined in one animal species, it can be used for humans by replacing the physiological, anatomical, biochemical, and thermodynamic variables used for the experimental animal, with the values for the corresponding parameters from humans. The accuracy of the model depends on the blood and tissue solubility, metabolism, and protein binding characteristics in various tissues and the physiology of the organism. The aim of the acute simulations for the present study was to reproduce experimental data from *in vivo* dosing studies NOT used in development of the model. Good agreement between the model and experimental results allow one to have greater confidence in extrapolating.

Mixtures

Toxicokinetic interactions may involve alterations of the absorption, distribution, metabolism, or elimination phase of one or more chemicals due to the influence of another chemical. There are numerous literature examples of absorption and elimination phase interaction, the vast majority of which occur at high dose levels however. Likewise, interactions affecting distribution, such as competition for protein binding and tissue saturation effects, are unlikely to occur at exposure concentrations

relevant for human exposures (Poulin & Krishnan, 1996). Thus, interaction at the metabolic level represents the most probable mechanistic basis for a number of interactions observed in chemical mixtures at environmentally relevant exposure levels.

The metabolism of individual OP insecticides has been well characterized; however, there is a lack of data regarding the *in vitro/in vivo* inhibition of ChE by combinations of OP compounds. A limited number of studies (DuBois, 1969; Karanth et al., 2001, 2004; Hazarika et al., 2003) have characterized the toxicological effects of exposures to binary OP insecticide mixtures. Even so, many of these studies do not address the larger issue of cumulative exposures to mixtures of pesticides at more realistic lower dosage levels. Keplinger and Deichmann (1967) found that exposure of laboratory animals to mixtures of ChE-inhibiting insecticides resulted in greater than additive effects on acute toxicity *in vivo*. However, a recent *in vivo* study by Timchalk et al. (2005) with binary mixtures of chlorpyrifos and diazinon showed that low-level binary mixtures exhibit additive responses with respect to ChE inhibition. Furthermore, Tahara et al. (2005) using an *in vitro* methodology, evaluated the toxicity of multiple binary combinations OP oxons based on the degree of inhibition of ChE activity, found the degree of inhibition was also generally additive. Similarly, a previous *in vitro* study in our laboratory (Richardson et al., 2001), with a binary mixture of chlorpyrifos-oxon and azinphos-methyl-oxon, noted dose additivity when both compounds were added simultaneously to brain tissue. More recently, Gordon et al. (2006) reported an antagonistic effect on rat brain ChE between the insecticides

chlorpyrifos and the carbamate carbaryl when administered in a 1:1 ratio, whereas a 2:1 mixture had additive effects on brain ChE. They suggested this resulted from the depletion of key detoxication esterases not directly associated with neural function.

Justification and Hypotheses

While there are approximately 30 commercially relevant OP insecticides, three such compounds were selected for the following reasons: coding, running, and validating a PBTK/TD model for more than three OP compounds would have presented unwarranted significant challenges given the present state-of-knowledge. Sufficient literature exists to support the development of a ternary mixture model using CP, MP, P, whereas insufficient data are available for other OP insecticides. However, mechanistic data on other OP insecticides could be incorporated within the current PBTK/TD model in the future for the extrapolation of the interactions of more complex mixtures once sufficient data are made available, since they share a similar toxic mechanism-of-action. Finally, the selection of the three OP insecticides in the present study are particularly valuable for the kinetic and dynamic analyses, since the onset-of-action, peak-effect, and the duration-of-action can be studied over a relatively short period of time (24hr); this is quite important in the collection of experimental data to validate the model since experimental techniques involved with the animals are extensive/time consuming.

The primary objectives of the current study were to: (1) develop and validate a PBTK/TD model that can be used to successfully predict the toxicokinetic disposition

and toxicodynamic response (ChE inhibition) of a ternary OP insecticide mixture: chlorpyrifos, methyl parathion and parathion; (2) test the assumption of additivity (ChE response), in linking the individual models (only single-compound models were used, no parameters specific for interaction effects were added to the models); (3) the existing database of PBTK/TD models for chemical mixtures is sparse; this study helps to expand that database. Furthermore, this model provides a strong foundation for future PBTK/TD model development of more complex OP insecticide mixtures. Chapter II describes the processes involved in developing the PBTK/TD model. Chapter III and IV describe the *in vivo* toxicokinetic and toxicodynamic studies, respectively, used to validate the PBTK/TD model. Lastly, Chapter V addresses general conclusions of the study.

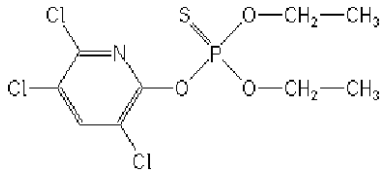

Chlorpyrifos

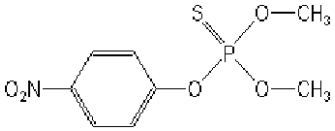

Methyl Parathion

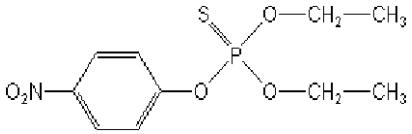

Parathion

Figure 1.1. Structures of chlorpyrifos, methyl parathion, parathion.

CHAPTER II

MODEL DEVELOPMENT

The PBTK/TD model was written as a program, using acslXtreme® Pharmacokinetic Toolkit Version 1.4 (AEgisTechnologies Group, Inc., Huntsville, AL), on a personal computer. Advanced Continuous Simulation Language (ACSL), is designed for modeling and evaluating the performance of continuous systems described by time-dependent, nonlinear differential equations. An important feature of ACSL is its sorting of continuous model equations, in contrast to digital programming languages such as FORTRAN where program execution depends on statement order. The Pharmacokinetic Toolkit®, used in concert with ACSL, is a collection of specialized PowerBlocks™ (PBTK/TD equations), that can be joined to model complex physiological processes. ACSL is commonly used in both pharmacology and toxicology for applications such as dosimetry, risk assessment, parameter estimation, and is cited extensively in the PBTK/TD modeling literature. There are other commercially available simulation software packages (SCoP®, STELLA®, PPP®, WinSAAM®, WinNonLin®; however, none are as user-friendly nor as comprehensive as acslXtreme® Pharmacokinetic Toolkit.

PBTK/TD Model Development Approach

PBTK/TD models have been developed for two of the individual compounds (Timchalk et al., 2002 (chlorpyrifos)), (Sultatos, 1990 (parathion)) used in the present study; making them ideal candidates for investigating mixture interactions without having to develop or validate a new PBTK/TD model for each compound. Nevertheless, a number of refinements were required for each model in order to construct a PBTK/TD model of predictive utility for the ternary mixture. Different modeling approaches (differences in parameters and underlying assumptions in the model structures, species used, sources for biological data etc.) were used for the models cited above. Therefore, the models could not simply be merged together as is. Thus, the ternary PBTK/TD model is a hybrid in essence, composed of the "best" parts of the two models, incorporating the needed changes to link the models under the assumption of additivity of ChE response. The PBTK/TD model for chlorpyrifos (Timchalk et al., 2002) served as a template, since this model was comparatively robust, requiring the least refinement of the two.

Given the importance of methyl parathion, discussed in Chapter I, the similarities/ differences in chemical structure and toxicity, as compared to chlorpyrifos and parathion, made its inclusion as the third OP insecticide of interest in the model a logical choice even though a PBTK/TD model has not been developed for methyl parathion. Sufficient literature, notably a somewhat recent review article of the pharmacokinetics and pharmacodynamics of methyl parathion by Kramer and

Ho (2002), and data from our laboratory allowed methyl parathion to be adequately modeled with chlorpyrifos and parathion.

Model Structure

The model consists of both organ-specific and lumped compartments. Organ-specific compartments were used to describe tissues directly involved in acute OP toxicity (i.e., brain, diaphragm, etc.) or tissues expected to significantly influence the toxicokinetics (blood, fat). The use of lumped compartments in the model helped to preserve a balance between parsimony of model structure, to maintain chemical mass balance, and to explicitly describe the physiology and biochemistry that determine the toxicokinetic behavior of the compounds. The model describes the time-course of absorption, distribution, and metabolism of chlorpyrifos, methyl parathion, parathion, their respective oxons, and detoxication products, as well as the inhibition of ChE by each oxon. As mentioned above, the two models were not merely "linked" as is, due to differences in modeling approaches used by each investigator and the need to eliminate redundancies between the two models, in order to construct a more efficient modeling system.

Figure 2.1 shows the resulting "hybrid" ternary mixture model, which describes the rat as a network of 6 tissue compartments; namely, adipose tissue, brain, diaphragm, liver, rapidly perfused tissues (representing viscera not explicitly described), slowly perfused tissues (primarily denoting muscle tissue), interconnected by systemic circulation and lung. The overall model consists of six PBTK/TD

models, 3 for the parent chemicals (chlorpyrifos, methyl parathion, parathion) and 3 for the oxon metabolites of each chemical. Each metabolite model is linked to its parent chemical model via the liver compartment. This is accomplished by considering the production rate of the metabolite as a reservoir for the parent chemical and as a source for the metabolite model. The estimated levels of the metabolites are then linked to a sub-model for AChE kinetics describing enzyme synthesis, degradation, inhibition and aging. The sub-model of AChE kinetics consists of 3 compartments, describing the mass balances for the free, inhibited, and aged forms of AChE.

For solving the equations in the ternary mixture model, a single set of rat physiological parameters and 3 sets of chemical-specific parameters (metabolic rates and partition coefficients for each compound) were used. These data were obtained from the literature. The model assumes that the toxicokinetic and toxicodynamic response in rats is independent of gender; the majority of the model parameters are based on those obtained from male rats, however. The absorption of the parent compounds, following oral gavage exposure, required the use of a two-compartment uptake model to simulate absorption. The two-compartment model incorporated 1^{st}-order rate equations to describe systemic uptake and transfer between compartments. The cytochrome 450 (CYP)-mediated activation and detoxication of the compounds was limited to the liver compartment. The parent compound models were linked to the oxon models that contained equations to describe the A-EST hydrolysis in both the liver and blood compartments. The CYP activation/detoxication and A-EST

detoxication were all described as Michaelis-Menton processes. Interactions of the oxon with B-EST (AChE, BuChE, and CaE) were modeled as 2nd-order processes occurring in the blood, brain, diaphragm and liver. The B-EST enzyme levels in blood, brain, diaphragm, and liver were calculated based on the enzyme turnover rates and enzyme activities reported by Maxwell et al. (1987), which were based on a balance between basal degradation and enzyme resynthesis. Following exposure to the respective oxons, the amount of available B-EST was determined by finding a balance between the bimolecular rate of inhibition and rate of B-EST regeneration (reactivation and resynthesis). In the present model, the detoxication products were formed by direct CYP metabolic conversion of the parent compounds and through A-EST mediated hydrolysis of the oxons and B-EST binding of the oxons. The selection of a reasonable set of model parameters was determined by evaluating the overall goodness of fit of the model against experimental data over the range of reported rate constants for enzyme affinities and activities.

In the current model, the total amount of absorbed parent compound is directly added to the liver compartment. However, once in the systemic circulation, only non-bound parent compound or metabolite was capable of entering the tissue compartments. The model structure for the inhibition of ChE by the compounds (oxons) in the selected tissues was based on the model structure developed by Gearhart et al. (1990), as modified by Timchalk et al. (2002). Since chlorpyrifos, methyl parathion, and parathion are all phosphorothionates, model parameters for chlorpyrifos reactivation and aging were also used for methyl parathion and

parathion, since the reactivation rates are similar, and aging is solely dependent on enzyme kinetics, regardless of the compound. Interactions between the compounds were explicitly described in the model at the level of metabolism through competition with CYP enzymes in the liver. At the response level, additivity of ChE response was assumed.

One of the objectives of the present study was to determine if the ternary OP mixture could be modeled solely using single-compound parameters; i.e., to address whether it is necessary to introduce separate interaction parameters for a mixture, as has been suggested by Tardif et al. (1997). As will be demonstrated in Chapters III and IV, a PBTK/TD mixture model can be successfully developed without the need for interaction experiments (i.e., explicit binary-interaction studies), at least in the case of simulations of low-dose exposures to a ternary OP insecticide mixture. The design of the current PBTK/TD model is sufficiently general and flexible in nature, such that it has the advantage of being applicable in the future to a variety of OP insecticides with minimal data input required. The model code is presented in Appendix A.

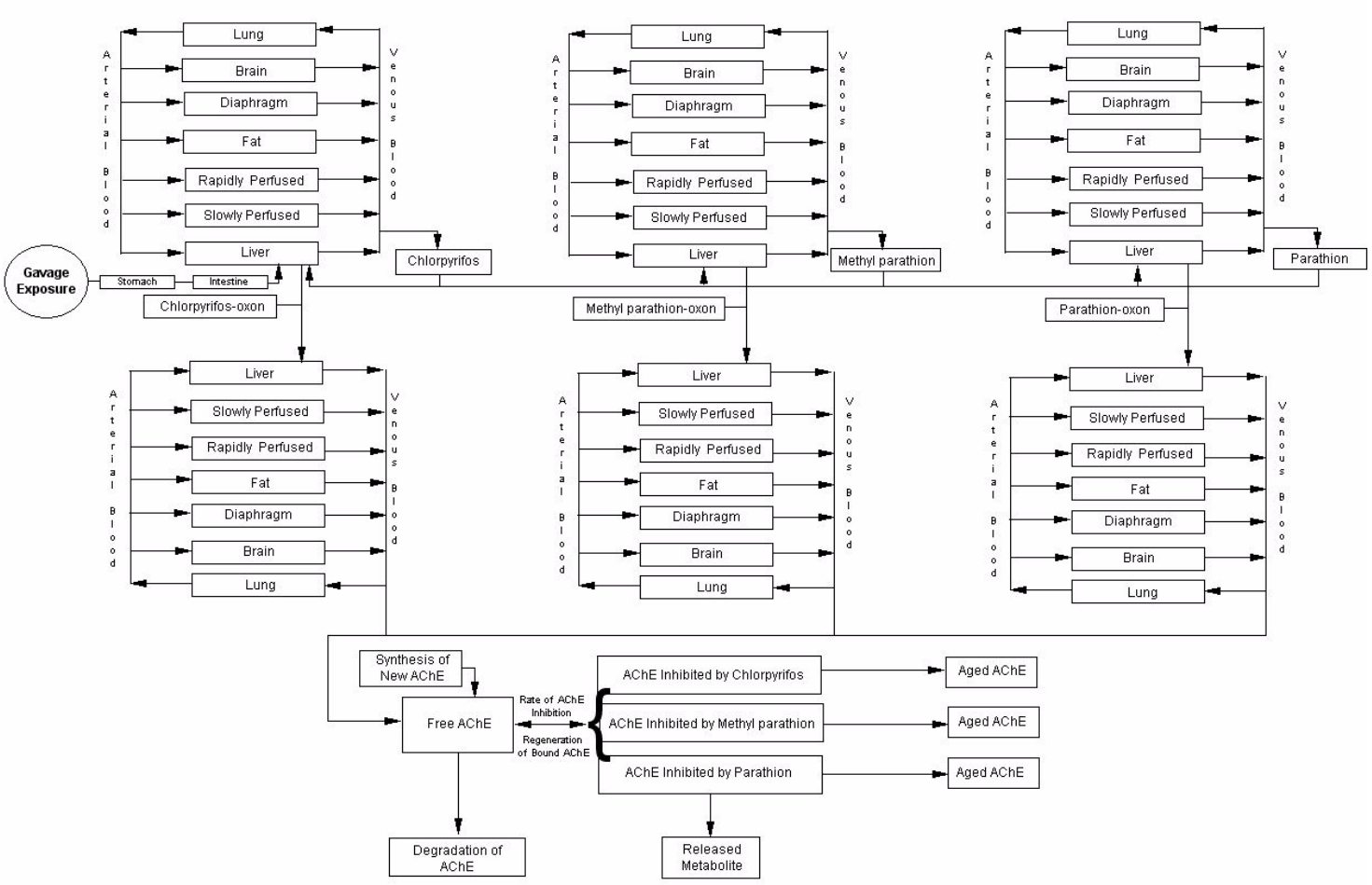

Figure 2.1. Schematic diagram of the ternary PBTK/TD mixture model. The model consists of six PBTK/TD models; 3 for the parent chemicals (chlorpyrifos, methyl parathion, parathion) and 3 for the metabolites of each chemical (their respective oxons). Each metabolite model is linked to its parent chemical model via the liver compartment. The metabolite models are linked to a sub-model for AChE kinetics; consisting of 3 sections describing the mass balances for free, inhibited, and aged forms of AChE.

CHAPTER III

MODEL VALIDATION: TOXICOKINETIC ANALYSES

Introduction

The principal objective of PBTK/TD modeling is prediction. In order to have confidence in the predictive power of a PBTK/TD model, the model must be validated. Model validation is a process in which the model's predictions are compared with experimental data NOT used in the creation of the model. Model validation is aimed only at demonstrating whether a model can produce reasonable accuracy within its realm of applicability, not that it embodies absolute truth, nor that it is the "best" model available. A model can never be proven wholly valid, only invalid.

The potential toxicity of an OP insecticide mixture is dependent upon several factors, namely, the amount delivered to the target tissue(s) and the balance between activation and detoxication. Toxicokinetic studies can provide important information on absorption, tissue compartmentalization of the parent compounds and their respective metabolites, and the time-course of compound transfer from one tissue compartment to another. Such information is central to fully describing the distribution, fate, and potential interaction patterns of each chemical within a mixture.

The objective of this portion of the study was to characterize the dosimetry of the parent compounds, their respective oxons, and detoxication products in selected tissues following oral gavage exposure to the ternary OP insecticide mixture.

Materials and Methods

Chemicals

Analytical grade chlorpyrifos, chlorpyrifos-oxon, methyl parathion, methyl paraoxon, parathion, paraoxon, 4-nitrophenol, TCP, and nitrophenyl valerate were provided by Dr. Howard W. Chambers, Department of Entomology and Plant Pathology, Mississippi State University, and were synthesized as previously described (Chambers et al., 1990). Analytical grade parathion and methyl parathion were re-crystallized from a generous gift from Monsanto Company (St. Louis, MO). Analytical grade chlorpyrifos and 3,5,6-trichloro-2-pyridinol, for synthesis of chlorpyrifos-oxon, were a generous gift from DowElanco Chemical (Indianapolis, IN). The same batch of each chemical was used throughout the study. Analytical grade ethyl acetate and acetonitrile were purchased from Burdick and Jackson (VWR International, West Chester, PA). Optima grade methanol was purchased from Fisher Scientific (Hampton, NH). All other chemicals were purchased from Sigma Chemical Co. (St. Louis, MO).

Animals and Treatments

Adult male Sprague-Dawley rats [Crl:CD(SD)BR] (280-330g) were obtained from Charles River Laboratories, Inc. Animals were housed in an AAALAC accredited facility and maintained in a temperature controlled room (22 ± 1^{o}C), 12:12 hour light/dark cycle, with food and water available *ad libitum*. Prior to dosing, food was withheld overnight (12hr) to allow for gastric emptying to minimize absorption of the mixture components by stomach contents following oral gavage administration. The Mississippi State University Animal Care and Use Committee approved all procedures.

Optimization-Dosage Range Finding

A pilot study was undertaken in order to determine the optimal dosage(s) for the mixture components used in the formal validation experiments, i.e., the dosage of each compound which was sufficient in magnitude to be detected (above the limit of detection (LOD)/limit of quantitation (LOQ) for each compound) via a gas chromatography (GC) methodology, outlined below, in the following tissues: blood, brain, diaphragm, liver, lung and skeletal muscle. The animals were starved overnight (12hr) prior to dosing, then received a combined oral administration, using a gavage needle of one of the following treatments: 50/1.0/1.0, 75/2.0/2.0, or 100/3.0/3.0 mg/kg of chlorpyrifos/methyl parathion/parathion. Corn oil was used as the vehicle. Following exposure, the animals were euthanized (stunning followed by decapitation)

at 3 time points (1hr, 4hr, 24hr) with one animal/time point/dosage combination. Brain, diaphragm, lung, liver and skeletal muscle were dissected out. The blood was collected and separated into serum and erythrocytes. Four hundred microliters of an acetic acid solution (2.5M) saturated with sodium chloride was added to halt metabolism and aid in the extraction process (Brzak et al., 1998).

An up-and-down approach was used for the optimization/pilot study. Initially, the highest 3 doses with 1 animal per time point was tested, and the animals observed closely for any signs of hypercholinergic activity. If there were no adverse signs, the tissues indicated were tested for the presence of the OP compounds and their respective metabolites. If the concentrations were within the range of analyte detectability then these dosages were used for the formal validation experiments. If the analytes could not be detected, the dosages were increased to obtain levels that yielded analyte detection, while concurrently not yielding overt signs of toxicity. If the initial dosages yielded toxic signs, then dosages were reduced to levels that did not yield signs. The dosages ultimately selected did not yield obvious signs of toxicity, in order to assure that cardiovascular function was not altered significantly, thus potentially invalidating the PBTK/TD models' general physiological assumptions.

Validation Experiments

Following the determination of the optimum dosages from the pilot study, the validation experiments commenced, which, as stated above, were used to test the

efficacy of the PBTK/TD model. The optimum dosages for the mixture components were determined to be 5.0mg/kg of chlorpyrifos, and 1.0mg/kg each of methyl parathion and parathion. This dosage combination was the lowest tested which remained above the LOD/LOQ for each compound using the GC methodology outlined below. However, the % brain AChE inhibition at these dosages was greater than sought, though no overt signs of toxicity were noted. Therefore, an additional dosage group was employed. Dosages of 2.5mg/kg of chlorpyrifos, and 0.5 mg/kg each of methyl parathion and parathion, which resulted in 10-15% brain AChE inhibition, was used to supplement the data acquired from the 5/ 1/ 1mg/kg dosage group, since these lower dosages could be assumed not to result in significant disruption of cardiovascular function.

Four time points of sacrifice were used for both dosage groups, 30min, 4, 12, and 24hr, with three treatment animals/time point/dosage group and two control animals/dosage group. Following exposure, rats were sacrificed by stunning followed by decapitation. Brain, diaphragm, liver, lung and skeletal muscle were dissected out and snap-frozen in liquid nitrogen and stored at -80^{o}C. Blood was collected and centrifuged at 400g for 5min to obtain the serum, which was also stored at -80^{o}C.

Toxicokinetic Analyses

In order to assess the accuracy of the model's predictions, analytical methods to quantify the levels of chlorpyrifos, chlorpyrifos-oxon, methyl parathion, methyl paraoxon, parathion, paraoxon, TCP, and 4-nitrophenol in the selected tissues, noted

above, were developed. Tissue homogenates, made in 0.05M Tris-HCl buffer/pH7.4, of brain (40mg/ml), lung (50mg/ml), diaphragm (75mg/ml), skeletal muscle (100mg/ml), plasma (1.5ml), and liver (100mg/ml) were used for the extractions. Extraction of the analytes was by addition of 4ml of ethyl acetate to 3ml of the homogenate or the plasma followed by mixing on a vortex mixer, with the layers separated by centrifugation (20min at 1600xg). An aliquot of the extract (3.0ml) was dried under a gentle stream of nitrogen and the residue resuspended in 100µl of acetonitrile to place the GC response within the linear range of the calibration curve. Samples (2µl) were injected into an Agilent Technologies 6890N GC in triplicate, using an autosampler. Tetrachlorvinphos (TCVP; 30µl) was used as the internal standard. The GC was equipped with both a nitrogen phosphorus detector (NPD) and an electron capture detector (ECD). Based on preliminary work during the optimization-dosage range finding pilot study, both detectors were required in order to detect all the compounds of interest. Separation using the ECD was achieved with a Restek RTX® -CL Pesticides column (30m x 0.32mm i.d. x 0.5µm film thickness; Restek, Bellefonte, PA, USA). Helium was used as the carrier gas, with argon (95%) and methane (5%) as the makeup gas. For the NPD, a Restek RTX®-5 column (30m x 0.32mm i.d. x 1.5µm film thickness; Restek, Bellefonte, PA, USA) was used. Hydrogen was used as the carrier gas and helium as the makeup. The temperature was ramped at a rate of 15^{o}C/min from 65 to 165 ^{o}C, which was held for 2min and then followed by a second ramp of 50 ^{o}C/min to a final temperature of 230^{o}C. The injector and detector temperatures were set at 275 and 300 ^{o}C, respectively. The compounds

of interest were identified by comparison of retention times with those of authentic standards. Similarly, the compounds were quantified by comparison with calibration curves constructed from standards containing a constant amount of TCVP and varying amounts of the compounds of interest. Calibration standards were prepared and extracted in parallel with the experimental samples.

Statistical Analysis

Calculation of the mean ± SEM (standard error of the mean) for the concentration-time profiles was the only formal statistical evaluation of the data conducted. The approach employed by the vast majority of PBTK/TD modelers, namely, comparing model output with the experimental observations exclusive of any formal statistical procedures, was adopted in the current study. Since the output processes of almost all real-world systems and simulations are non-stationary and autocorrelated, none of the classical statistical tests are directly applicable. Given that the PBTK/TD model is only a crude approximation of the real physiological system, a null hypothesis that the natural system and model are the same is obviously false. The more apt question that must be answered is whether or not the differences between the actual biological system and the model are significant enough to affect the conclusions which are derived from the model. For such conclusions, an "eyeball approach" is the best available at present, and employed in the current study.

Results

The majority of the parent compounds, CP-oxon, and both of the detoxication products (TCP, 4-NP) were extractable/quantifiable from all tissues of interest (blood, brain, diaphragm, liver, lung and skeletal muscle) with the 5mg/kg of CP and 1mg/kg of MP and P, respectively, dosage group. MP, P, and their respective oxons were below limits of quantitation for the lower dosage group (2.5mg/kg (CP), 0.5mg/kg (MP, P), respectively). The extraction recovery efficiencies and GC retention times are listed in Table 3.1 and 3.2, respectively. Calibration curves of peak area ratios of all compounds and the internal standard were linear (r^2 ranged from 0.9232 to 0.9840).

Concentration of analytes for CP followed the order TCP>>CP>>CPXN in all tissues (Figures 3.1-3.6). Concentration of analytes for MP and for P followed the order 4-NP>>MP or P in all tissues (Figures 3.1-3.6). The respective oxons of MP and P were below the limits of quantitation for both dosage groups. A general trend in the concentration of all the compounds quantified in tissues was: liver > blood > brain > lung > diaphragm > skeletal muscle. The data suggest that all three compounds are rapidly absorbed and metabolized. Peak CP concentrations were attained by 4hr, with the exception of the liver, with a peak occurrence at 30min. Peak concentrations of MP were attained by 30min in all tissues. Peak P concentrations were attained by 12hr, with the exception of the liver, 30min. The toxicokinetics of the individual compounds were not altered by the presence of the others; i.e. peak concentrations of

CP (4hr), MP (30min), P (12hr) would be expected for an individual exposure to the respective compounds. This is further confirmed by the PBTK/TD model's accurate simulation of these data. With respect to CP-oxon, when detected, the levels generally agreed quite well with the AChE inhibition pattern in the target tissues, i.e., the greater the amount of oxon present, the greater the inhibition of AChE observed (Chapter IV). Furthermore, the overall higher levels of CP present in the tissues, as compared to both MP and P, link the dominant trend of maximal ChE inhibition (4hr, Chapter IV) with that of the CP toxicokinetics.

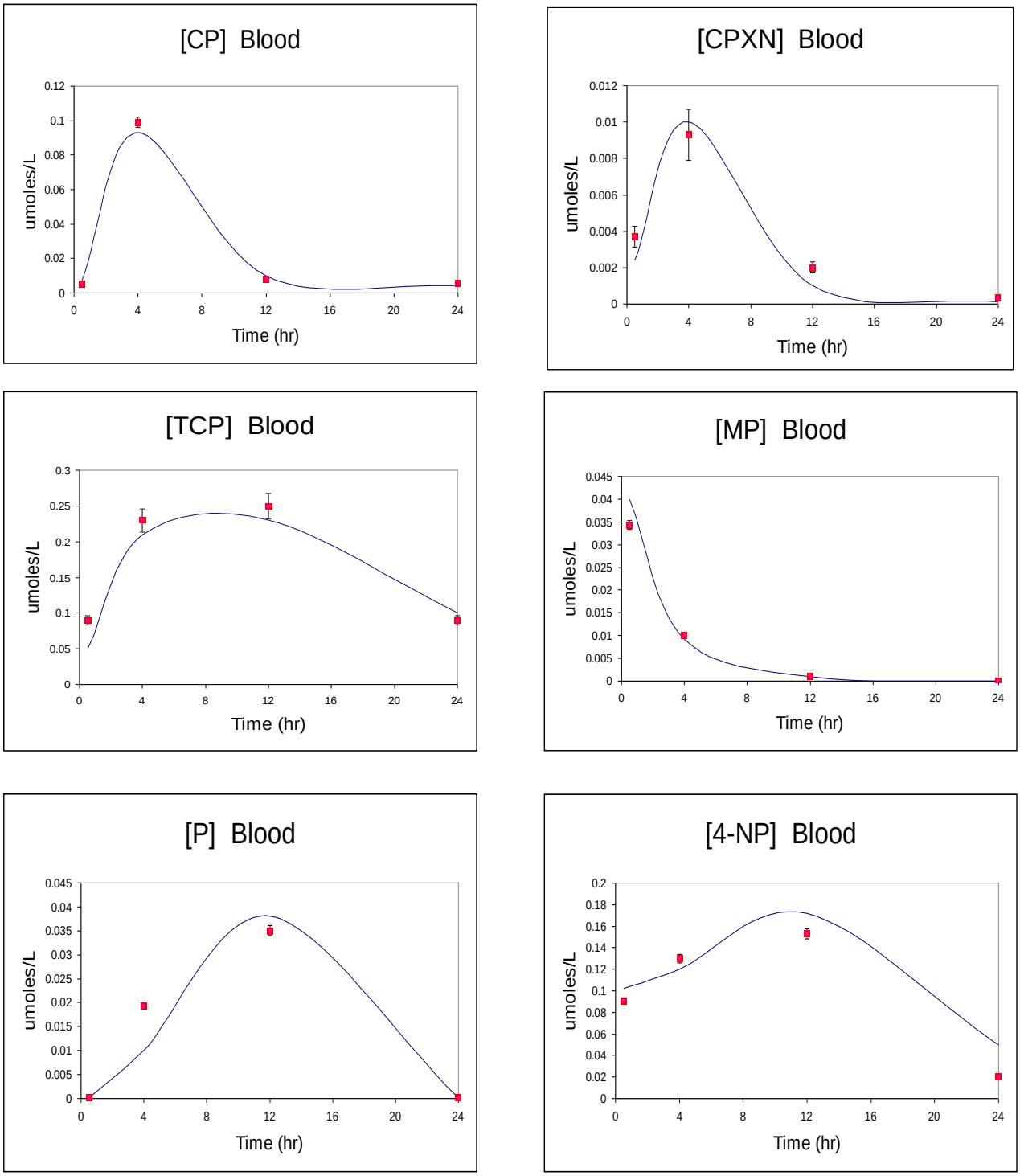

Figure 3.1. Concentration-time profiles of chlorpyrifos (CP), chlorpyrifos oxon (CPXN), 3,5,6-trichloro-2-pyridinol (TCP), methyl parathion (MP), parathion (P), 4-nitrophenol (4-NP) in blood following exposure to a mixture of 5, 1, 1mg/kg of CP, MP and P, respectively. Experimental data (symbols), means ± SEM (n = 3) and simulations (lines).

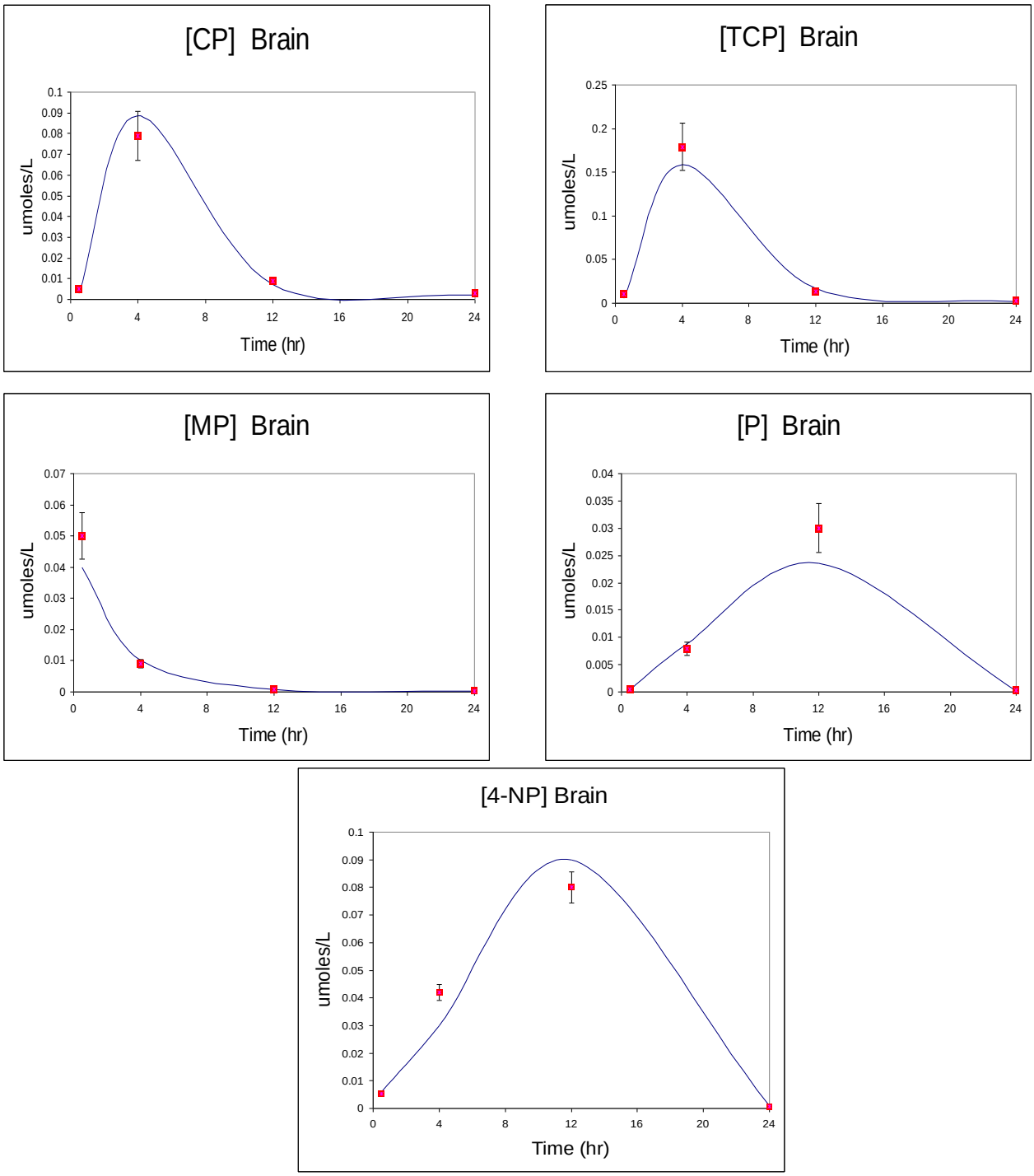

Figure 3.2. Concentration-time profiles of chlorpyrifos (CP), 3,5,6-trichloro-2-pyridinol (TCP), methyl parathion (MP), parathion (P), 4-nitrophenol (4-NP) in brain following exposure to a mixture of 5, 1, 1mg/kg of CP, MP and P, respectively. Experimental data (symbols), means ± SEM (n = 3) and simulations (lines).

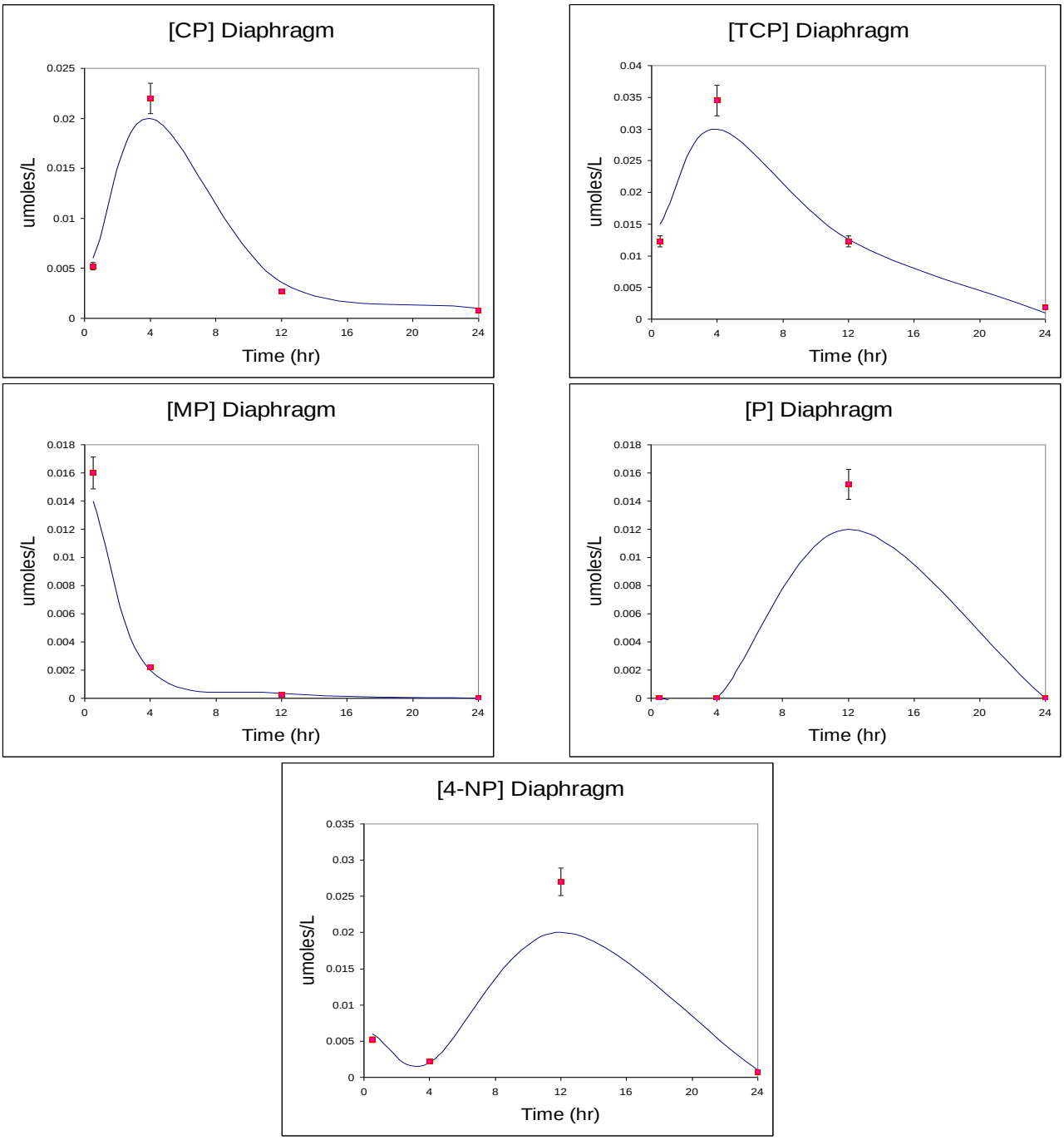

Figure 3.3. Concentration-time profiles of chlorpyrifos (CP), 3,5,6-trichloro-2-pyridinol (TCP), methyl parathion (MP), parathion (P), 4-nitrophenol (4-NP) in diaphragm following exposure to a mixture of 5, 1, 1mg/kg of CP, MP and P, respectively. Experimental data (symbols), means ± SEM (n = 3) and simulations (lines).

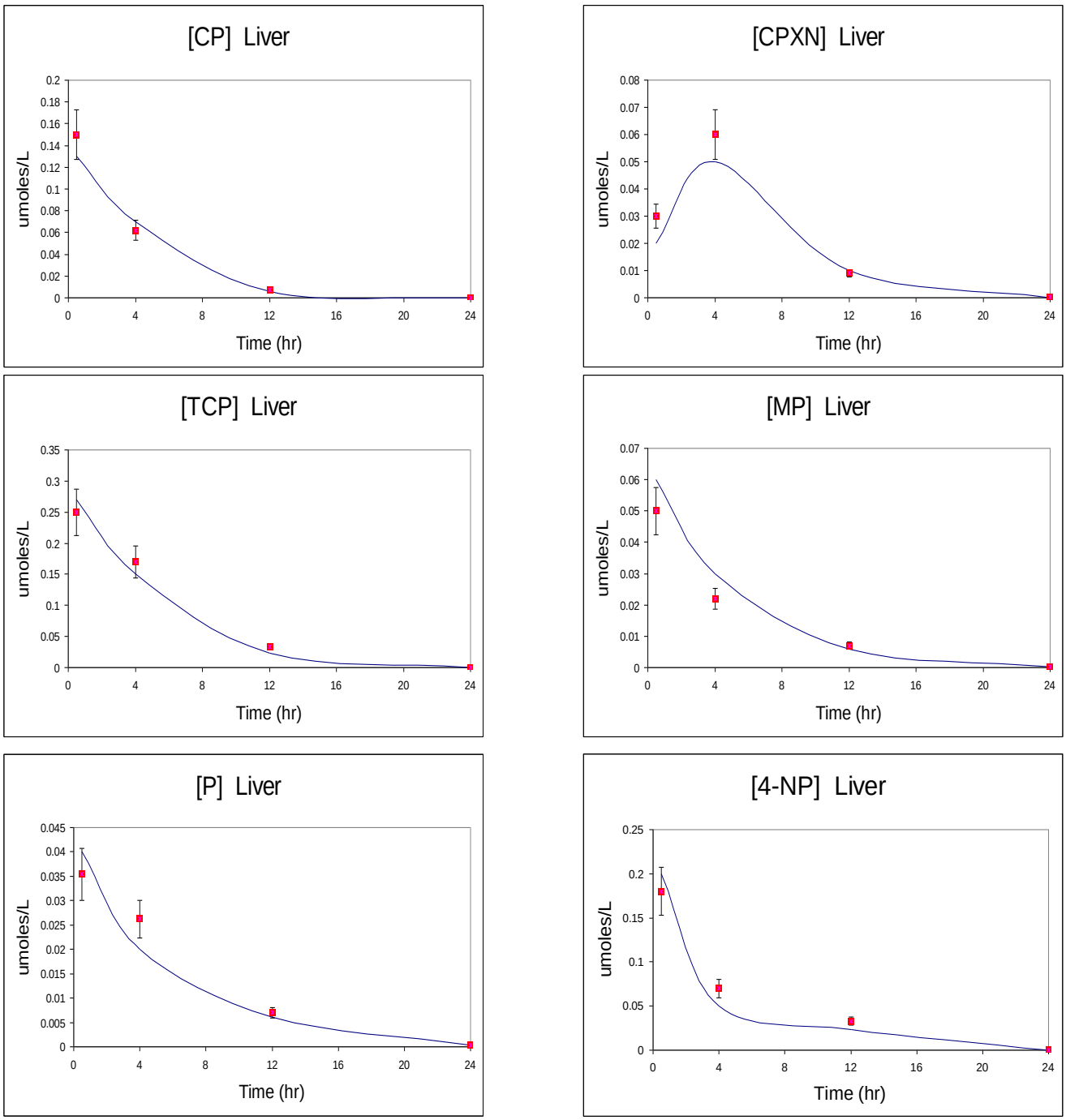

Figure 3.4. Concentration-time profiles of chlorpyrifos (CP), chlorpyrifos oxon (CPXN), 3,5,6-trichloro-2-pyridinol (TCP), methyl parathion (MP), parathion (P), 4-nitrophenol (4-NP) in liver following exposure to a mixture of 5, 1, 1mg/kg of CP, MP and P, respectively. Experimental data (symbols), means ± SEM (n = 3) and simulations (lines).

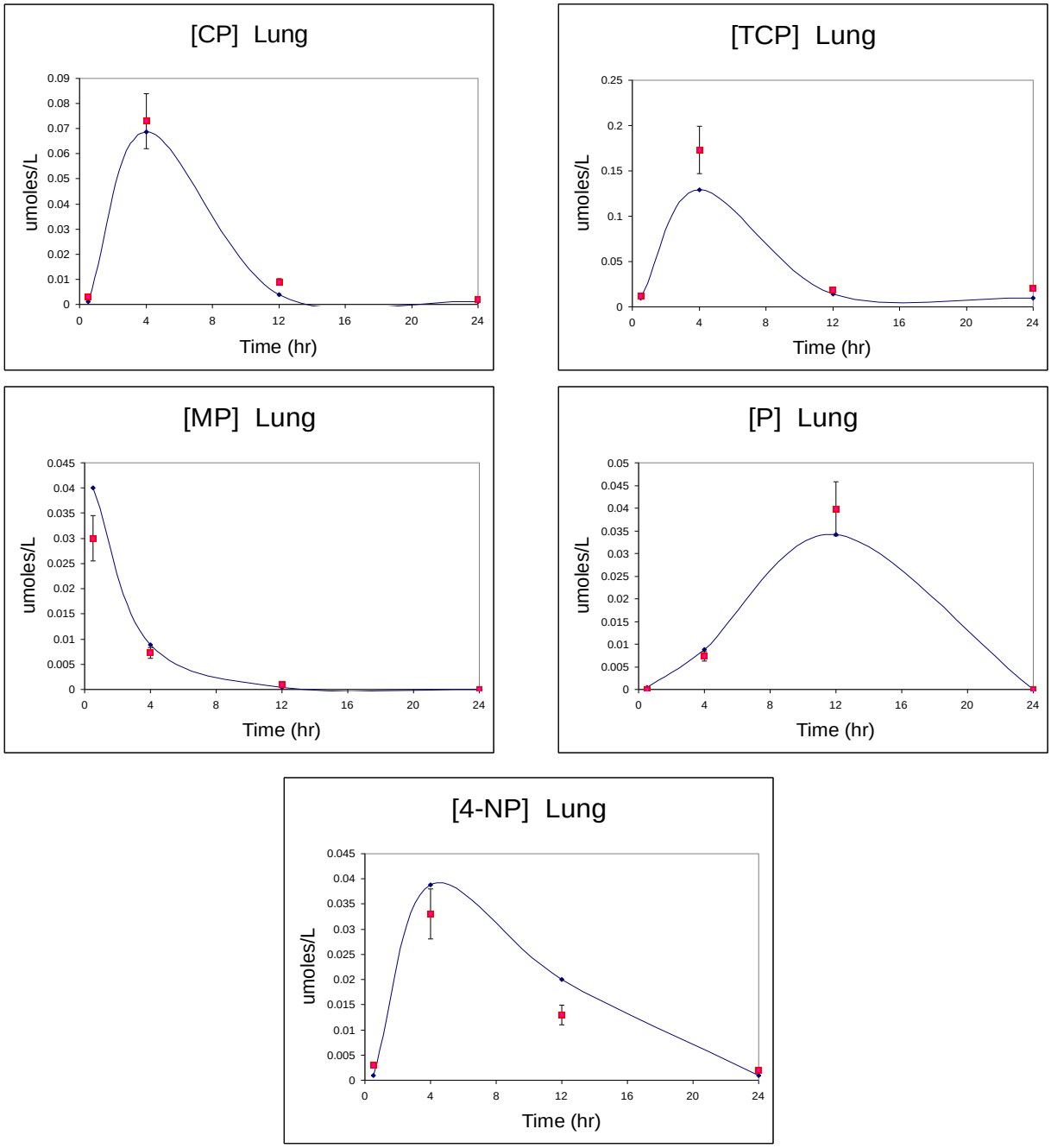

Figure 3.5. Concentration-time profiles of chlorpyrifos (CP), 3,5,6-trichloro-2-pyridinol (TCP), methyl parathion (MP), parathion (P), 4-nitrophenol (4-NP) in lung following exposure to a mixture of 5, 1, 1mg/kg of CP, MP and P, respectively. Experimental data (symbols), means ± SEM (n = 3) and simulations (lines).

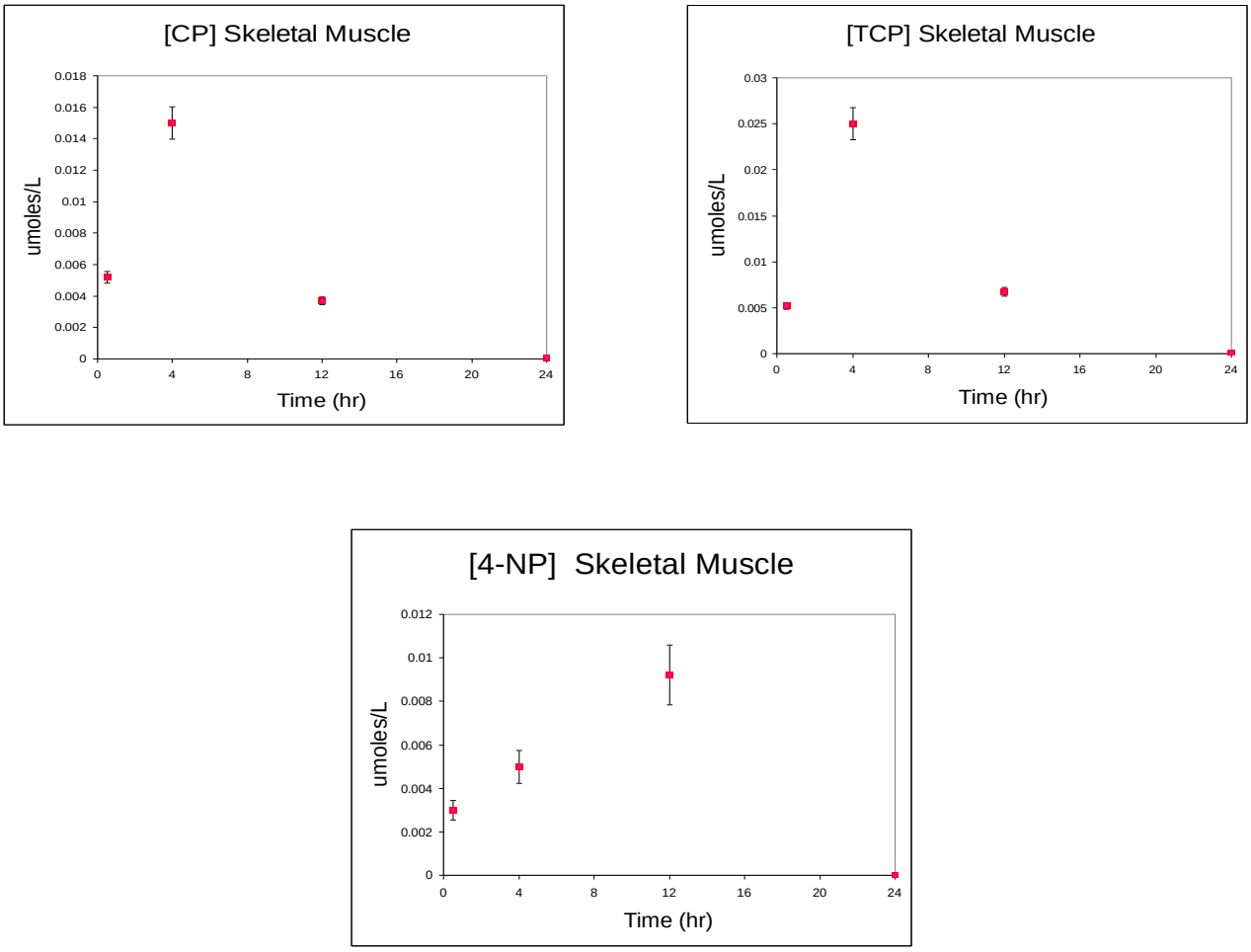

Figure 3.6. Concentration-time profiles of chlorpyrifos (CP), 3,5,6-trichloro-2-pyridinol (TCP), 4-nitrophenol (4-NP) in skeletal muscle following exposure to a mixture of 5, 1, 1mg/kg of CP, MP and P, respectively. Experimental data (symbols), means ± SEM (n = 3) and simulations (lines).

Discussion

The toxicokinetics of CP, MP, P, CP-oxon, and the detoxication products (TCP, 4-NP) were quantified in the tissues of interest (blood, brain, diaphragm, liver, lung and skeletal muscle) with the 5mg/kg of CP and 1mg/kg of MP and P, respectively, dosage group. MP, P, and their respective oxons were below the limits of quantitation for the lower dosage group (2.5mg/kg (CP), 0.5mg/kg (MP,P, respectively)), as were the oxons of both MP and P for the higher dosage group. MP, P, and their respective oxons were below the limits of quantitation at these dosages likely because they are efficiently extracted by the liver and metabolized (deactivated) rapidly. The toxicokinetics of CP-oxon were only sufficiently characterized in the blood and liver samples. Levels of the 3 oxons in other tissues were well below the limits of quantitation, likely due to the chemical instability and reactivity of the oxons, and/or the limited amount formed at the low dosages used in the present study.

The occurrence of peak levels of MP at the 30min time point in all tissues suggests that MP is rapidly absorbed and distributed. Protein binding in the blood can be assumed to play a significant role in the case of CP and P, however, since their toxicokinetic profiles illustrate their presence in blood for extended periods of time, as compared to MP. Future studies may benefit from examining earlier time points in order to better characterize the toxicokinetics of MP. Furthermore, additional time points between 30min and 12hr would also be of value in order to more closely

examine the concentration intersections of the compounds at these points, and their relation to the resulting ChE inhibition described in Chapter IV. It is unfortunate that the toxicokinetics of the oxons were difficult to characterize; although it was feasible to identify CP-oxon in the blood and liver, the observed results were very close to the analytical limits of quantitation. The oxons (all three) were readily quantifiable at the higher dosages used in the pilot studies; however, at such dosages the animals either died or displayed significant "cholinergic crisis" signs, making such dosages inadequate for any meaningful validation studies to be used for the PBTK/TD model. The limited number of quantifiable oxon samples thus made it particularly difficult to adequately model the oxon toxicokinetics. However, over the higher dosage range evaluated, the model predictions and measured concentrations were reasonably comparable given the limitations of the data.

As will be shown in the following chapter (IV), the model was able to accurately predict ChE inhibition quite well, even though the oxon toxicokinetic data were limited in the present study. The presence of the parent compounds, specifically their time of maximal concentration, in the selected tissues appears to be a good predictor of ChE inhibition. It should be kept in mind that mere concentration of the various compounds is but one factor in the determination of the magnitude and extent of ChE inhibition in the target and non-target tissues.

The detoxication products, 4-NP and TCP, were detected in all target tissues as well as in liver and plasma. Given that 4-NP and TCP were detected more readily than the parent compounds indicates that metabolism, and perhaps esterase

phosphorylation, occurred quite readily. Brain, diaphragm, and lungs showed significant levels of 4-NP and TCP, as compared to the parent compounds, suggesting that these tissues are likely active in extrahepatic metabolism; some of this may have resulted from phosphorylation of serine esterases, and dearylation as well. Extrahepatic metabolism of the parent compounds in the mixture, whether activation or detoxication, may have significant impact in acute exposures to OP insecticides. Hence, metabolic activity of target sites, particularly peripheral target sites such as brain, diaphragm, lungs, etc., may be a critical factor in determining acute toxicity levels. Chronic toxicity also may depend on target site metabolic activities, especially since occupational exposures are repetitive and cumulative in nature, and moreover since OP insecticides, in the prototypical dermal or respiratory exposure routes may circumvent the liver. Although chronic toxicity was not investigated in the present study per se, the current PBTK/TD model has the flexibility to explore such scenarios; which are otherwise difficult or unethical to test in real-life.

TABLE 3.1

Extraction Recovery Efficiencies

	Percent Recovery of Compounds							
Tissue	CP	CPXN	TCP	MP	MPXN	P	PX	4-NP
Brain	87.93 (5.44)	79.50 (2.84)	82.75 (8.68)	84.92 (7.99)	72.31 (8.97)	78.19 (6.10)	73.89 (11.56)	82.99 (5.04)
Blood	74.83 (3.97)	76.66 (6.41)	76.11 (8.53)	88.30 (2.99)	75.89 (12.01)	71.00 (8.17)	83.92 (3.59)	86.52 (3.22)
Diaphragm	78.38 (6.10)	75.00 (5.88)	69.32 (10.92)	71.88 (9.84)	73.12 (9.31)	74.50 (6.44)	72.49 (7.78)	81.89 (5.29)
Lung	79.72 (12.42)	74.59 (5.98)	77.92 (5.56)	76.92 (3.82)	68.91 (7.66)	67.93 (5.92)	75.89 (9.31)	77.12 (10.02)
Liver	89.47 (3.81)	67.31 (8.68)	83.59 (3.58)	66.79 (5.51)	69.33 (2.99)	77.92 (5.90)	68.29 (12.94)	84.43 (6.62)
Skeletal Muscle	75.83 (10.62)	73.22 (9.83)	77.53 (6.31)	69.40 (7.84)	72.63 (3.90)	66.08 (4.79)	69.23 (9.01)	82.61 (8.17)

Each value represents the mean (±SEM) of 3 determinations. Chlorpyrifos (CP), chlorpyrifos oxon (CPXN), 3,5,6-trichloro-2-pyridinol (TCP), methyl parathion (MP), methyl paraoxon (MPXN), parathion (P), paraoxon (PXN), 4-nitrophenol (4-NP).

TABLE 3.2

Retention Times of Compounds

Compound	Retention Time (min) ECD	NPD
Chlorpyrifos	14.13 (±0.05)	18.52 (±0.05)
Chlorpyrifos oxon	8.02 (±0.05)	18.36 (±0.05)
Methyl parathion	14.26 (±0.05)	15.51 (±0.05)
Methyl paraoxon	8.32 (±0.05)	13.33 (±0.05)
Parathion	14.97 (±0.05)	18.58 (±0.05)
Paraoxon	14.86 (±0.05)	16.54 (±0.05)
TCP	8.06 (±0.05)	6.14 (±0.05)
4-nitrophenol	10.28 (±0.05)	10.73 (±0.05)

CHAPTER IV

MODEL VALIDATION: TOXICODYNAMIC ANALYSES

Introduction

The Food Quality Protection Act of 1996 mandates that all pesticides acting through a common mechanism of toxicity undergo cumulative risk assessments. The primary concern is that exposure to multiple members of a common-mechanism group might pose a health risk even if the individual components of the mixture are present at levels below their respective no-observed-adverse-effect levels. OP insecticides were the first class of chemicals to undergo a cumulative risk assessment (US EPA, 2002). As such, they share a common mechanism of toxicity, the inhibition of AChE, resulting in accumulation of acetylcholine in cholinergic synapses and excessive stimulation of cholinergic pathways in central and peripheral nervous tissues.

The potential toxicity of an OP insecticide mixture is dependent upon a combination of the amount delivered to the target systems and the balance between activation and detoxication. Many OP insecticides, including the ones in the present study, are phosphorothionates (possessing a P=S group) and are weak anticholinesterases; they must be bioactivated by CYP450 to their oxon metabolites (possessing a P=O group) which are potent anticholinesterases. The oxons can inhibit

a variety of serine esterases including AChE in target tissues, i.e., brain, as well as non-target esterases (carboxylesterases), in non-target tissues, i.e. blood and liver. The inhibition of non-target esterases stoichiometrically destroys oxon molecules and is an effective form of protection of the target, brain AChE, from inhibition.

As acknowledged in Chapter I, limited experimental data are available on the effects (esterase inhibition) of mixtures of OP insecticides; such information would be of great value in cumulative risk assessments. The toxicodynamic analyses of the present study were designed with the following objective: to perform *in vivo* experiments to quantitate the inhibition of AChE and CbxE following exposure to a ternary OP insecticide mixture; composed of chlorpyrifos, methyl parathion and parathion. These data were used to validate the PBTK/TD model simulations.

Materials and Methods

Chemicals

Analytical grade chlorpyrifos, chlorpyrifos-oxon, methyl parathion, methyl paraoxon, parathion, paraoxon, 4-nitrophenol, TCP, and 4-nitrophenyl valerate were provided by Dr. Howard W. Chambers, Department of Entomology and Plant Pathology, Mississippi State University, and were synthesized as previously described (Chambers et al., 1990). Analytical grade parathion and methyl parathion were re-crystallized from a generous gift from Monsanto Company (St. Louis, MO). Analytical grade chlorpyrifos and 3,5,6-trichloro-2-pyridinol, for synthesis of

chlorpyrifos-oxon, were a generous gift from DowElanco Chemical (Indianapolis, IN). The same batch of chemicals was used throughout the study. All other biochemicals were purchased from Sigma Chemical Co. (St. Louis, MO).

Animals and Treatments

Adult male Sprague-Dawley rats [Crl:CD(SD)BR] (280-330g) were obtained from Charles River Laboratories, Inc. Animals were housed in an AAALAC accredited facility and maintained in a temperature controlled room (22 ± 1)^{o}C, 12:12 hour light/dark cycle, with food and water available *ad libitum*. Prior to dosing, food was withheld overnight (12hr) to allow for gastric emptying, to minimize the adsorption of the mixture components by stomach contents following oral gavage administration. The Mississippi State University Animal Care and Use Committee approved all procedures.

Acetylcholinesterase Assay

The tissues used for this component were isolated along with the tissue samples used for the toxicokinetic analyses (Chapter III). Frozen samples of brain, diaphragm, lung, and skeletal muscle were assayed using an established technique in our lab (Ellman et al., 1961; as modified in Chambers and Chambers, 1989) to determine the amount of cholinesterase activity. Tissues were homogenized in 0.05M Tris-HCl (pH 7.4, 25°C): brain 40mg/ml, lung 200mg/ml, diaphragm 100mg/ml, and skeletal muscle 100mg/ml. The chromagen, 0.024M 5,5-dithio-bis(2-nitrobenzoic

acid) (DTNB) and the substrate, 0.1M acetylthiocholine (ATCH) were mixed in a ratio of 2:1 and diluted 1:10 with warm 0.05M Tris-HCl. In a microplate, 155µl of warm Tris-HCl and 18.75µl of the diluted DTNB/ATCH mixture were added into eight wells. Into three wells, 10µl of 0.01M eserine sulfate was added to correct for non-ChE hydrolysis of the substrate. The reaction was initiated by addition of 25µl of the homogenate to all eight wells. Using a Phenix Sunrise® plate reader, readings were taken every 5sec for 5min. The average slope of the three eserine sulfate blanks were subtracted from the average slope of the five sample wells. This corrected slope was used to calculate specific activity. Employing the same method, 10µl of undiluted serum per well was used to determine the serum ChE activity.

Diaphragm, lung, and skeletal muscle homogenates were filtered through polyester fiberfill twice to remove large particulates. The ChE activity was determined by adding 100µl of DTNB, 30µl of ATCH, 1.8ml of 0.05 Tris-HCl, and 100µl of homogenate into a cuvette and placed into a Perkin-Elmer Lambda 25 spectrophotometer. Readings were taken every 5sec for 2min. To correct for particulates settling during the assay and causing reading errors, the average slope between 25sec and 2min was used to calculate specific activity.

Carboxylesterase Assay

For the carboxylesterase (CbxE) analyses, liver and plasma samples were assayed spectrophotometrically using 4-nitrophenyl valerate as the substrate (Chambers et al., 1990). Serum was diluted 1:19 with 0.05M Tris-HCl and liver was

homogenized 5mg/ml with 0.05 Tris-HCl. Diluted serum and homogenized liver (40µl) samples were added to each of six test tubes containing 1.8ml of cold Tris-HCl buffer. Paraoxon (20µl of 0.1M solution) was added to the last two of each set to completely inhibit the CbxE activity and correct for non-CbxE hydrolysis of substrate. After incubating in a warm, shaking waterbath for 10min, 20µl of nitrophenyl valerate was added and incubated for 5min. The reaction was terminated by addition of 0.5ml of 2% Tris-SDS and each sample was read spectrophotometrically at 405nm. The average of the two paraoxon blanks was subtracted from the average of the remaining four tubes.

Protein Quantification

Protein concentrations for all of the tissues were determined by the method of Lowry et al. (1951). The serum was diluted 1:19, diaphragm 1:5, lung 1:4, and skeletal muscle 1:4 with 0.05M Tris-HCl to give absorbance readings in the linear range of the 50µg and 200µg standards. Brain and liver were not diluted. The protein concentrations were used to calculate AChE and CbxE specific activity as nmoles product min^{-1} mg $protein^{-1}$.

Statistical Analysis

Calculation of the mean ± SEM (standard error of the mean) for the AChE and CbxE percent inhibition-time profiles was the only formal statistical evaluation of the data conducted. The approach employed by the vast majority of PBTK/TD modelers,

namely, comparing model output with the experimental observations exclusive of any formal statistical procedures, was adopted in the current study. Since the output processes of almost all real-world systems and simulations are non-stationary and autocorrelated, none of the classical statistical tests are directly applicable. Given that the PBTK/TD model is only a crude approximation of the real physiological system, a null hypothesis that the natural system and model are the same is clearly false. The more apt question posed is whether or not the differences between the biological system and the model are significant enough to affect the conclusions which are derived from the model. For such conclusions, an "eyeball approach" is the best available at present.

Results

The results of the present study demonstrate a clear dose- and time-dependent inhibition of tissue ChE activity. The extent of *in vivo* tissue sensitivity followed the order: serum > liver > lung > diaphragm > brain > skeletal muscle. Following exposure to both dosages of the mixture, AChE activity was rapidly inhibited by 30min and reached maximal inhibition by 4hr in all tissues (Figures 4.1, 4.2, 4.4, 4.8, 4.9, 4.11), with the exception of muscle and serum, maximal inhibition occurred at 12hr (Figures 4.5, 4.6, 4.12, 4.14). Liver and serum CbxE maximal inhibition was present by 4hr for both dosage groups (Figures 4.3, 4.7, 4.10, 4.13). Cholinesterase inhibition in the tissues ranged from 11- 37% for the lower dosage, and 29-93% for

the higher dosage group; with few exceptions, inhibition was generally additive and was supported by the model simulations.

The percent activity of AChE and CbxE following exposure to both dosage groups was significantly different from control at 30min through 24hr. Very little to slow recovery of AChE and CbxE activity was seen in the tissues from the 12hr – 24hr time points, following the window of maximal inhibition within the tissues (4hr -12hr); i.e. enzyme activity did not return to control levels through 24hr post-dosing. As mentioned above, inhibition was generally additive at most time points and in most tissues with the lower dosage group. However, with the higher dosage group, deviations from additivity were seen particularly in the diaphragm and lung (Figures 4.9, 4.11). In these instances, the model overestimated the percent inhibition at the early time points, 30min – 4hr and underestimated the percent ChE inhibition at 24hr, in the case of the diaphragm. In addition, the model overestimated at 4hr and underestimated at 12hr CbxE inhibition in the serum (Figure 4.7, 4.13) for both dosage groups. The model was not able to accurately simulate muscle AChE inhibition following exposure to both dosage groups, the experimental data, however, are shown in Figures 4.5, 4.12. With that said, the experimental data did follow the basic trend of the model simulations, however; accurately predicting the time point of maximal inhibition, and model fits were 80% or greater for any particular data set.

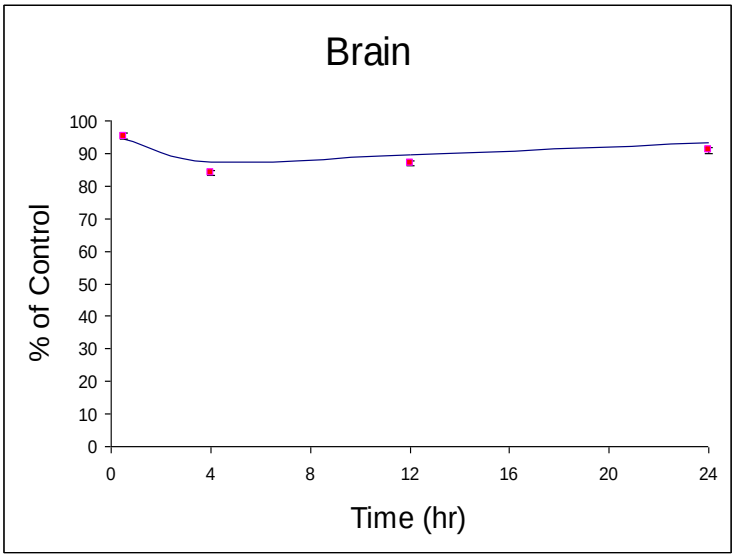

Figure 4.1. Time-course of inhibition of brain cholinesterase activity in adult male rats following exposure to 2.5, 0.5, 0.5mg/kg of chlorpyrifos, methyl parathion and parathion respectively. Experimental data (symbols), means ± SEM (n = 3) and simulations (lines).

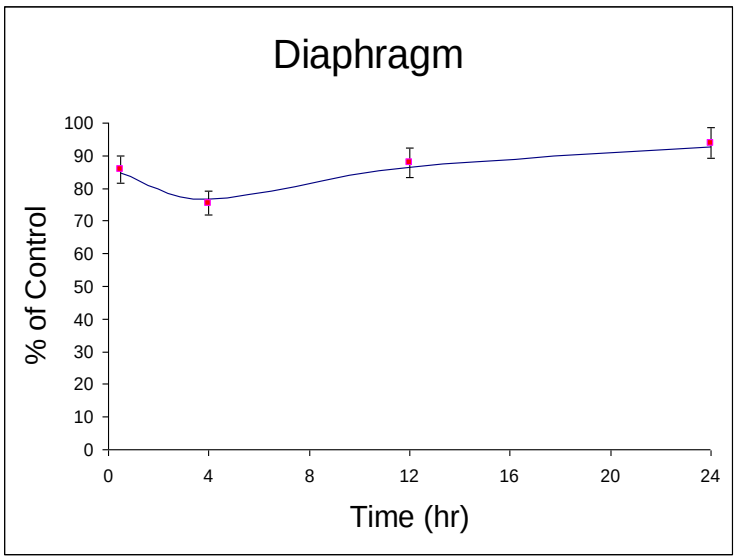

Figure 4.2. Time-course of inhibition of diaphragm cholinesterase activity in adult male rats following exposure to 2.5, 0.5, 0.5mg/kg of chlorpyrifos, methyl parathion and parathion, respectively. Experimental data (symbols), means ± SEM (n = 3) and simulations (lines).

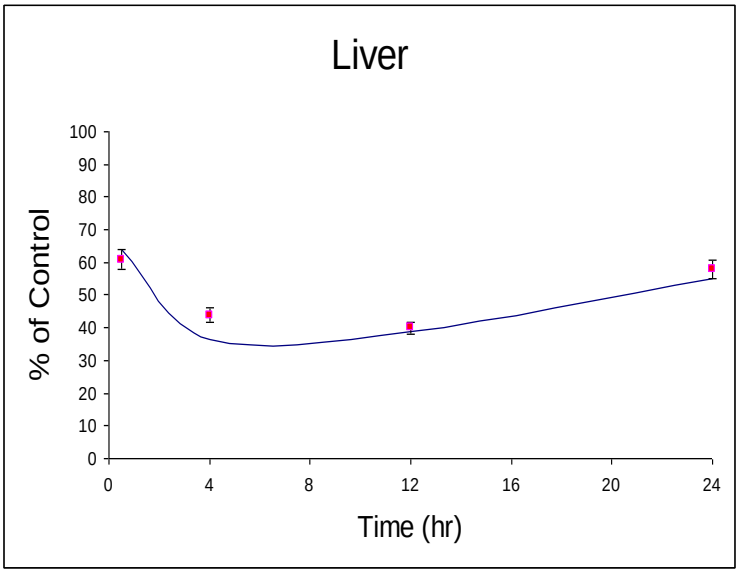

Figure 4.3. Time-course of inhibition of liver carboxylesterase activity in adult male rats following exposure to 2.5, 0.5, 0.5mg/kg of chlorpyrifos, methyl parathion and parathion, respectively. Experimental data (symbols), means ± SEM (n = 3) and simulations (lines).

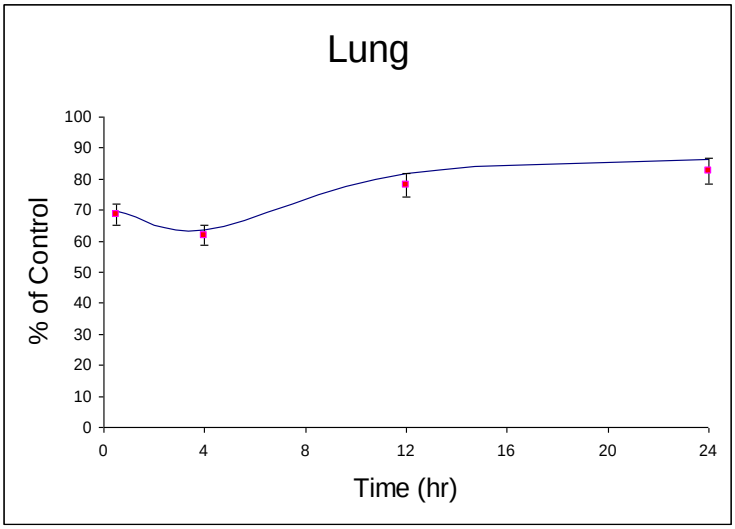

Figure 4.4. Time-course of inhibition of lung cholinesterase activity in adult male rats following exposure to 2.5, 0.5, 0.5mg/kg of chlorpyrifos, methyl parathion and parathion, respectively. Experimental data (symbols), means ± SEM (n = 3) and simulations (lines).

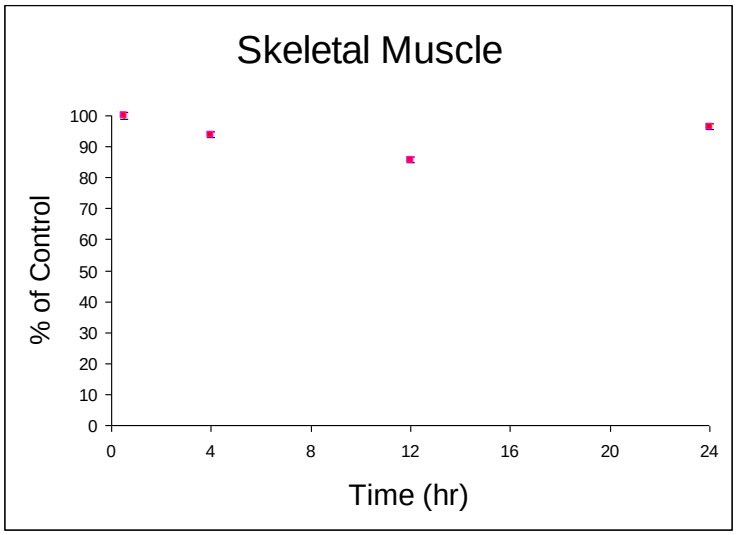

Figure 4.5. Time-course of inhibition of skeletal muscle cholinesterase activity in adult male rats following exposure to 2.5, 0.5, 0.5mg/kg of chlorpyrifos, methyl parathion and parathion, respectively. Experimental data (symbols), means ± SEM (n = 3).

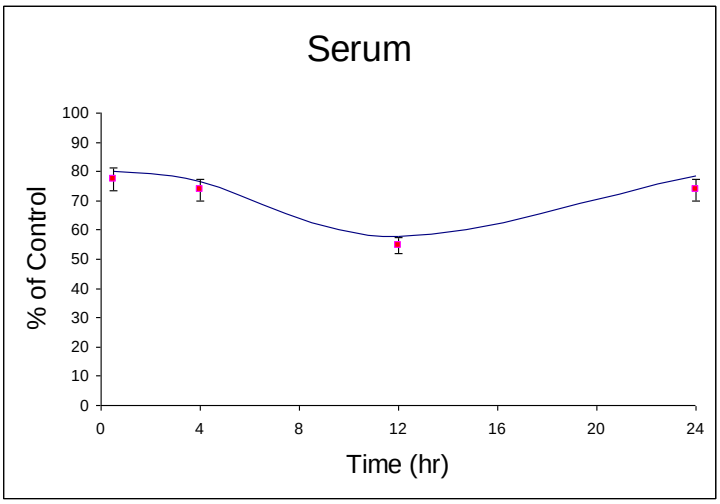

Figure 4.6. Time-course of inhibition of serum cholinesterase activity in adult male rats following exposure to 2.5, 0.5, 0.5mg/kg of chlorpyrifos, methyl parathion and parathion, respectively. Experimental data (symbols), means ± SEM (n = 3) and simulations (lines).

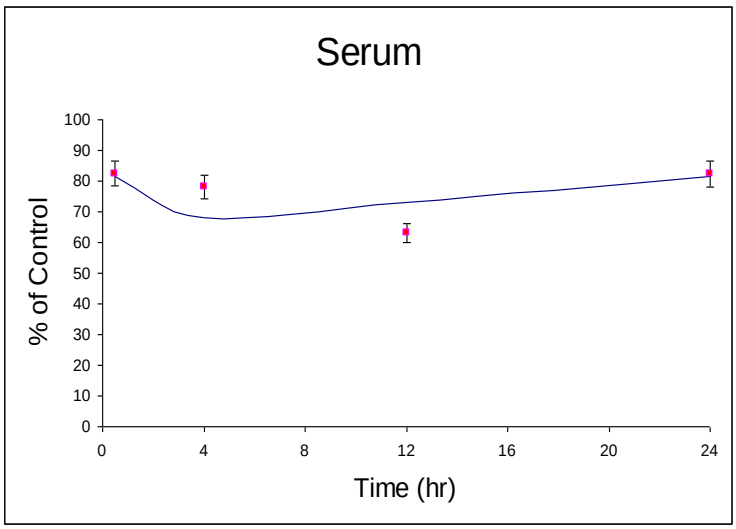

Figure 4.7. Time-course of inhibition of serum carboxylesterase inhibition in adult male rats following exposure to 2.5, 0.5, 0.5mg/kg of chlorpyrifos, methyl parathion and parathion, respectively. Experimental data (symbols), means ± SEM (n = 3) and simulations (lines).

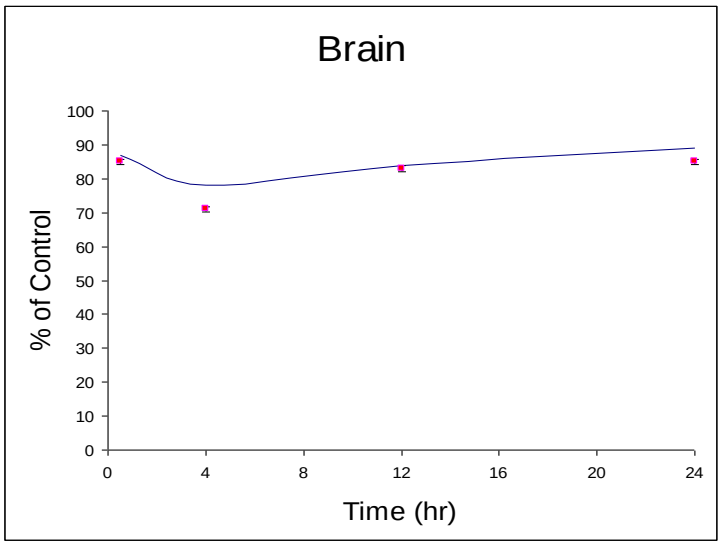

Figure 4.8. Time-course of inhibition of brain cholinesterase activity in adult male rats following exposure to 5, 1, 1mg/kg of chlorpyrifos, methyl parathion and parathion, respectively. Experimental data (symbols), means ± SEM (n = 3) and simulations (lines).

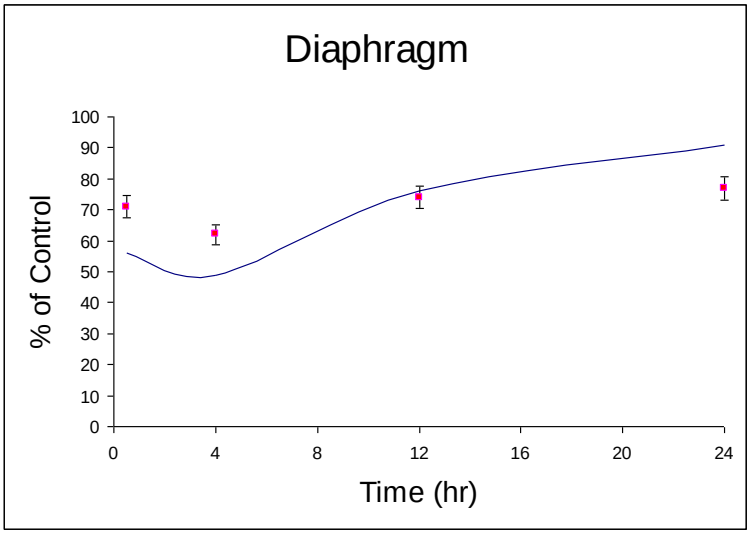

Figure 4.9. Time-course of inhibition of diaphragm cholinesterase activity in adult male rats following exposure to 5, 1, 1mg/kg of chlorpyrifos, methyl parathion and parathion, respectively. Experimental data (symbols), means ± SEM (n = 3) and simulations (lines).

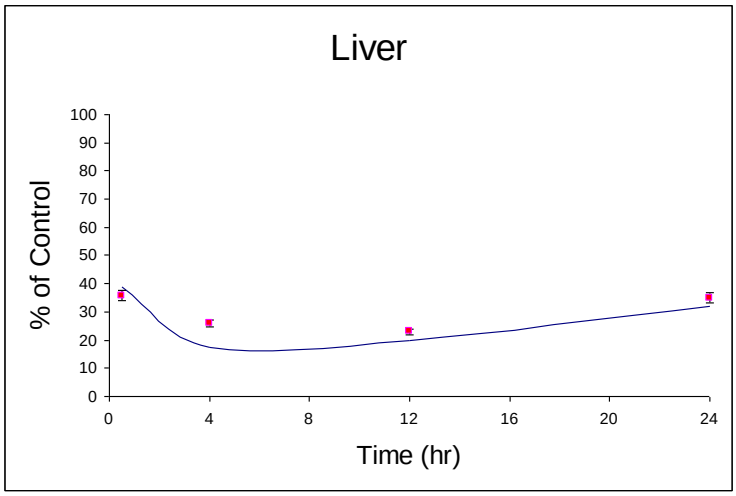

Figure 4.10. Time-course of inhibition of liver carboxylesterase activity in adult male rats following exposure to 5, 1, 1mg/kg of chlorpyrifos, methyl parathion and parathion, respectively. Experimental data (symbols), means ± SEM (n = 3) and simulations (lines).

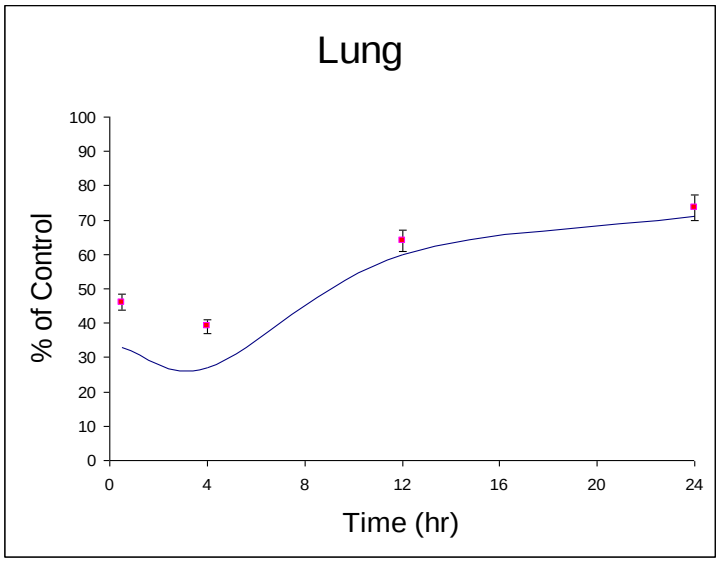

Figure 4.11. Time-course of inhibition of lung cholinesterase activity in adult male rats following exposure to 5, 1, 1mg/kg of chlorpyrifos, methyl parathion and parathion, respectively. Experimental data (symbols), means ± SEM (n = 3) and simulations (lines).

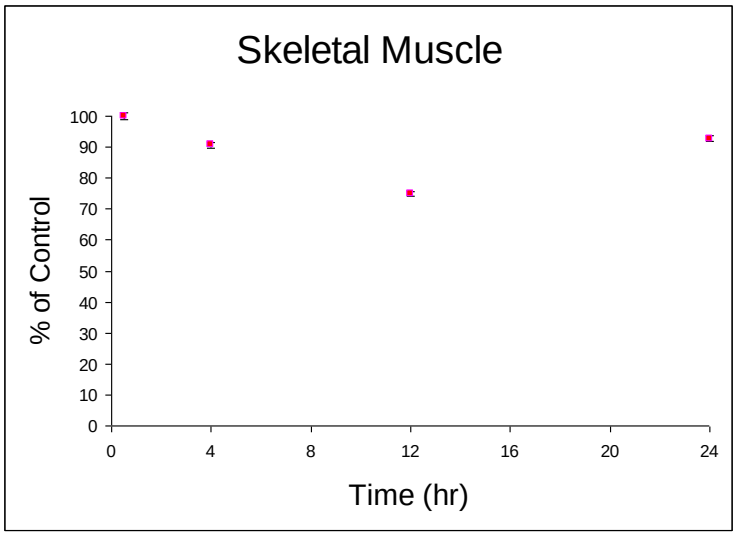

Figure 4.12. Time-course of inhibition of skeletal muscle cholinesterase activity in adult male rats following exposure to 5, 1, 1mg/kg of chlorpyrifos, methyl parathion and parathion, respectively. Experimental data (symbols), means ± SEM (n = 3).

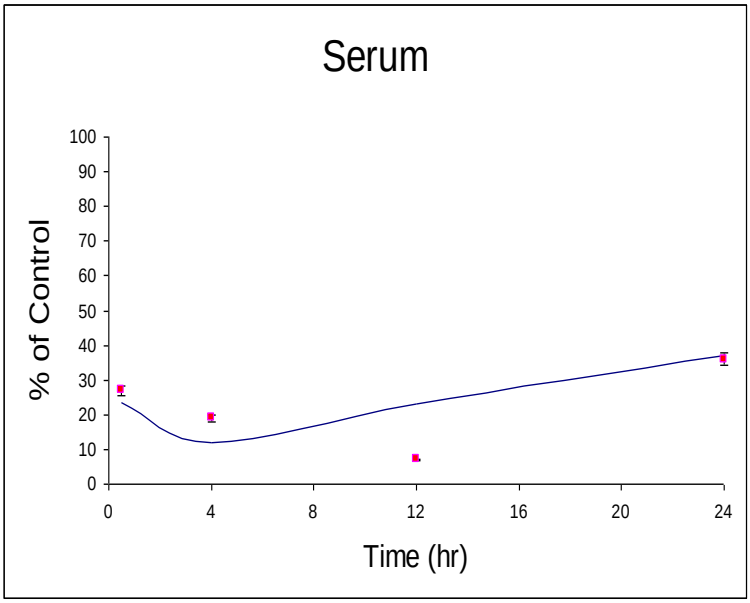

Figure 4.13. Time-course of inhibition of serum carboxylesterase activity in adult male rats following exposure to 5, 1, 1mg/kg of chlorpyrifos, methyl parathion and parathion, respectively. Experimental data (symbols), means ± SEM (n = 3) and simulations (lines).

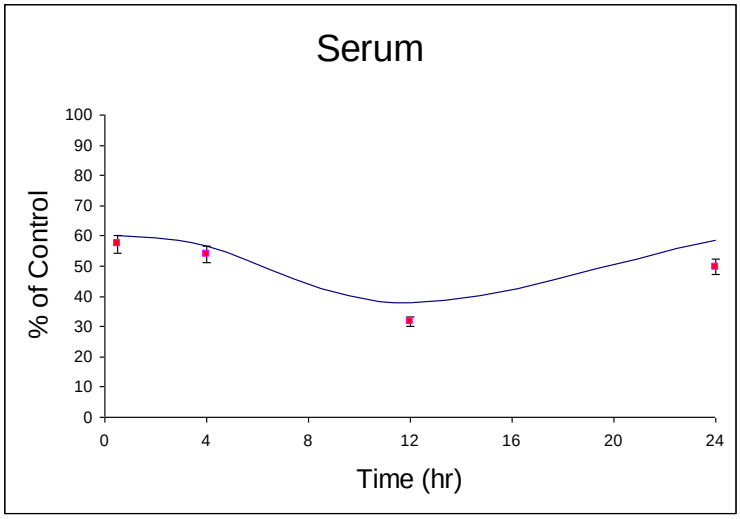

Figure 4.14. Time-course of inhibition of serum cholinesterase activity in adult male rats following exposure to 5, 1, 1mg/kg of chlorpyrifos, methyl parathion and parathion, respectively. Experimental data (symbols), means ± SEM (n = 3) and simulations (lines).

Discussion

The pattern of AChE and CbxE inhibition appears to be largely dominated by CP, which agrees well with the toxicokinetic data presented in Chapter III. It can be inferred that both MP and P are contributing to the rapid inhibition seen at 30min and responsible for the extended inhibition and slow recovery evident from 12hr-24hr time points. The "protective enzymes" within the body are serum ChE and CbxE, and liver CbxE. Inhibition of these protective enzymes leads to a greater amount of the mixture of parent compounds and/or their respective oxons from being able to reach target tissues and inhibit AChE. With the higher dosage group, these protective esterases are significantly inhibited, as shown in Figures 4.10, 4.13, 4.14. Slightly higher dosages, compared to those used in the current study, would be expected to lead to saturation of these protective enzymes and potentially lead to greater inhibition than expected, since more oxon molecules would potentially be available to inhibit target tissue AChE. However, it has been suggested that only a minimal amount of AChE is required to maintain normal physiological function, i.e., homeostasis (Ellin, 1982).

There appear to be some antagonistic effects among the compounds; there were less-than-additive effects present in the diaphragm and lung at the higher dosage exposure. However, since the experimental data for the pattern of brain AChE inhibition was shown to agree well with the model simulations, it can be assumed that

metabolism of the compounds in the liver was occurring at a normal rate. Thus, the interaction may be at the level of distribution, or at the level of the target site itself. The pattern of inhibition in the diaphragm and lung is not similar to that of serum AChE inhibition, which implies that serum AChE is not contributing to this pattern in any significant fashion.

Although the model could not adequately simulate skeletal muscle per se (this tissue was modeled as a lumped-compartment), the experimental inhibition data appear to reflect the smaller amount of blood flow, and less delivery of active metabolites as compared to some of the more well-perfused tissues in the model. The amount of inhibition was small and relatively inconsequential (Figures 4.5, 4.12) at the dosage levels used in the current study. The limited blood flow to skeletal muscle likely explains the shift of maximal AChE inhibition to 12hr, as compared to 4hr for the other tissues.

The determining factor for how an OP insecticide mixture will react within the body varies with tissue and time of sampling. As mentioned above, there appears in some instances to be an interaction, i.e., antagonism, among the compounds in the diaphragm and the lung. This interaction may be occurring at either the level of metabolic activation in the liver, the distribution of the compounds to the tissue(s), interaction with non-target esterases, interaction with the target site, or a combination of the above. However, the results presented here demonstrate that the ability of the active metabolite of each compound to inhibit serum ChE and/or serum and liver CbxE plays an important role in the degree/pattern of ChE inhibition following

exposure to an OP mixture. The model and experimental results highlight the protective role of CbxE (inhibition was 70-90 % in the liver and serum, while the inhibition of brain AChE activity was 15-30 %). The inhibition of liver CbxE by the individual compounds is reflective of the *in vitro* potency of the active metabolites of the three OP insecticides. CP-oxon is a much better inhibitor of CbxE than either MP-oxon or P-oxon, and the results of the mixture followed a pattern of inhibition similar to that of CP alone. Regarding serum CbxE, however, the inhibition by the individual compounds was not reflective of the *in vitro* potency of the active metabolites of the three OP insecticides. Experimentally, exposure to the mixture did not follow the pattern of inhibition predicted by the model; instead CbxE inhibition appeared to be dominated by P-oxon and/or an interaction with CP-oxon that resulted in delayed maximal inhibition, as compared to the effects predicted by the compounds alone. Ma and Chambers (1994) have reported that P is activated more efficiently than is CP, while CP is detoxified more efficiently than P. CP-oxon is also a much more potent inhibitor of CbxE than is P-oxon (Chambers et al., 1990). Theoretically, this higher affinity of CP-oxon for CbxE would lead to greater non-specific binding by CP-oxon compared to P-oxon, thus decreasing the amount of CP-oxon that would be available to reach the target enzyme. Additionally, the higher lipophilicity of CP compared to P could lead to CP being sequestered by some tissues (Chambers and Carr, 1993). Sequestrations would decrease the bioavailability of CP, thereby reducing the immediate impact of the compound on target tissues. This reduction may play a role in the lower LD50 of P as compared to CP.

There is comparatively very little detoxication potential in the brain; the potential variable rates of detoxication among the compounds that are very likely in blood, are not likely to confound experimental data/model simulation interpretation in other tissues. Experimental data/ model simulation agreement in serum are much less consistent presumably because of the presence of additional detoxication mechanisms, such as CbxE and BuCh. Differences in the pattern of inhibition in the mixture as compared to that of the individual compounds, may be partially the result of competition for P450-meditated bioactivation. The patterns may also be due to different affinities of the oxons for AChE and CbxE. The model fit for serum CbxE to the experimental data could not be improved by adjusting the parameters associated with CbxE reactivation, aging, or degradation. Optimization of the rate constants (Ki) for CP-oxon and P-oxon resulted in a somewhat better fit, but failed to fully reconcile the differences between the predicted percent peak inhibition (4hr) and the experimentally determined percent peak inhibition (12hr). Model parameters, metabolic constants Vmax and Km, and binding/dissociation constants of free/bound AChE for the mixture were reevaluated and the fit was only minimally improved. The serum concentrations were only secondarily influenced by Vmax and Km. With values giving the smallest bile residuals, a significant change in the fit for serum concentrations could only be obtained by changes to other parameters, notably protein binding ratios. Aside from the discrepancies observed with the serum, very little model "fitting" (i.e., finding a mathematical equation and a set of parameter values

such that the values predicted by the model are close to the observed experimental values) was required.

In toxicokinetic interactions, the presence of a second or third chemical alters the kinetics such that a unit of administered dose no longer produces a unit of dose at the target tissue. In toxicodynamic interactions, the presence of other compounds alters the dynamics such that a unit tissue dose no longer produces a unit of response. B-EST (i.e., AChE, BuChE, and CbxE) inhibition is an integrated function of target-tissue dosimetry, esterase affinity for the oxon, and the number of available esterase binding sites in each tissue compartment. In this regard, improvements in the predictive capability of the current model could be obtained with data that better characterize the time-course of specific esterase activities in blood over a broad range of compound exposure.

A particular concern in mammals is exposure to lipophilic compounds, such as CP. Following exposure of P, for example, in rats, if mortality does not occur within 24-48hr, the rat will generally survive. However, it has been demonstrated that high-dosage acute exposures to CP can produce mortality 4 days post-exposure (Chambers and Carr 1993). With chronic exposures, the body compensates for chronic inhibition of AChE by reduction of ACh receptor number, which reduces the impact of high levels of ACh in the synapse. Generally, down-regulation of receptor numbers does not occur following an acute exposure. Description of such dynamic processes would be valuable to include in future PBTK/TD models to expand their

use for chronic exposure conditions. However, problems with properly describing such dynamic processes exist, as will be discussed in Chapter V.

CHAPTER V

GENERAL CONCLUSIONS

The PBTK/TD model in the present study was developed, using a framework from published individual PBTK/TD models, as a quantitative tool for assessing OP insecticide dosimetry and cholinesterase inhibition in rats. The PBTK/TD modeling approaches used in the current study are ideally suited for assessing dosimetry and biological responses following exposures to OP insecticide mixtures, and for development of "family models" that can be used for related compounds and/or metabolites. Overall, the PBTK/TD model successfully predicts dosimetry and cholinesterase inhibition in the selected tissues. The present study demonstrates the utility of using previously developed individual models and *in vitro/in vivo* data from the open literature to construct a reliable mixture model. Cholinesterase inhibition in selected tissues peaked at 4hr, ranged from 11- 37% for the lower dosage group, and 29-93% for the higher dosage group, and was generally additive; the overall mixture response appeared driven by CP. Model predictions diverged from the experimental data for serum, but for other tissues there was good agreement. The model is used to describe a complex set of multivariate data; hence it is not surprising that some over- and underestimation occurred. The model fit for the experimental data is quite good, considering the diverse sources of data used in the creation of the model; the shapes

of the predicted curves are generally accurate. The assumption of response additivity holds for low dosage exposures, which are likely to be encountered in environmental/occupational settings. An assumption of additivity at higher dosages than those used in the current study may not be appropriate in all tissues, particularly those tissues involved in maintaining respiratory function. This is likely only a concern in those instances of occupational accidents or other such non-typical/extreme exposure scenarios. Model development is an iterative process; the model is improved/revised as more data become available. Therefore, the model is not "complete" per se; it can be improved upon as more data are acquired. The model is sufficiently flexible that a similar approach could be readily applied to other multiple combinations of OP insecticides, provided necessary data are available in the literature and/or through focused experimental studies, to address the impact of variable OP exposure scenarios and the impact of sensitive sub-populations for the risk assessment of OP insecticides.

OP insecticides commonly co-occur in the environment, which can potentially lead to antagonistic, additive, or synergistic neurotoxicity. When considering combined action of chemicals at low dosages, one is left to contemplate if real "interactions" are likely to occur. There is little uncertainty that the combined toxic action of compounds is a dose-dependent phenomenon. At low doses, physicochemical interactions are of relatively little importance and toxicokinetic and toxicodynamic interactions may be atypical. At very low doses, even receptor occupancy and competition for receptors may be of little importance. Therefore,

interactions such as potentiation or antagonism may not be very relevant in the low-dose region. This study indicates that the joint toxicity of anticholinesterase mixtures can be accurately predicted from the knowledge of individual chemicals within a mixture; OP insecticides are non-interactive in terms of AChE inhibition, and it is possible to estimate the cumulative neurotoxicity of mixtures by response addition, at least at low dosage exposure levels.

The primary function of PBTK/TD models is prediction of concentrations/effects of various environmental toxicants, and/or their metabolites in different organ systems. However, most such models view physiological systems as static, unable to respond to physiological changes/insults (Clewell et al., 2003; Krishnan et al., 2001; Welling, 1996). This assumption of "static" physiological systems is not realistic for chemicals that are stressors, especially neurotoxic chemicals such as OP insecticides. Some recent attempts have been made to include physiological changes in PBTK/TD models, these efforts however do not integrate the changes directly into the modeling process; they provide fixed time-dependent functions which have extremely limited applicability to very narrow dosing regimens (Lu et al., 2006). By using integral or delay terms in modeling approaches, it may be possible to model/account for more complex reactant physiological behavior; i.e., changes in cardiac output. Such approaches, however, are beyond the scope of the current study. While the current model has adjustable parameters to allow fitting to experimental data, the degree of adjustment is often limited by physical and biological considerations. The difficulty produced by this circumstance is, in fact, one

of the advantages of modeling; a purely empirical fit would not illuminate internal inconsistencies in the experimental data. In many instances, the modeler is restrained by his scientific principles from assigning values to critical coefficients, and this restraint may ultimately lead to a better understanding and description of the mixture metabolic processes.

Although the current PBTK/TD model successfully describes the toxicokinetics and toxicodynamics of the compounds over the dosages used, it is important to recognize that even the low dosages evaluated in the current study are still significantly greater than typical aggregate (total dietary and residential) human exposures. For example, in both adults and children, potential nonoccupational aggregate exposures to CP are estimated to range from 0.0002 mg/kg-day (adults) to 0.0005 mg/kg-day (infants and small children) (Cochran, 2002), which is many-fold below the lowest dosage (0.5mg/kg) used in the present study. Based upon the observed dose response, where the parent compounds and oxons were nondetectable and ChE activity was minimally depressed at the lower dosage, it is hypothesized that a significant first-pass metabolism, would be observed at environmentally relevant doses. In this regard, a number of recent studies have demonstrated that intestinal epithelial cells have CYP metabolic capacity and are capable of significantly altering oral bioavailability of drugs and chemicals in animals and humans (Obach et al., 2001; Paine et al., 1999; Zhang, et al., 1999). A number of CYP isoforms residing within the intestine have been shown to metabolize many OP insecticides, including chlorpyrifos and parathion (Butler and Murphy, 1997; Fabrizi et al., 1999; Sams et

al., 2000). In addition, P-glycoproteins (multidrug resistance proteins) are located in the apical borders of intestinal cells, and are known to be up-regulated and bound by CP-oxon (Lanning et al., 1996). Thus, an unknown amount of first-pass detoxication and activation could occur in the intestines, and oxon that is generated in enterocytes would be subject to removal by P-glycoproteins. Since the current model does not incorporate intestinal metabolism or P-glycoprotein removal of oxon, it is probable that the model overestimates low-dose oral bioavailability, thereby potentially overestimating dosimetry and dynamic response. This presumed overestimation in fact was evident in some tissues in the present study at both the toxicokinetic and toxicodynamic levels.

The current PBTK/TD model can function as a constructive tool for helping design and focus future experimental research. The capacity of the model to accurately predict dosimetry and response is limited by the adequacy of the model parameters and limitations of experimental data. As with all models, developing and validating a PBTK/TD model is an iterative process and highlights existing confines of understanding of critical biological processes that help identify important data gaps. In the process of refining the model to fit the data, several key model parameters that impact the model fit to data sets were noted. The parameter with the strongest consequence to data fit was plasma protein binding to the compounds and, to a slightly lesser extent, the oxons. Improved parameter estimates for the inhibition of oxons with B-EST, and in particular CbxE tissue inhibition kinetic parameters would be helpful in the future. Although the formation of oxons can be inferred from

the inhibition of ChE activities, the amount formed as well as the toxicokinetics had limited detection at the dosage levels used in the present study. This is primarily a reflection of the half-life of the compounds; for example, a 60-fold difference exists between the half-lives of paraoxon and parathion in rats (Eigenberg et al., 1983). In addition, the oxons are sufficiently reactive that they do not remain stable for any appreciable length of time. Such factors as the length of time esterases remain inhibited, the potency of the oxons as anticholinesterases, and the competition of the compounds for enzymes of metabolism are probably the main contributing factors to non-additive levels of ChE inhibition. Predicting effects of mixtures *in vivo* thus requires knowledge of both activation and detoxication potentials, potencies of the oxons as ChE and CbxE inhibitors, ability of the oxons to serve as substrates for A-esterases, and time/sequence of exposure to the compounds.

Clearly, it is impossible to conduct all of the necessary laboratory experiments on toxicant effects, dosages, time frames, and routes of administration, not only for OP insecticides, but for all environmentally-relevant toxicants. PBTK/TD modeling, when based on logical approaches and concrete data, can help provide useful predictions on dosimetry and effects. Occasionally, models must be developed with an absence of data sets; when this occurs certain assumptions must be made from similar data or certain simplifications must be used in the model. The endpoint of easily measured ChE inhibition in the present study does make the modeling of OP-molecular interactions easier compared to the modeling of many toxicants that do not covalently bind to targets, or that exert as-yet-undefined molecular actions. With any

modeling exercise, the accuracy of the model is limited by the quality of the data. When model predictions and data are incompatible, the data can be wrong, the model can be wrong, or both can be wrong to varying degrees. It is imperative to bear in mind that PBTK/TD models do not replace well planned experimental studies. Rather, they are adjuncts which serve to capitalize on the utility of experimental results, assist in more precise planning of other experiments and help design cost-effective studies. As such, they are tools to aid in identifying and hopefully reduce some of the many uncertainties inherently associated with the risk assessment process. Ultimately, well-organized assessments based on experimentation, PBTK/TD modeling, and realistic monitoring and sound scientific judgment will result in rational and successful risk management decisions. PBTK/TD models offer promise in understanding and possibly screening for interactive effects of chemical mixtures; however, a great deal of validation is necessary before they can be applied to chemical mixture assessments. Instead of "validation", some in the PBTK/TD modeling community have recently suggested validation be described instead as "juxtaposition" of model predictions with the experimental data. This purportedly treats the experimental data and the model predictions on a more even level; the debate is primarily one of semantics however. At present, is it questionable if a computer model can fully represent the complexity of the physiology and interactions of higher-order chemical mixtures in living biologic systems; the future of *in silico* modeling appears bright however, with momentous advances made with each passing year.

REFERENCES

Abbas, R., Hayton, W. (1997) A physiologically based pharmacokinetic and pharmacodynamic model for paraoxon in rainbow trout. Toxicol. Appl. Pharmacol. 145, 192-201.

Albers, J. (1999). Analysis of chlorpyrifos exposure and human health: expert panel report. Journal of Toxicology and Environmental Health, Part B, 2, 301-324.

Aldridge, W. and Reiner, E. (1972) Enzyme inhibitors as substrates. In A. Neuberger and E. Tatum (Eds.), North-Holland Research Monographs, Frontiers of Biology, Vol.26. North-Holland, London. p.236.

Amitai, G., Moorad, D., Adani, R. (1998) Inhibition of acetylcholinesterase and butyrylcholinesterase by chlorpyrifos-oxon. Biochem. Pharmacol. 56, 293-299.

Andersen, M., Gargas, M., Clewell, H. (1987) Quantitative evaluation of the metabolic interactions between trichloroethylene and 1, 1 dichloroethylene in vivo using gas uptake methods. Toxicol. Appl. Pharm. 89, 149-157.

Andersen, M., Clewell, H., Gargas, M., Smith, F. (1987) Physiologically based pharmacokinetics and the risk assessment process for methylene chloride. Toxicol. Appl. Pharmacol. 87, 185-205.

Andersen, M. (1995) Development of physiologically based pharmacokinetic and physiologically based pharmacodynamic models for applications in toxicology and risk assessment. Toxicol Lett. 79, 35-44.

Atterberry, T. Burnett, W. Chambers, J. (1997) Age-related differences in parathion and chlorpyrifos toxicity in male rats, target and nontarget esterase sensitivity and cytochrmone P450-mediated metabolism. Toxicol. Appl. Pharmacol. 147, 411-418.

Bakke, J., Feil, V. Price, C (1976) Rat urinary metabolites from TCP. J. Environ. Sci Health B. 3, 225-230.

Benke, G., Murphy, S. (1974) Anticholinesterase action of methylparathion, parathion and azinphosmethyl in mice and fish: onset and recovery of inhibition. Bull Environ Contam Toxicol 12, 117-122.

Berends, F., Posthumus, C., Sluys, I. (1959) The chemical basis of the "aging process" of DFP-inhibited pseudocholinesterase. Biochem Biophys Acta 34, 576-578.

Berends, F. (1964) Stereospecificity in the reactivation and ageing of butyrylcholinesterase inhibited by organophosphates with an asymmetrical P-atom. Biochem Biophys. Acata. 81, 190-193.

Bischoff, K., Dedrick, R. (1968) Thiopental pharmacokinetics. J. Pharm Sci 57: 1346-1351.

Brown, R., Delp, M., Lindstedt, L. (1997) Physiological parameter values for physiologically based pharmacokintetic models. Toxicol. Ind. Health.

Brzak, K., Harms, D., Bartels, M., Nolan, R. (1998) Determination of chlorpyrifos, chlorpyrifos-oxon, and 3,5,6-trichloro-2-pyridinol in rat and human blood. J. Analy. Toxicol. 129, 56-60.

Butler, A., Murray, M (1997) Biotransformation of parathion in human liver: Participation of CYP3A4 and its inactivation during microsomal parathion oxidation. J. Pharmacol. Exp. Ther. 280, 966-973.

Carr, R. Chambers, J. (1992) Inhibition and aging of acetylcholinesterase in central and peripheral tissues following a single exposure of chlorpyrifos. Toxicologist. 12, 42.

Carr, R., and Chambers, J. (1996) Kinetic analysis of the *in vitro* inhibition, aging, and reactivation of brain acetylcholinesterase from rat and channel catfish by paraoxon and chlorpyrifos oxon. Toxicol. Appl. Pharamcol. 139, 363-373.

Carr, R., Chambers, W., Chambers, J., Oppenheimer, S., Richardson, J. (2003) Modeling the interactions of mixtures of organophosphorus insecticides with cholinesterase. Electr. J. Diff. Equat. 10, 89-99.

Castor, W., Poncelet, J., Simon, A. (1956) Tissue weights of the rat. Normal values determined by dissection and chemical methods. Proc. Soc. Exp. Biol. Med. 91, 122-126.

Chambers, J., Chambers, H. (1989) Oxidative desulfuration of chlorpyrifos, chlorpyrifos-methyl, and leptophos by rat brain and liver. J. Biochem Toxicol. 4, 201-203.

Chambers, H., Chambers, J. (1989) An investigation of acetylcholinesterase inhibition and aging and choline acetyltransferase activity following a high level acute exposure to paraoxon. Pestic Biochem Physiol 33, 125-131.

Chambers, J., Forsyth, C., Chambers, H. (1989) Bioactivation and detoxication of organophosphorus insecticides in rat brain. In Intermediary Xenobiotic Metabolism; Methodology, Mechanisms and Significance (J. Caldwell, D. Hutson, and G. Paulson, Eds.), pp.99-115. Taylor and Francis, Basingstoke, England.

Chambers, J. and Chambers, H., (1989) Oxidative desulfuration of chlorpyrifos, chlorpyrifos-methyl, and leptophos by rat brain and liver. J. Biochem. Toxicol. 4, 201-203.

Chambers, H., Brown, B., Chambers, J. (1990) Noncatalytic detoxication of six organophosphorus compounds by rat liver homogenates. Pestic Biochem Physiol 36, 308-315.

Chambers, J., Carr, R. (1993) Inhibition patterns of brain acetylcholinesterase and hepatic and plasma aliesterases following exposures to three phosphorothionate insecticides and their oxons in rats. Fundam Appl Toxicol 21, 111-119.

Chanda, S., Mortensen, S., Moser, V., Padilla, S. (1997) Tissue-specific effects of chlorpyrifos on carboxylesterase and cholinesterase activity in adult rats: An in vitro and in vivo comparison. Fund Appl. Toxicol. 38, 148-157.

Chiu, Y., Main, A., Dauterman, W. (1969) Affinity and phosporylation constants of a series of O,O-dialkyl malaoxon and paraoxon with acetylcholinesterease. Biochem. Pharmacol. 18. 2171-2177.

Clement, J., (1984) Role of aliesterase in organophosphate poisoning. Fundam Appl. Toxicol. 4, 96-105.

Clothier, B. Johnson, M, Reiner E (1981) Interaction of some trialkyl phosphorothiolates with acetylcholinesterase: Characterization of inhibition, aging, and reactivation. Biochem Biophys. Acta. 660, 306-316.

Cochran, R. (2002) Appraisal of risks from nonoccupational exposure to chlorpyrifos. Regul. Toxicol. Pharmacol. 35(1): 105-21.

Cohen, S., Williams, R., Killinger, J. (1985) Comparative sensitivity of bovine and rodent acetylcholinesterase to *in vitro* inhibition by organophosphate insecticides. Toxicol. Appl. Pharmacol. 81: 452-459.

DuBois, K. (1969) Combined effects of pesticides. Can. Med. Assoc. J. 100, 173-179.

Ecobichon, D. and Comeau, A. (1973) Pseudocholinesterases of mammalian plasma: Physiochemical properties and organophosphate inhibition in eleven species. Toxicol. Appl. Pharmacol. 24, 92-100.

Eigenberg, D., Pazdernik, T., Doull, J. (1983) Hemoperfusion and pharmacokinetic studies with parathion and paraoxon in the rat and dog. Drug Met Dispo 11: 366-370.

Ellin, R. (1982) Anomalies in theories and therapy of intoxication by potent organophosphorus anticholinesterase compounds. Gen Pharmacol 13, 455-466.

Ellman, G., Courtney, K., Andres, V., Featherstone, R. (1961) A new and rapid colorimetric determination of acetylcholinesterase activity. Biochem Pharamcol 7, 88-95.

El-Masri, H., Mumtaz, M., Yushak, M. (2004) Application of physiologically-based pharmacokinetic modeling to investigate the toxicological interaction between chlorpyrifos and parathion in the rat. Environ. Tox. Pharm. 16, 57-71.

Environmental Protection Agency (EPA), Recognition and management of pesticide poisonings. EPA 735-R-98-0.03, 1999.

Enwick, A. (1994) Toxicokinetics-pharmacokinetics in toxicology. In Principles and Methods of Toxicology, 3rd ed. (A.W. Hayes, Ed.), pp 101-147. Raven Press, New York.

Fabrizi, L., Gemma, S., Testai, E., Vittozzi, L. (1999) Identification of the cytochrome P450 isoenzymes involved in the metabolism of diazinon in the rat liver. J. Biochem. Mol. Toxicol. 13, 53-61.

Gallo, M. and Lawryk, N. (1991) Organic phosphorus pesticides. In handbook of Pesticide Toxicology (W. J. Hayes, Jr. and E. R. Laws, Jr., Eds.) Academic Press, New York.

Gaines, T. (1969) Acute toxicity of pesticides. Toxicol Appl. Pharmacol. 14, 515-534.

Garcia-Repetto, R., Martinez, D. , Repetto, M (1995) Coefficient of distribution of some organophosphorus pesticides in rat tissue. Vet Human Toxicol. 37, 226-229.

Garcia-Repetto, R., Martinez, D. , Repetto, M. (1997) Biodisposition study of the organophosphorus pesticide, methyl parathion. Bull. Environ. Contam. Toxicol. 59 901-908.

Gearhart, J., Jepson, G., Clewell, H. (1990) Physiologically based pharmacokinetic and pharmacodynamic model for the inhibition of acetylcholinesterase by diisopropylfluruorophosphate. Toxicol. Appl. Pharmacol. 106, 295-310.

Gearhart, J., Jepson, G., Clewell, H., Andersen, M., Conolly, R. (1994) Physiologically based pharmacokinetic model for the inhibition of acetylcholinesterease by organophosphate esters. Environ Health Perspect. 102:11 51-60.

Gibson, J., Chen, W., Peterson, R. (1999) How to determine if an additional 10x safety factor is needed for chemicals: A case study with chlorpyrifos. Toxicol Sci. 48, 117-122.

Gordon, C., Herr, D., Gennings, C., Graff, J., McMurray, M., Hamm, A., Mack, C. (2006) Thermoregulatory response to an organophosphate and carbamate insecticide mixture: Testing the assumption of dose-additivity. Toxicology, 217, 1-13.

Haddad, S., Pelkis, M., Krishnan, K., (1996) A methodology for solving physiologically based pharmacokinetic models without the use of simulation software. Toxicol. Lett. 85. 113-126.

Haddad, S., Tardif, R., Krishnan, K. (1999) Physiological modeling of the toxicokinetic interactions in a quaternary mixture of aromatic hydrocarbons. Toxicol Appl. Pharmacol. 161, 249-257.

Hahn, T., Ruhnke, M., Luppa, H. (1991) Inhibition of acetylcholinesterase and butyrlcholinesterase by the organophosphorus insecticide methylparathion in the central nervous system of the Golden Hamster (Mesocricetus auratus) Acta Histochem 91, 13-19.

Harris, L, Fleisher, J Clark, J. (1966) Dealkylation and loss of capacity for reactivation of cholinesterases inhibited by sarin. Science 154, 404-406.

Hattis, D., White, P., Marmorstein, L. (1990) Uncertainties in pharmacokinetic modeling for perchloroethylene. Risk Analysis. 10, 449-458.

Hobbiger, F Sadler, P (1959) Protection against lethal organophosphate poisoning by quaternary pyridine aldoximes. Brit. J. Pharmacol. 14, 192-201.

International Life Sciences Institute-Risk Sciences Institute (ILSI-RSI). Physiological Parameter Values for PBPK Models. Report prepared under a cooperative agreement with OHEA. Environmental Protection Agency, Washington, DC, 1994.

Ioerger, B., Smith, J. (1993) Multi-residue method for the extraction and detection of organophosphate pesticides and their primary and secondary metabolites from beef tissue using HPLC. J. Agric. Food Chem. 41, 303-307.

Kacham, R., Karanth, S., Baireddy, P., Liu, J., Pope, C. (2006) Interactive toxicity of chlorpyrifos and parathion in neonatal rats: role of esterases in exposure sequence-dependent toxicity. Toxicol. Appl. Pharmacol. 210, 142-149.

Karczmar, A. G. (1984) Acute and long lasting actions of organophosphorus agents. Fundam. Appl. Toxicol. 4, 1-17.

Karanth, S., Olivier, K., Liu, J., Pope, C. (2001) *In vivo* interaction between chlorpyrifos and parathion in adult rats: sequence of administration can markedly influence toxic outcome. Toxicol. Appl. Pharmacol. 177, 247-255.

Karanth, S., Liu, J., Olivier, K., Pope, C. (2004) Interactive toxicity of the organophosphorus insecticides chlorpyrifos and methyl parathion in adult rats. Toxicol. Appl. Pharmacol. 196, 183-190.

Kararli, T. (1995) Comparison of the gastrointestinal anatomy, physiology, and biochemistry of humans and commonly used laboratory animals. Biopharm. Drug Dispos. 16, 351-380.

Keplinger, M., and Deichmann, W. (1967) Acute toxicity of combinations of pesticides. Toxicol. Appl. Pharmacol. 10, 586-595.

Kidd, H. and James, D. R., Eds. The Agrochemicals Handbook, Third Edition. Royal Society of Chemistry Information Services, Cambridge, UK, 1991. 5-14.

Knaak, J. Raabe, O., Blancato, J. Use of a multiple pathway and multiroute PBPK model for predicting organophosphorous pesticide toxicity. In J. N. Blancato, R. N. Brown, C.C. Dary, and M.A. Saleh (Eds.), Biomarkers for Agrochemicals and Toxic Substances, ACS Symposium Series, 643. American Chemical Society, Washington, DC, 1996.

Kootsey, J., Kohn, M., Feezor., D. (1986) SCoP: an interactive simulation control program for micro and minicomputers. Bull. Math Biol. 48, 427-441.

Konemann, W, and Pieters, M. (1996) Confusion of concepts in mixture toxicology. Food Chem.Toxicol. 34, 1025-1031.

Kramer, R., Ho, I. (2002) Pharmacokinetics and pharmacodynamics of methyl parathion. Chinese Medical Journal (Taipei) 65, 187-199.

Langenburg, J. De Jong, L. Otto P Benschop H. (1988) Spontaneous and oxime-induced reactivation of acetylcholinesterae inhibited by phosphoramidetases. Arch. Toxicol. 62, 305-310.

Lanning, C., Fine, R., Sachs, C (1996) Chlorpyrifos oxon interacts with the mammalian multidrug-resistance protein, P-glycoprotein. J. Toxicol. Environ. Health 47, 395-407.

Lowry, O., Rosebrough, N., Rarr, A, Randall, R. (1951) Protein determination with the Folin phenol reagent. J. Biol. Chem. 193, 266-275.

Lu, F. (1995) A review of the acceptable daily intakes of pesticides assessed by the World Health Organization. Reg. Toxicol. Pharmacol. 21, 351-364.

Ma, T. and Chambers, J. (1994). Kinetic parameters of desulfuration and dearylation of parathion and chlorpyrifos by rat liver microsomes. Food Chem. Toxicol. 32, 763-767.

Ma, T. and Chambers, J. (1995) A kinetic analysis of hepatic microsomal activation of parathion and chlorpyrifos in control and phenobarbital-treated rats. J. Biochem. 10, 63-68.

Maxwell, D., Lenz, D., Groff, W. (1987) The effect of blood flow and detoxication on *in vivo* cholinesterase inhibition by soman in rats. Toxicol. Appl Pharmacol. 88, 66-76.

Maxwell, D., Vlahacos, C. Lenz, D. (1988) A pharmacodynamic model for soman in rats. Toxicol. Lett. 43, 175-188.

Maxwell, D. (1992) The specificity of carboxylesterase protection against the toxicity of organophosphorus compounds. Toxicol. Appl. Pharmacol. 114, 306-312.

McCollister, S., Kociba, R., Humiston, C. (1974) Studies on the acute and long-term oral toxicity of chlorpyrifos. Food Cosmetic Toxicol. 12, 45-61.

McDougal, J., Jepson, G., Clewell, H. (1986) A physiological pharmacokinetic model for dermal absorption of vapors in the rat. Toxicol. Appl. Pharmacol.

Meister, R.T., Ed. Farm Chemicals Handbook '99, Meister Publishing Company: Willoughby, OH, 1999.

Menzel, D., Wolpert, R., Boger, J. (1987) Resources available for simulation in toxicology: specialized computers, generalized software and communication networks. Drinking Water Health 8, 229-254.

Michalek, H., Meneguz, A., Bisso, G. (1982) Mechanisms of recovery of brain acetylcholinesterase in rats during chronic intoxication by isoflurophate. Arch Toxicol 5: 116-119.

Miyamoto J. (1963) Studies on the mode of action of organophosphorus compounds. Part I. Metabolic fate of P^{32} labeled sumithion and methylparathion in guinea pig and white rat. Agri. Bio Chem. 27, 381-389.

Mortensen, S., Brimijoin, S. Hooper, M. (1998) Comparison of the *in vitro* sensitivity of rat acetylcholinesterase to chlorpyrifos oxon: What do IC50 values represent? Toxicol. Appl. Pharmacol. 148, 46-49.

Moser, V. (1995) Comparisons of the acute effects of cholinesterase inhibitors using a neurobehavioral screening battery in rats. Neurotoxicol Teratol. 17, 617-625.

Murphy, S. (1986) Toxic effects of pesticides. In Casarett and Doull's Toxicology; The Basic Science of Poisons, 5th edition. pp 519-581. McGrawHill, New York.

Neal, R. (1980) Microsomal metabolism of thiono-sulfur compounds, mechanisms, and toxicological significance. In Reviews in Biochemical Toxicology; Vol.2, pp. 131-172. Elsevier-North Holland, New York.

Nolan, R., Rick, D., Freshour, N. (1984) Chlorpyrifos: pharmacokinetics in human volunteers. Toxicol. Appl. Pharmacol. 73, 8-15.

Nostrandt, A. Padilla, S, Moser, V. (1997) The relationship of oral chlorpyifos: effects on behavior, cholinesterase inhibition, and muscarinic receptor density in rat. Pharmacol . Biochem. Behav. 58, 15-23.

Obach, R., Zhang, Q. Dunbar, D., Kaminsky, L., (2001). Metabolic characterization of the major human small intestine cytochrome P450s. Drug Metab. Dispos. 29, 347-352.

ORNL (2000). Appendix G: Inhibition of cholinesterases and an evaluation of the methods used to measure cholinesterase activity. Oak Ridge National Laboratory. J. Toxicol. Environ. Health 59, 519-526.

Paine, M., Schmiedlin, P., Watkins, P. (1999) Cytochrome P450 1A1 expression in human small bowel: Interindividual variation and inhibition by ketoconazole. Drug Metab. Dispo. 27, 360-364.

Poet, T., Kousba, A., Dennison, S., Timchalk, C. (2004) Physiologically based pharmacokinetic/pharmacodynamic model for the organophosphorus pesticide diazinon. Neurotox. 25, 1013-1030

Pond, A., Chambers, H., Chambers, J. (1995) Organophosphate detoxification potential of various rat tissues via A-esterase and aliesterase activity. Toxicol. Lett. 78, 245-252.

Poulin, P. and Krishnan, K. (1995) An algorithm for predicting tissue:blood partition coefficients of organic chemicals from n-octonol:water partition coefficient data. J. Toxicol. Environ. Health 46, 117-129.

Ramsey, J., Anderson, M. (1984) A physiologically based description of the inhalation pharmacokinetics of styrene in rats and humans. Toxicol. Appl. Pharmacol 73, 159-175.

Rane, A., Wilkinson, G., Shand, D. (1977). Prediction of hepatic extraction ratio from *in vitro* measurement of intrinsic clearance. J. Phamacol. Exp. Ther. 200, 420-424.

Richardson, J., Chambers, H., Chambers, J. (2001) Analysis of the additivity of *in vitro* inhibition of cholinesterase by mixtures of chlorpyrifos-oxon and azinphos-methyl-oxon. Toxicol Applied Pharm. 172, 128-139.

Rosenstock, L., Keifer, M., Daniell, W. (1991) Chronic central nervous system effects of acute organophosphate pesticide intoxication. Lancet. 338, 223-7.

Sams, C., Mason, H., Rawbone, R. (2000) Evidence for the activation of organophosphate pesticides by cytochrome P450 3A4 and 2D6 in human liver microsomes. Toxicol. Lett. 116, 217-221.

Satoh, T. (1987) Role of carboxylesterases in xenobiotic metabolism. In Reviews in Biochemical Toxicology (E. Hodgsen, J. Bend, and R. Philpot, Eds.) Vol. 8, pp. 155-181. Elsevier, New York.

Savage, E., Keefe, T., Mounce, L., (1988) Chronic neurological sequelae of acute organophosphate pesticide poisoning. Arch Environ Health 42, 38-45.

Schalm, O. Ed (1961) Veterinary hematology. Lea and Febiger, Philadelphia, PA.

Silver, A. (1974) The biology of Cholinesterase. North-Holland Publishing Company, Amsterdam, Netherlands.

Simcox, N., Fenske, R., Wolz, S., Lee, I., Kalman, D. (1995) Pesticides in household dust and soil: exposure pathways for children of agricultural families. Environ. Health. Perspect. 103 (12), 1126-1134.

Singh, A. (1986). Kinetic analysis of acetylcholinesterase inhibition by combinations of acephate and methamidophos. Toxicology 42, 143-156.

Solana, R., Gennings, C., Carter, W., Anderson, D., Lennox, W., Carchman, R., Harris, L. (1990). Evaluation of the efficacy of two carbamates, physostigmine and pyridostigmine, when used in conjunction for protection against organophosphate exposure. Fundam. Appl. Toxicol. 15, 814-819.

Staats, D., Fisher, J., Conolly, R. (1991) Gastrointestinal absorption of xenobiotics in physiologically based pharmacokinetic models. A two-compartment description. Drug Metab. Disp. 19, 144-148.

Steel, S. (1991). The new chemical gate keepers. Farm J., 40-42.

Sultatos, L., Costa, L. Murphy, S. (1982) Determination of organophosphorus insecticides, their oxygen analogs and metabolites by high pressure liquid chromatography. Chromatographia 15, 669-671.

Sultatos, L., and Murphy, S. (1983). Kinetic analyses of the microsomal biotransformation of the phosphorothionate insecticides chlorpyrifos and parathion. Fundam Appl. Toxicol. 3, 16-21.

Sultatos, L., Shao, M., Murphy, S. (1984). The role of hepatic biotransformation in mediating the acute toxicity of the phosphorothionate insecticide chlorpyrifos. Toxicol. Appl. Pharmacol. 73, 60-68.

Sultatos, L., Minor, L. (1986) Factors affecting the biotransformation of the pesticide parathion by the isolated perfused mouse liver. Drug Metab. Dispos. 14, 214-220.

Sultatos, L. (1990) A physiologically based pharmacokinetic model of parathion based on chemical-specific parameters determined *in vitro*. J. Amer. Col. Toxicol. 9, 611-619.

Sultatos, L. (1994) Mammalian toxicology of organophosphorus pesticides. J. Toxicol. Environ. Health 43, 271-289.

Tahara, M., Kubota, R., Nakazawa, H., Tokunaga, H., Nishimura, T. (2005) Use of cholinesterase activity as an indicator for the effects of combinations of organophosphorus pesticides in water from environmental sources. Water Res. 39, 5112-5118.

Tardif, R., Lapare, S., Krishnan, K. (1993) Physiologically based modeling of the toxicokinetic interaction between toluene and xylene in the rat. Toxicol. Appl Pharm 120, 266-273.

Tardif, R., Brodeur, J., Krishnan, K. (1997). Physiologically-based pharmacokinetic modeling of a ternary mixture of alkyl benzenes in rats and humans. Toxicol. Appl. Pharmacol. 144, 120-134.

Teuschler, L., Klaunig, J., Carney, E., Chambers, J., Connolly, R., Gennings, C., Giesy, J., Hertzberg, R., Klaassen, C., Kodell, R., Paustenbach, D., and Yang, R. (2002) Support of science-based decisions concerning the evaluation of the toxicology of mixtures: A new beginning. Reg Toxicol. 36, 34-39.

Timchalk, C., Nolan, R. Mendrala, A., Mattsson, J. (2002) A physiologically based pharmacokinetic and pharmacodynamic model for the organophosphate insecticide chlorpyrifos in rats and humans. Toxicol. Sci. 66, 34-53.

Timchalk, C., Poet, T., Hinman, M., Busby, A., Kousba, A. (2005) Pharmacokinetic and pharmacodynamic interaction for a binary mixture of chlorpyrifos and diazinon in the rat. Toxicol. Appl. Pharmacol. 205, 31-42.

Traina, M., Serpietri, L. (1984) Changes in the levels and forms of rat plasma cholinesterase during chronic diisopropylphosphorofluoridate intoxication. Biochem Pharmacol 33, 645-653.

Vale, J. (1998) Toxicokinetic and toxicodynamic aspects of organophosphate poisoning. Toxicol. Lett. 102-103, 649-652.

Vandekar, M., Heath, D. (1957) The reactivation of cholinesterase after inhibition *in vivo* by some dimethyl phosphate esters. J. Biochem. 67, 202-208.

Waldron-Lechner, D., Abdel-Rahman, M. (1986) Kinetics of carbaryl and malathion in combination in the rat. J. Toxicol. Environ. Health 18 (2), 241-256.

Wallace, K. B. (1992) Species-selective toxicity of organophosphorus insecticides: A pharmacodynamic phenomena. In: Organophosphates Chemistry , Fate, and Effects. Academic Press, San Diego, CA.

Wang, C. and Murphy, S. (1982) Kinetic analysis of species differences in acetylcholinesterase sensitivity to organophosphate insecticides. Toxicol. Appl. Pharmacol. 66, 409-419.

Wenthold, R., Mahler, H., Moore, W. (1974) The half-life of acetylcholinesterase in mature rat brain. J. Neurochem 22, 941-943.

Wilkinson, G (1987). Prediction of *in vivo* parameters of drug metabolism and distribution from *in vitro* studies. In: Pharmacokinetics in Risk Assessment, vol. 8. Washington, DC: National Academy Press, pp.80-95.

Wilson, I. (1952) Acetylcholinesterase. Reactivation of alkyl phosphate-inhibited enzyme. J. Biol. Chem. 199, 113-120.

Zhang, Q., Dunbar, D., Ostrowska, A., Zeisloft, S., Yang, J. (1999) Characterization of human small intestinal cytochrome P450. Drug Metab. Dispos. 27, 804-809.

APPENDIX A

ACSL PROGRAM CODE

! OPS.CSL A PHYSIOLOGICALLY-BASED TOXICOKINETIC AND TOXICODYNAMIC (PBTK/TD) MODEL FOR A TERNARY ORGANOPHOSPHORUS INSECTICIDE MIXTURE IN RATS

```
! JULIAN T. PITTMAN

'-------------------------------------------------------------'
  PROGRAM SWEEP

INITIAL

  L1.CONTINUE
  CALL INITD

OPEN(FILE='OUTPUT.DAT')

ALGORITHM IALG=2 $ 'GEAR INTEGRATION ALGORITHM FOR STIFF SYSTEMS'

!-----TIMING COMMANDS-----!

CONSTANT TSTOP=0.5! 4! 12! 24  ! LENGTH OF SIMULATION (H)
CONSTANT POINTS=1000          ! NUMBER OF SIMULATED DATA POINTS
CINT=TSTOP/POINTS           ! COMMUNICATION INTERVAL (H)
TM=T*60                     ! HOURS TO MINUTES CONVERSION
TD=T/24                     ! HOURS TO DAYS CONVERSION
w=t
schedule cat1 .at.tchng
cizone=0!1.0

!-----PHYSIOLOGICAL PARAMETERS-----!

CONSTANT BW=0.22            ! BODY WEIGHT (KG)
CONSTANT QCC=15             ! CARDIAC OUTPUT (L/H/KG BW)
CONSTANT QHC=0.25     ! PROPORTION OF CARDIAC OUTPUT TO HEART AND
LUNGS
CONSTANT QDC=0.006      ! PROPORTION OF CARDIAC OUTPUT TO DIAPHRAGM
CONSTANT QLC=0.25           ! PROPORTION OF CARDIAC OUTPUT TO LIVER
CONSTANT QBRC=0.03          ! PROPORTION OF CARDIAC OUTPUT TO BRAIN
CONSTANT QFC=0.09           ! PROPORTION OF CARDIAC OUTPUT TO FAT
CONSTANT VHC=0.04     ! FRACTION HEART AND LUNGS TISSUE VOLUME (L/L
BW)
CONSTANT VDC=0.0003          ! FRACTION DIAPHRAGM VOLUME (L/L BW)
CONSTANT VLC=0.04           !  FRACTION LIVER TISSUE VOLUME (L/L BW)
CONSTANT VBRC=0.06          ! FRACTION BRAIN TISSUE VOLUME (L/L BW)
CONSTANT VFC=0.07           ! FRACTION BODY FAT VOLUME (L/L BW)
CONSTANT VAC=.0185       ! FRACTION POOLED VENOUS BLOOD VOLUME (L/L
BW)
CONSTANT VVC=.05555         ! FRACTION ATERIAL BLOOD VOLUME (L/L BW)

!-----CHLORPYRIFOS-SPECIFIC PARAMETERS-----!
```

```
CONSTANT MW=350.57          ! MOLECULAR WEIGHT (G/MOL)
CONSTANT VMAX1=74421!57003  ! LIVER CP450 VMAX1 (µM/H/KG BW)
CONSTANT VMAX2=80!273!0     ! LIVER CP450 VMAX2 (µM/H)
CONSTANT VMAX2= 1.8085*vmax1!74421!57003 ! LIVER CP450  VMAX1
(µM/H/KG BW)
CONSTANT KM1=240            ! LIVER CP450 MICHAELIS-MENTON KM1
(µM/L)
CONSTANT KM2=250!16.1       ! LIVER CP450 MICHAELIS-MENTON KM2
(µM/L)
CONSTANT KM2=1.64*km1!16.1  ! LIVER CP450 MICHAELIS-MENTON KM2
CONSTANT PH=23            ! HEART AND LUNGS/BLOOD PART. COEF.
CONSTANT PD=6             ! DIAPHRAGM/BLOOD PART. COEF.
CONSTANT PL=22            ! LIVER/BLOOD PART. COEF.
CONSTANT PBR=33           ! BRAIN/BLOOD PART. COEF.
CONSTANT PF=435           ! FAT/BLOOD PART. COEF.
CONSTANT PSK=6            ! SKIN/BLOOD PART. COEF.
CONSTANT PR=10            ! RICHLY PERFUSED TISSUE/BLOOD PART. COEF.
CONSTANT PS=6             ! SLOWLY PERFUSED TISSUE/BLOOD PART. COEF.

!-----CHLORPYRIFOS-OXON-SPECIFIC PARAMETERS-----!

CONSTANT MWW=334.5          ! MOLECULAR WEIGHT OXON (G/MOL)
CONSTANT MWW=190.0          ! MOLECULAR WEIGHT TCP (G/MOL)
CONSTANT VMAX3=179!273!     ! PLASMA A-ESTERASE VMAX (µM/H/KG BW)
CONSTANT KM3=2.86         ! PLASMA A-ESTERASE MICHAELIS-MENTON KM
(µM/L)
CONSTANT VMAX4=179.4       ! LIVER A-ESTERASE VMAX (µM/H/KG BW)
CONSTANT KM4=1.64         ! LIVER A-ESTERASE MICHAELIS-MENTON KM
(µM/L)
CONSTANT PHH=19            ! HEART/BLOOD PART. COEF.
CONSTANT PDD=4.9           ! DIAPHRAGM/BLOOD PART. COEF.
CONSTANT PLL=17            ! LIVER/BLOOD PART. COEF.
CONSTANT PBRR=26           ! BRAIN/BLOOD PART. COEF.
CONSTANT PFF=342           ! FAT/BLOOD PART. COEF.
CONSTANT PSKK=6            ! SKIN/BLOOD PART. COEF.
CONSTANT PRR=8.1           ! RICHLY PERFUSED TISSUE/BLOOD PART. COEF.
CONSTANT PSS=4.9           ! SLOWLY PERFUSED TISSUE/BLOOD PART. COEF.

!-----METHYLPARATHION-SPECIFIC PARAMETERS-----!

CONSTANT MW=263.23             ! MOLECULAR WEIGHT (G/MOL)
CONSTANT VMAX1=24.28!29.09     ! LIVER CP450 VMAX1 (MG/H/KG BW)
CONSTANT VMAX2=34.29!33.53     ! LIVER CP450 VMAX2 (MG/H)
CONSTANT VMAX2= 1.8085*vmax1!35.38!32.96  ! LIVER CP450 VMAX1
(MG/H/KG BW)
CONSTANT KM1=21.64             ! LIVER CP450 MICHAELIS-MENTON KM1
(MG/L) CONSTANT KM2=36.385!23.76  ! LIVER CP450 MICHAELIS-MENTON KM2
(MG/H/KG BW)
CONSTANT KM2=2.0384*km1!24.757 ! LIVER CP450 MICHAELIS-MENTON KM2
(MG/H/KG BW)
CONSTANT PH=5             ! HEART AND LUNGS/BLOOD PART. COEF.
CONSTANT PD=8             ! DIAPHRAGM/BLOOD PART. COEF.
CONSTANT PL=7             ! LIVER/BLOOD PART. COEF.
```

```
CONSTANT PBR=29          ! BRAIN/BLOOD PART. COEF.
CONSTANT PF=80           ! FAT/BLOOD PART. COEF.
CONSTANT PR=4            ! RICHLY PERFUSED TISSUE/BLOOD PART. COEF.
CONSTANT PS=2            ! SLOWLY PERFUSED TISSUE/BLOOD PART. COEF.

!-----METHYLPARAOXON-SPECIFIC PARAMETERS-----!

CONSTANT MWW=247.02         ! MOLECULAR WEIGHT (G/MOL)
CONSTANT VMAX3=54.93! 65! 102.5!49.30 !PLASMA A-ESTERASE VMAX (MG/H)
CONSTANT KM3=82.49       ! PLASMA A-ESTERASE MICHAELIS-MENTON KM
(MG/L)
CONSTANT VMAX4=93!112.4!92.97    ! LIVER A-ESTERASE VMAX (MG/H)
CONSTANT KM4=66.38!75.51  ! LIVER A-ESTERASE MICHAELIS-MENTON KM
(MG/L)
CONSTANT PHH=1.07           ! HEART/BLOOD PART. COEF.
CONSTANT PDD=1.08           ! DIAPHRAGM/BLOOD PART. COEF.
CONSTANT PLL=1.09           ! LIVER/BLOOD PART. COEF.
CONSTANT PBRR=1.27          ! BRAIN/BLOOD PART. COEF.
CONSTANT PFF=1.18           ! FAT/BLOOD PART. COEF.
CONSTANT PRR=1.09           ! RICHLY PERFUSED TISSUE/BLOOD PART.
COEF.
CONSTANT PSS=1.07           ! SLOWLY PERFUSED TISSUE/BLOOD PART.
COEF.

!-----PARATHION-SPECIFIC PARAMETERS-----!

CONSTANT MW=291.27                ! MOLECULAR WEIGHT (G/MOL)
CONSTANT VMAX1=13.596!15.9!14.19  ! LIVER CP450  VMAX1 (MG/H/KG BW)
CONSTANT VMAX2=24.54!28.72!16.39  ! LIVER CP450 VMAX2 (MG/H)
CONSTANT VMAX2= 1.8085*vmax1!13.596!15.9!14.19 ! LIVER CP450  VMAX1
(MG/H/KG BW)
CONSTANT KM1=10.508!math7.573  ! LIVER CP450 MICHAELIS-MENTON KM1
(MG/L)
CONSTANT KM2=24.699!15.437 ! LIVER CP450 MICHAELIS-MENTON KM2
(MG/H/KG BW)
CONSTANT KM2=2.0384*km1!15.437 ! LIVER CP450 MICHAELIS-MENTON KM2
(MG/H/KG BW)
CONSTANT PH=3.8            ! HEART AND LUNGS/BLOOD PART. COEF.
CONSTANT PD=8              ! DIAPHRAGM/BLOOD PART. COEF.
CONSTANT PL=3.8            ! LIVER/BLOOD PART. COEF.
CONSTANT PBR=2.78          ! BRAIN/BLOOD PART. COEF.
CONSTANT PF=96.7           ! FAT/BLOOD PART. COEF.
CONSTANT PSK=8.7           ! SKIN/BLOOD PART. COEF.
CONSTANT PR=3.8            ! RICHLY PERFUSED TISSUE/BLOOD PART.
COEF.
CONSTANT PS=2              ! SLOWLY PERFUSED TISSUE/BLOOD PART.
COEF.

!-----PARAOXON-SPECIFIC PARAMETERS-----!

CONSTANT MWW=275.21         ! MOLECULAR WEIGHT (G/MOL)
CONSTANT VMAX3=48.72!57!93.6!39.21 ! PLASMA A-ESTERASE VMAX (MG/H)
CONSTANT KM3=61.92       ! PLASMA A-ESTERASE MICHAELIS-MENTON KM
(MG/L)
```

```
CONSTANT VMAX4=80!93.6!76.51  ! LIVER A-ESTERASE VMAX (MG/H)
CONSTANT KM4=50.08!55.04      ! LIVER A-ESTERASE MICHAELIS-MENTON KM
(MG/L)
CONSTANT PHH=1.07           ! HEART/BLOOD PART. COEF.
CONSTANT PDD=1.08           ! DIAPHRAGM/BLOOD PART. COEF.
CONSTANT PLL=1.09           ! LIVER/BLOOD PART. COEF.
CONSTANT PBRR=1.27          ! BRAIN/BLOOD PART. COEF.
CONSTANT PFF=1.18           ! FAT/BLOOD PART. COEF.
CONSTANT PSKK=.95           ! SKIN/BLOOD PART. COEF.
CONSTANT PRR=1.09           ! RICHLY PERFUSED TISSUE/BLOOD PART.
COEF.
CONSTANT PSS=1.07           ! SLOWLY PERFUSED TISSUE/BLOOD PART.
COEF.

!-----DERIVED PARAMETERS-----!

QC=QCC*BW**0.74             ! CARDIAC OUTPUT (L/H)
QH=QHC*QC                   ! BLOOD FLOW TO HEART AND LUNGS (L/H)
QD=QDC*QC                   ! BLOOD FLOW TO DIAPHRAGM (L/H)
QL=QLC*QC                   ! BLOOD FLOW TO LIVER (L/H)
QBR=QBRC*QC                 ! BLOOD FLOW TO BRAIN (L/H)
QF=QFC*QC                   ! BLOOD FLOW TO FAT (L/H)
QR=0.76*QC-QL-QBR        ! BLOOD FLOW TO RAPIDLY PERFUSED TISSUES
(L/H)
QS=.24*QC-QF-QSK-QD       ! BLOOD FLOW TO SLOWLY PERFUSED TISSUES
(L/H)
VH=VHC*BW                   ! VOLUME OF HEART AND LUNGS (L)
VD=VDC*BW                   ! VOLUME OF DIAPHRAGM (L)
VL=VLC*BW                   ! VOLUME OF LIVER (L)
VBR=VBRC*BW                 ! VOLUME OF BRAIN (L)
VF=VFC*BW                   ! VOLUME OF FAT (L)
VS=0.82*BW-VF-VSK-VD        ! VOLUME OF SLOWLY PERFUSED TISSUES (L)
VR=0.09*BW-VL-VBR-VH        ! VOLUME OF RAPIDLY PERFUSED TISSUE (L)
VV=VVC*BW                   ! VOLUME OF POOLED VENOUS BLOOD (L)
VA=VAC*BW                   ! VOLUME OF ARTERIAL BLOOD (L)

!-----EXPOSURE DEFINITION-----!

DOSE=CDOSE*BW               ! CHLORPYRIFOS ORAL DOSE
DOS=CDOS*BW
DOSS=CDOSS*BW

DOSEO=CDOSEO*BW             ! CHLORPYRIFOS-OXON ORAL DOSE
DOSO=CDOSO*BW
DOSSO=CDOSSO*BW

DOSE=MPDOSE*BW              ! METHYLPARATHION ORAL DOSE
DOS=MPDOS*BW
DOSS=MPDOSS*BW

DOSEO=MPDOSEO*BW            ! METHYLPARAOXON ORAL DOSE
DOSO=MPDOSO*BW
DOSSO=MPDOSSO*BW
```

```
DOSE=PDOSE*BW                ! PARATHION ORAL DOSE
DOS=PDOS*BW
DOSS=PDOSS*BW

DOSEO=PDOSEO*BW              ! PARAOXON ORAL DOSE
DOSO=PDOSO*BW
DOSSO=PDOSSO*BW

CONSTANT CDOSE=0             ! CHLORPYRIFOS ORAL DOSE (MG/KG)
CONSTANT CDOS=0
CONSTANT CDOSS=0

CONSTANT MPDOSE=0            ! METHYLPARATHION ORAL DOSE (MG/KG)
CONSTANT MPDOS=0
CONSTANT MPDOSS=0

CONSTANT PDOSE=0             ! PARATHION ORAL DOSE (MG/KG)
CONSTANT PDOS=0
CONSTANT PDOSS=0

CONSTANT KA=1                ! FIRST ORDER ORAL UPTAKE RATE (1/HR)
CONSTANT KAA=1
CONSTANT KAAA=1

IF (PDOSE.EQ.0.) KA=0.       ! IF NO ORAL DOSE SET ABSORPTION RATE
TO 0
IF (DOS.EQ.0) KAA=0.
IF (DOSS.EQ.0) KAAA=0.

CONSTANT CDOSEO=0            ! CHLORPYRIFOS-OXON ORAL DOSE (MG/KG)
CONSTANT CDOSO=0
CONSTANT CDOSSO=0

CONSTANT MPDOSEO=0           ! METHYLPARAOXON ORAL DOSE (MG/KG)
CONSTANT MPDOSO=0
CONSTANT MPDOSSO=0

CONSTANT PDOSEO=0            ! PARAOXON ORAL DOSE (MG/KG)
CONSTANT PDOSO=0
CONSTANT PDOSSO=0

CONSTANT KAB=1               ! OXON FIRST ORDER ORAL UPTAKE RATE
(1/HR)
CONSTANT KAAC=1
CONSTANT KAAAD=1

IF (PDOSEO.EQ.0.) KAB=0.     ! IF NO ORAL DOSE SET ABSORPTION RATE
TO 0
IF (DOSO.EQ.0) KAAC=0.
IF (DOSSO.EQ.0) KAAAD=0.

!-----SWEEP CONSTANTS-----!

CONSTANT CMN=.25            ! SWEEP PARAMETER
```

```
CONSTANT CMX=.25            ! SWEEP PARAMETER
CONSTANT CDL=.25            ! SWEEP PARAMETER

CONSTANT MPMN=.25           ! SWEEP PARAMETER
CONSTANT MPMX=.25           ! SWEEP PARAMETER
CONSTANT MPDL=.25           ! SWEEP PARAMETER

CONSTANT PMN=.25            ! SWEEP PARAMETER
CONSTANT PMX=.25            ! SWEEP PARAMETER
CONSTANT PDL=.25            ! SWEEP PARAMETER

!---------- PHARMACODYNAMIC MODEL PARAMETERS----------!

'** ACHE DYNAMIC PARAMETERS IN THE BRAIN TISSUE**'

CONSTANT ACTD=3255.6  ! TOTAL ENZYME CONC. (PM) IN DIAPHRAGM
(EBD)(BED)
CONSTANT ACTL=3466.7         ! TOTAL ENZYME CONC. (PM) IN LIVER
CONSTANT ACTH=2604           ! TOTAL ENZYME CONC. (PM) IN HEART
CONSTANT ACTM=2036!2790.9!500   ! TOTAL ENZYME CONC. (PM) IN RBSC
BLOOD
CONSTANT ACTV=2790.9!498      ! TOTAL ENZYME CONC. (PM) IN VENOUS
BLOOD
CONSTANT ACTMP=725.7!2036!2790.9!500   ! TOTAL ENZYME CONC. (PM) IN
RBSC BLOOD
CONSTANT ACT=31227.3       ! TOTAL ENZYME CONC. (PM) IN BR CON. add
pbs
CONSTANT Ki=1.45!.9           ! INHIBITION ACHE (PM-1 H-1) add pbs
CONSTANT Ki2=.00000125        ! INHIBITION ACHE (PM-1 H-1) add pbs
CONSTANT K2=50                ! add pbs
CONSTANT zz=3                 ! add pbs
CONSTANT K5=.08!.114 !08      ! REGENERATION OF ACHE (H-1)
CONSTANT K6=.01               ! AGING OF ACHE (H-1)
CONSTANT K8=.0107             ! DEGENERATION OF ACHE (H-1)
CONSTANT K7ab= 334.2
CONSTANT K7al=37.1
CONSTANT K7ah=27.9
CONSTANT K7abl=21.7!5.35!29.9      ! RBSCS ACHE SYNTHSIS
CONSTANT K7ablP=7.7!21.7!5.35!29   ! PLASMA ACHE SYNTHSIS
CONSTANT K7ad=34.8!25.2

'** BUTYRYLCHOLINESTERASE PHARMACODYNAMIC PARAMETERS**'

CONSTANT ACTBUb=14646       ! TOTAL ENZYME CONC. (PM) IN BRAIN
CONSTANT ACTBUL=2305       ! TOTAL ENZYME CONC. (PM) IN LIVER (EBT)
(BET)
CONSTANT ACTBUD=3422.2     ! TOTAL ENZYME CONC. (PM) IN DIAPHRAGM
(EBD)(BED)
CONSTANT ACTBUH=3425         ! TOTAL ENZYME CONC. (PM) IN HEART
CONSTANT ACTBUM=3761!2050    ! TOTAL ENZYME CONC. (PM) IN  PLASMA
CONSTANT ACTBUM=2050         ! TOTAL ENZYME CONC. (PM) IN  BLOOD
CONSTANT ACTBUV=2050         ! TOTAL ENZYME CONC. (PM) IN  VENOUS
BLOOD
```

```
CONSTANT Ki2B=.00002044!.000005    ! optIM INHIBITION
BUTERYLCHOLINESTERASE (PM-1 H-1)
CONSTANT K5B=.08            ! REGENERATION OF (H-1)
CONSTANT K6B=.01            ! AGING (H-1)
CONSTANT K7bb=156.7!34.13!43.17!34.1329994   ! SYNTHESIS OF BRAIN
ACHE (H-1)
CONSTANT K7bl=24.7          ! SYNTHESIS OF LIVER ACHE
CONSTANT K7db=36.62         ! SYNTHESIS OF DIAPHRAGM ACHE
CONSTANT K7bbl=40.24!21.9   ! SYNTHESIS OF PLASMA BUCHE ADJUSTED TO
PLASMA VOLUME
CONSTANT K7bh=36.6            ! SYNTHESIS OF HEART ACHE
CONSTANT K7bblv=21.935        ! SYNTHESIS OF VENOUS TOTAL ADJUSTED
TO VENOUS VOLUME

'** CARBOXYLESTERASE PHARMACODYNAMIC PARAMETERS**'

CONSTANT ACTCEb=163636.37         ! TOTAL ENZYME CONC. (PM) IN BRAIN
CONSTANT ACTCEbf=426262.63        ! TOTAL ENZYME CONC. (PM) IN BRAIN
II
CONSTANT ACTCEL=5310000           ! TOTAL ENZYME CONC. (PM) IN LIVER
CONSTANT ACTCELf=13822500         ! TOTAL ENZYME CONC. (PM) IN LIVER
caeII
CONSTANT ACTCEH=440986.667        ! TOTAL ENZYME CONC. (PM) IN HEART
CONSTANT ACTCEHf=11480833.330     ! TOTAL ENZYME CONC. (PM) IN HEART
II
CONSTANT ACTCEM=1244881.245       ! TOTAL ENZYME CONC. (PM) IN
ARTERIAL BLOOD
CONSTANT ACTCEV=1244881.245       ! TOTAL ENZYME CONC. (PM) IN
VENOUS BLOOD
CONSTANT ACTCEMf=3242424.242      ! TOTAL ENZYME CONC. (PM) IN
ARTERIAL BLOOD II
CONSTANT ACTCEVf=3242424.242      ! TOTAL ENZYME CONC. (PM) IN
VENOUS BLOOD II
CONSTANT ACTCED=866666.6667       ! TOTAL ENZYME CONC. (PM) IN
DIAPHRAGM
CONSTANT ACTCEDf=311666.6667      ! TOTAL ENZYME CONC. (PM) IN
DIAPHRAGM II
CONSTANT Ki2C=0.0000312!0.00000625 ! INHIBITION CARBOXYL ESTERASE
(PM-1 H-1)
CONSTANT K5C=.08             ! REGENERATION OF (H-1)
CONSTANT K6C=.01             ! AGING OF (H-1)
CONSTANT K7C=1751            ! SYNTHESIS OF CAE I
CONSTANT K7CF=4561           ! SYNTHESIS OF CAE II
(K8*ACTCEBF,10107)
CONSTANT K7bc=1751           ! SYNTHESIS OF CAE I BRAIN (H-1)
CONSTANT K7lc=56817          ! SYNTHESIS OF LIVER CAE I
CONSTANT K7dc=9273.3         ! SYNTHESIS OF DIAPHRAGM CAE I
CONSTANT K7blc=13320.2       ! SYNTHESIS OF BLOOD CAE I
CONSTANT K7hc=4718.6         ! SYNTHESIS OF HEART CAE I
CONSTANT K7bd=4561           ! SYNTHESIS OF BRAIN CAE II(H-1)
CONSTANT K7ld=147900.8       ! SYNTHESIS OF LIVER CAE II
CONSTANT K7dd=3334.8         ! SYNTHESIS OF DIAPHRAGM CAE II
CONSTANT K7bld=34693.9       ! SYNTHESIS OF BLOOD CAE II
CONSTANT K7hd=122844.9
```

```
CONSTANT K8C=.0107           ! DEGENERATION OF (H-1)

END                          ! END OF INITIAL

!-------------------------------------------------------------!

DYNAMIC

WRITE(99,10)T,PCHE
10..FORMAT(F12.5,F12.5,F12.5)
DISCRETE CAT1
CIZONE=48!24
!w=t-24
schedule cat2 .at. t+48!24
END

DISCRETE cat2
CIZONEe=96!48
!w=t-48
schedule cat3 .at. t+48
END

DISCRETE cat3
scdosop=.75
!w=t-72
CIZONE=144!72!0
schedule cat4 .at. t+48
END

DISCRETE cat4
!w=t-96
CIZONE=192!96
schedule cat5 .at. t+48!
END

DISCRETE cat5
!w=t-120
CIZONE=240!120!0
schedule cat6 .at. t+48!
END

DISCRETE cat6
CIZONE=288!144!1
schedule cat7 .at. t+48!
END

DISCRETE cat7
scdosop=1.35
CIZONE=336!168!0
schedule cat8 .at. t+48
END

DISCRETE cat8
CIZONE=384!192!1
```

```
schedule cat9 .at. t+48!.0083
END

DISCRETE cat9
CIZONE=432!0
schedule cat10 .AT. T+48
END

DISCRETE cat10
CIZONE=480!1
schedule cat11 .at. t+48!.0083
END

DISCRETE cat11
CIZONE=264!0
schedule cat12 .at. t+48
END

DISCRETE cat12
CIZONE=288!1
schedule cat13 .at. t+48!
END

DISCRETE cat13
CIZONE=312!0
schedule cat14 .at. t+48
END

DISCRETE cat14
CIZONE=336!!1
schedule cat15 .at. t+48!.0083
END

DISCRETE cat15
CIZONE=360!0
schedule cat16 .AT. T+48
END

DISCRETE cat16
CIZONE=384!1
schedule cat17 .at. t+48!.0083
END

DISCRETE CAT17
CIZONE=408
!w=t-24
schedule cat18 .at. t+48
END

DISCRETE cat18
CIZONE=432
!w=t-48
schedule cat19 .at. t+48
END
```

```
DISCRETE cat19
!w=t-72
CIZONE=456!0
schedule cat20 .at. t+48
END

DISCRETE cat20
!w=t-96
CIZONE=480
schedule cat2 .at. t+48!
END

DISCRETE cat21
CIZONE=504
schedule cat2 .at. t+48
END

END

!---------------------------------------------------------------!

DERIVATIVE
!K1=K2*ZZ
!KM2=2.0384*KM1
!KM3=1.3264*KM4
!VMAX2=1.8085*VMAX1
!VMAX4=1.642*VMAX3

!-----CONDITION FOR TERMINATION OF THE RUN-----!

TERMT (T.GE.TSTOP)

!-----OP EXPOSURE-----!

!-----ORAL DOSE MIXTURE-----!

RMR=-KA*MR                    ! RATE OF CHANGE IN THE STOMACH
MR=DOSE*EXP(-KA*T)            ! AMOUNT REMAINING IN THE STOMACH
RAO=KA*MR                     ! RATE OF AMOUNT ABSORBED
AO=INTEG(RAO,0.)              ! AMOUNT ABSORBED

RMRR=-KAA*MRR
MRR=DOS*EXP(-KAA*(T-8))
RAOO=KAA*MRR
AOO=INTEG(RAOO,0.)

RMRS=-KAAA*MRS
MRS=DOSS*EXP(-KAAA*(T-16))
RAOP=KAAA*MRS
AOP=INTEG(RAOP,0.)

!-----OXON EXPOSURE-----!
```

```
!-----ORAL DOSE OF MIXTURE-----!
RMRB=-KAB*MRB                 ! RATE OF CHANGE IN THE STOMACH
MRB=DOSEO*EXP(-KAB*T)         ! AMOUNT REMAINING IN THE STOMACH
RAOB=KAB*MRB                  ! RATE OF AMOUNT ABSORBED
AOB=INTEG(RAOB,0.)            ! AMOUNT ABSORBED

!----- CHLORPYRIFOS IN VENOUS BLOOD-----!

RAV=(QF*CVF+QL*CVL+QS*CVS+QR*CVR+QBR*CVBR+QSK*CVSK+IV+QD*CVD)...
-QC*CV+rscap               ! RATE OF CHLOPYRIFOS INPUT TO THE VENOUS
BLOOD(MG/H)
AV=INTEG(RAV,0.)            ! AMOUNT IN THE VENOUS BLOOD (MG)
CV=AV/VV                    ! CONCENTRATION (MG/KG)

!-----CHLORPYRIFOS-OXON IN VENOUS BLOOD-----!

RAVO=(QF*CVFF+QL*CVLL+QS*CVSS+QR*CVRR+QBR*CVBRR+QSK*CVSKK+ivo+QD*CVD
D)...
-QC*CVO-RAM3+rsca-RINHCEVM-RINHCEVFM-RINHBUVM-RINHvM!RAG!+scA
! RATE OF CHLORPYRIFOS-OXON INPUT TO THE VENOUS BLOOD (MG/H)
AVO=INTEG(RAVO,0.)          ! AMOUNT IN THE VENOUS BLOOD (MG)
CVO=AVO/VV                  ! CONCENTRATION (MG/KG)
ABV=CVO*1000000000/MWW

!-----A-ESTERASE ENZYME HYDROLYSIS OF CHLORPYRIFOS-OXON IN THE
VENOUS BLOOD -----!

RAM3=(VMAX3*CVO)/(KM3+CVO)  ! RATE OF CHLORPYRIFOS-OXON
HYDROLYSIS(MG/H)
AM3=INTEG(RAM3,0.)          ! AMOUNT OF HYDROLYSED CHLORPYRIFOS-
OXON(MG)

!----- CHLORPYRIFOS-OXON IN ARTERIAL BLOOD-----!

RAT=(QC*(CHHH-CAT))-RAM4-RINHCEMM-RINHCEMFM-RINHBUMM-RINHMM!
                            ! RATE OF CHANGE (MG/HR)
AAT=INTEG(RAT,0.)           ! AMOUNT (MG)'
CAT=AAT/VA                  ! CONCENTRATION (MG/L)
ABM=CAT*1000000000/MWW      ! CONCENTRATION PM

RAM4=(VMAX3*CAT)/(KM3+CAT)
AM4=INTEG(RAM4,0.)

!-----CHLORPYRIFOS IN HEART+LUNGS-----!

RAH=QC*(CV-CA)              ! RATE OF CHANGE (MG/HR)
AH=INTEG(RAH,0.)            ! AMOUNT (MG)'
CH=AH/VH                    ! CONCENTRATION HEART/LUNGS (MG/L)
CA=CH/PH                    ! CONCENTRATION ARTERIAL HEART (MG/L)

!-----CHLORPYRIFOS-OXON IN HEART+LUNGS-----!

RAAH=(QC*(CVO-CHHH))-RINHCEHM-RINHCEHFM-RINHBUHM-RINHHM
                            ! RATE OF CHANGE (MG/HR)
```

```
AHH=INTEG(RAAH,0.)          ! AMOUNT (MG)'
CHH=AHH/VH                  ! CONCENTRATION (MG/L)
ABH=CHH*1000000000/MWW
CHHH=CHH/PHH

!-----CHLORPYRIFOS IN DIAPHRAGM-----!

RAD=QD*(CA-CVD)             ! RATE OF CHANGE (MG/HR)
AD=INTEG(RAD,0.)            ! AMOUNT (MG)'
CD=AD/VD                    ! CONCENTRATION (MG/L)
!ABH=CDD*1000000000/MWW
CVD=CD/PD                   ! CONCENTRATION IN VENOUS OUTFLOW (MG/L)

!-----CHLORPYRIFOS-OXON IN DIAPHRAGM-----!

RADD=(QD*(CAT-CVDD))-RINHCEDFM-RINHCEDM-RINHBUDM-RINHDM
! RATE OF CHANGE (MG/HR)
ADD=INTEG(RADD,0.)          ! AMOUNT (MG)
CDD=ADD/VD                  ! CONCENTRATION (MG/L)
ABD=CVDD*1000000000/MWW
!ABD=CVDD*1000000000/MWW
CVDD=CDD/PDD                ! CONCENTRATION IN VENOUS OUTFLOW (MG/L)

!-----CHLORPYRIFOS IN LIVER-----!

RAL=(QL*(CA-CVL))-RAM1-RAM2+RAO+RAOO+RAOP ! RATE OF CHANGE (MG/HR)
AL=INTEG(RAL,0.)            ! AMOUNT (MG)
CL=AL/VL                    ! CONCENTRATION (MG/L)
CVL=AL/(VL*PL)              ! CONCENTRATION IN VENOUS OUTFLOW (MG/L)

!-----CHLORPYRIFOS METABOLISM IN LIVER-----!

RAM1=(VMAX1*CVL)/(KM1+CVL)  ! RATE OF CHANGE (MG/HR)
AM1=INTEG(RAM1,0.)          ! AMOUNT (C-OXON) (MG)
RAM2=(VMAX2*CVL)/(KM2+CVL)
AM2=INTEG(RAM2,0.)          ! AMOUNT (TCP) (MG)

!-----CHLORPYRIFOS-OXON IN LIVER-----!

RALL=(QL*(CAT-CVLL))+RAM1-RAMM+raob-RINHCELM-RINHCELFM...
-RINHBULM-RINHLM            ! RATE OF CHANGE (MG/HR)
ALL=INTEG(RALL,0.)          ! AMOUNT (MG)
CLL=ALL/VL                  ! CONCENTRATION (MG/L)
ABL=CVLL*1000000000/MWW
!ABL=CLL*1000000000/MWW
CVLL=ALL/(VL*PLL)           ! CONCENTRATION IN VENOUS OUTFLOW (MG/L)

!-----CHLORPYRIFOS-OXON METABOLISM IN LIVER-----!

RAMM=(VMAX4*CVLL)/(KM4+CVLL)
AMM=INTEG(RAMM,0.)          ! AMOUNT (TCP) (MG)

!-----CHLORPYRIFOS IN BRAIN-----!
```

```
RABR=QBR*(CA-CVBR)          ! RATE OF CHANGE (MG/HR)
ABR=INTEG(RABR,0.)          ! AMOUNT (MG)
CBR=ABR/VBR                 ! CONCENTRATION (MG/L)
CVBR=ABR/(VBR*PBR)          ! CONCENTRATION IN VENOUS OUTFLOW (MG/L)

!-----CHLORPYRIFOS-OXON IN BRAIN-----!

RABRR=(QBR*(CAT-CVBRR))-RINHCEBM-RINHCEBFM-RINHBUBM-RINHMC
! RATE OF CHANGE (MG/HR)
ABRR=INTEG(RABRR,0.)        ! AMOUNT (MG)
CBRR=ABRR/VBR               ! CONCENTRATION (MG/L)
AB=CBRR*1000000000/MWW

CVBRR=ABRR/(VBR*PBRR)       ! CONCENTRATION IN VENOUS OUTFLOW (MG/L)

!-----CHLORPYRIFOS IN FAT-----!

RAF=QF*(CA-CVF)             ! RATE OF CHANGE (MG/HR)
AF=INTEG(RAF,0.)            ! AMOUNT (MG)
CF=AF/VF                    ! CONCENTRATION (MG/L)
CVF=AF/(VF*PF)              ! CONCENTRATION VENOUS OUTFLOW (MG/L)

!-----CHLORPYRIFOS-OXON IN FAT-----!

RAFF=QF*(CAT-CVFF)          ! RATE OF CHANGE (MG/HR)
AFF=INTEG(RAFF,0.)          ! AMOUNT (MG)
CFF=AFF/VF                  ! CONCENTRATION (MG/L)
CVFF=AFF/(VF*PFF)           ! CONCENTRATION IN VENOUS OUTFLOW (MG/L)


!-----CHLORPYRIFOS IN SLOWLY PERFUSED TISSUES-----!

RAS=QS*(CA-CVS)             ! RATE OF CHANGE (MG/HR)
AS=INTEG(RAS,0.)            ! AMOUNT (MG)
CS=AS/VS                    ! CONCENTRATION (MG/L)
CVS=CS/PS                   ! CONCENTRATION IN VENOUS OUTFLOW (MG/L)

!-----CHLORPYRIFOS-OXON IN SLOWLY PERFUSED TISSUES-----!

RASS=QS*(CAT-CVSS)          ! RATE OF CHANGE (MG/HR)
ASS=INTEG(RASS,0.)          ! AMOUNT (MG)
CSS=ASS/VS                  ! CONCENTRATION (MG/L)
CVSS=CSS/PSS                ! CONCENTRATION IN VENOUS OUTFLOW (MG/L)

!-----CHLORPYRIFOS IN RAPIDLY PERFUSED TISSUES-----!

RAR=QR*(CA-CVR)             ! RATE OF CHANGE (MG/HR)
AR=INTEG(RAR,0.)            ! AMOUNT (MG)
CR=AR/VR                    ! CONCENTRATION (MG/L)
CVR=CR/PR                   ! CONCENTRATION IN VENOUS OUTFLOW (MG/L)

!-----CHLORPYRIFOS-OXON IN RAPIDLY PERFUSED TISSUES-----!

RARR=QR*(CAT-CVRR)          ! RATE OF CHANGE (MG/HR)
```

```
ARR=INTEG(RARR,0.)          ! AMOUNT (MG)
CRR=ARR/VR                  ! CONCENTRATION (MG/L)
CVRR=CRR/PRR                ! CONCENTRATION IN VENOUS OUTFLOW (MG/L)

!-----CHLORPYRIFOS -> TCP) Model 1-----!

CONSTANT KmHcp= 24.0          ! CONCENTRATION (µM/L)
CONSTANT VmHcp= 273.0         ! RATE OF CHANGE (µM /HR)

!-----LIVER(OXON ->TCP) AEST Model 2-----!

CONSTANT KMlst= 240.0         ! CONCENTRATION (µM/L)
CONSTANT VMl= 74421.0         ! RATE OF CHANGE (µM /HR)

!-----BLOOD(OXON -> TCP) AEST Model 2-----!

CONSTANT KMblst= 250.0        ! CONCENTRATION (µM/L)
CONSTANT VMbl= 57003.0        ! RATE OF CHANGE (µM /HR)

!----- METHYLPARATHION IN VENOUS BLOOD-----!

RAV=(QF*CVF+QL*CVL+QS*CVS+QR*CVR+QBR*CVBR+QSK*CVSK+IV+QD*CVD)...
-QC*CV+rscap               ! RATE OF METHYLPARATHION INPUT TO THE
VENOUS BLOOD(MG/H)
AV=INTEG(RAV,0.)            ! AMOUNT IN THE VENOUS BLOOD (MG)
CV=AV/VV                    ! CONCENTRATION (MG/KG)

!-----METHYLPARAOXON IN VENOUS BLOOD-----!

RAVO=(QF*CVFF+QL*CVLL+QS*CVSS+QR*CVRR+QBR*CVBRR+QSK*CVSKK+ivo+QD*CVD
D)...
-QC*CVO-RAM3+rsca-RINHCEVM-RINHCEVFM-RINHBUVM-RINHvM!RAG!+scA
!RATE OF METHYLPARAOXON INPUT TO THE VENOUS BLOOD(MG/H)
AVO=INTEG(RAVO,0.)          ! AMOUNT IN THE VENOUS BLOOD (MG)
CVO=AVO/VV                  ! CONCENTRATION (MG/KG)
ABV=CVO*1000000000/MWW

!-----A-ESTERASE ENZYME HYDROLYSIS OF METHYLPARAOXON IN VENOUS
BLOOD-----!

RAM3=(VMAX3*CVO)/(KM3+CVO)  ! RATE OF METHYLPARAOXON HYDROLYSIS
(MG/H)
AM3=INTEG(RAM3,0.)          ! AMOUNT OF HYDROLYSED METHYLPARAOXON
(MG)


!-----METHYLPARAOXON IN ARTERIAL BLOOD-----!

RAT=(QC*(CHHH-CAT))-RAM4-RINHCEMM-RINHCEMFM-RINHBUMM-RINHMM!
                            ! RATE OF CHANGE (MG/HR)
AAT=INTEG(RAT,0.)           ! AMOUNT (MG)'
CAT=AAT/VA                  ! CONCENTRATION (MG/L)
ABM=CAT*1000000000/MWW      ! CONCENTRATION PM
```

```
RAM4=(VMAX3*CAT)/(KM3+CAT)
AM4=INTEG(RAM4,0.)

!-----METHYLPARATHION IN HEART+LUNGS-----!

RAH=QC*(CV-CA)              ! RATE OF CHANGE (MG/HR)
AH=INTEG(RAH,0.)            ! AMOUNT (MG)'
CH=AH/VH                    ! CONCENTRATION HEART/LUNGS (MG/L)
CA=CH/PH                    ! CONCENTRATION ARTERIAL (MG/L)

!-----METHYLPARAOXON IN HEART+LUNGS-----!

RAAH=(QC*(CVO-CHHH))-RINHCEHM-RINHCEHFM-RINHBUHM-RINHHM
                            ! RATE OF CHANGE (MG/HR)
AHH=INTEG(RAAH,0.)          ! AMOUNT (MG)'
CHH=AHH/VH                  ! CONCENTRATION (MG/L)
ABH=CHH*1000000000/MWW

CHHH=CHH/PHH

!-----METHYLPARATHION IN DIAPHRAGM-----!

RAD=QD*(CA-CVD)              ! RATE OF CHANGE (MG/HR)
AD=INTEG(RAD,0.)             ! AMOUNT (MG)'
CD=AD/VD                     ! CONCENTRATION (MG/L)
!ABH=CDD*1000000000/MWW

CVD=CD/PD                    ! CONCENTRATION IN VENOUS OUTFLOW (MG/L)

!-----METHYLPARAOXON IN DIAPHRAGM-----!

RADD=(QD*(CAT-CVDD))-RINHCEDFM-RINHCEDM-RINHBUDM-RINHDM
                            ! RATE OF CHANGE (MG/HR)
ADD=INTEG(RADD,0.)          ! AMOUNT (MG)
CDD=ADD/VD                  ! CONCENTRATION (MG/L)
ABD=CVDD*1000000000/MWW
!ABD=CVDD*1000000000/MWW

CVDD=CDD/PDD                ! CONCENTRATION IN VENOUS OUTFLOW (MG/L)

!-----METHYLPARATHION IN LIVER-----!

RAL=(QL*(CA-CVL))-RAM1-RAM2+RAO+RAOO+RAOP
                            ! RATE OF CHANGE (MG/HR)
AL=INTEG(RAL,0.)            ! AMOUNT (MG)
CL=AL/VL                    ! CONCENTRATION (MG/L)

CVL=AL/(VL*PL)              ! CONCENTRATION IN VENOUS OUTFLOW (MG/L)

!-----METHYLPARATHION METABOLISM IN LIVER-----!

RAM1=(VMAX1*CVL)/(KM1+CVL)  ! RATE OF CHANGE (MG/HR)
AM1=INTEG(RAM1,0.)          ! AMOUNT (METHYLPARAOXON) (MG)
RAM2=(VMAX2*CVL)/(KM2+CVL)
```

```
AM2=INTEG(RAM2,0.)          ! AMOUNT (PNP) (MG)

!-----METHYLPARAOXON IN LIVER-----!

RALL=(QL*(CAT-CVLL))+RAM1-RAMM+raob-RINHCELM-RINHCELFM...
-RINHBULM-RINHLM            ! RATE OF CHANGE (MG/HR)
ALL=INTEG(RALL,0.)          ! AMOUNT (MG)
CLL=ALL/VL                  ! CONCENTRATION (MG/L)
ABL=CVLL*1000000000/MWW
!ABL=CLL*1000000000/MWW

CVLL=ALL/(VL*PLL)           ! CONCENTRATION IN VENOUS OUTFLOW (MG/L)

!-----METHYLPARAOXON METABOLISM IN LIVER-----!

RAMM=(VMAX4*CVLL)/(KM4+CVLL)
AMM=INTEG(RAMM,0.)          ! AMOUNT (PNP) (MG)

!-----METHYLPARATHION IN BRAIN-----!

RABR=QBR*(CA-CVBR)          ! RATE OF CHANGE (MG/HR)
ABR=INTEG(RABR,0.)          ! AMOUNT (MG)
CBR=ABR/VBR                 ! CONCENTRATION (MG/L)
CVBR=ABR/(VBR*PBR)          ! CONCENTRATION IN VENOUS OUTFLOW (MG/L)

!-----METHYLPARAOXON IN BRAIN-----!

RABRR=(QBR*(CAT-CVBRR))-RINHCEBM-RINHCEBFM-RINHBUBM-RINHMc
                            ! RATE OF CHANGE (MG/HR)
ABRR=INTEG(RABRR,0.)        ! AMOUNT (MG)
CBRR=ABRR/VBR               ! CONCENTRATION (MG/L)
AB=CBRR*1000000000/MWW

CVBRR=ABRR/(VBR*PBRR)       ! CONCENTRATION IN VENOUS OUTFLOW (MG/L)

!-----METHYLPARATHION IN FAT-----!

RAF=QF*(CA-CVF)             ! RATE OF CHANGE (MG/HR)
AF=INTEG(RAF,0.)            ! AMOUNT (MG)
CF=AF/VF                    ! CONCENTRATION (MG/L)
CVF=AF/(VF*PF)              ! CONCENTRATION VENOUS OUTFLOW (MG/L)

!-----METHYLPARAOXON IN FAT-----!

RAFF=QF*(CAT-CVFF)          ! RATE OF CHANGE (MG/HR)
AFF=INTEG(RAFF,0.)          ! AMOUNT (MG)
CFF=AFF/VF                  ! CONCENTRATION (MG/L)
CVFF=AFF/(VF*PFF)           ! CONCENTRATION IN VENOUS OUTFLOW (MG/L)


!-----METHYLPARATHION IN SLOWLY PERFUSED TISSUES-----!

RAS=QS*(CA-CVS)             ! RATE OF CHANGE (MG/HR)
AS=INTEG(RAS,0.)            ! AMOUNT (MG)
```

```
CS=AS/VS                    ! CONCENTRATION (MG/L)
CVS=CS/PS                   ! CONCENTRATION IN VENOUS OUTFLOW (MG/L)

!-----METHYLPARAOXON IN SLOWLY PERFUSED TISSUES-----!

RASS=QS*(CAT-CVSS)          ! RATE OF CHANGE (MG/HR)
ASS=INTEG(RASS,0.)          ! AMOUNT (MG)
CSS=ASS/VS                  ! CONCENTRATION (MG/L)
CVSS=CSS/PSS                ! CONCENTRATION IN VENOUS OUTFLOW (MG/L)

!-----METHYLPARATHION IN RAPIDLY PERFUSED TISSUES-----!

RAR=QR*(CA-CVR)             ! RATE OF CHANGE (MG/HR)
AR=INTEG(RAR,0.)            ! AMOUNT (MG)
CR=AR/VR                    ! CONCENTRATION (MG/L)
CVR=CR/PR                   ! CONCENTRATION IN VENOUS OUTFLOW (MG/L)

!-----METHYLPARAOXON IN RAPIDLY PERFUSED TISSUES-----!

RARR=QR*(CAT-CVRR)          ! RATE OF CHANGE (MG/HR)
ARR=INTEG(RARR,0.)          ! AMOUNT (MG)
CRR=ARR/VR                  ! CONCENTRATION (MG/L)
CVRR=CRR/PRR                ! CONCENTRATION IN VENOUS OUTFLOW (MG/L)

!----- PARATHION IN VENOUS BLOOD-----!

RAV=(QF*CVF+QL*CVL+QS*CVS+QR*CVR+QBR*CVBR+QSK*CVSK+IV+QD*CVD)...
-QC*CV+rscap                ! RATE OF PARATHION INPUT TO THE VENOUS
BLOOD(MG/H)
AV=INTEG(RAV,0.)            ! AMOUNT IN THE VENOUS BLOOD (MG)
CV=AV/VV                    ! CONCENTRATION (MG/KG)

!-----PARAOXON IN VENOUS BLOOD-----!

RAVO=(QF*CVFF+QL*CVLL+QS*CVSS+QR*CVRR+QBR*CVBRR+QSK*CVSKK+ivo+QD*CVD
D)...
-QC*CVO-RAM3+rsca-RINHCEVM-RINHCEVFM-RINHBUVM-RINHvM!RAG!+scA
! RATE OF PARAOXONN INPUT TO THE VENOUS BLOOD(MG/H)
AVO=INTEG(RAVO,0.)          ! AMOUNT IN THE VENOUS BLOOD (MG)
CVO=AVO/VV                  ! CONCENTRATION (MG/KG)
ABV=CVO*1000000000/MWW

!-----A-ESTERASE ENZYME HYDROLYSIS OF PARAOXON IN THE VENOUS BLOOD--
---!

RAM3=(VMAX3*CVO)/(KM3+CVO)  ! RATE OF PARAOXON HYDROLYSIS (MG/H)
AM3=INTEG(RAM3,0.)          ! AMOUNT OF HYDROLYSED PARAOXON (MG)

!----- PARAOXON IN ARTERIAL BLOOD-----!

RAT=(QC*(CHHH-CAT))-RAM4-RINHCEMM-RINHCEMFM-RINHBUMM-RINHMM!
                             ! RATE OF CHANGE (MG/HR)
AAT=INTEG(RAT,0.)            ! AMOUNT (MG)'
CAT=AAT/VA                   ! CONCENTRATION (MG/L)
```

```
ABM=CAT*1000000000/MWW       ! CONCENTRATION PM

RAM4=(VMAX3*CAT)/(KM3+CAT)
AM4=INTEG(RAM4,0.)

!-----PARATHION IN HEART+LUNGS-----!

RAH=QC*(CV-CA)              ! RATE OF CHANGE (MG/HR)
AH=INTEG(RAH,0.)            ! AMOUNT (MG)'
CH=AH/VH                    ! CONCENTRATION HEART/LUNGS (MG/L)
CA=CH/PH                    ! CONCENTRATION ARTERIAL (MG/L)

!-----PARAOXON IN HEART+LUNGS-----!

RAAH=(QC*(CVO-CHHH))-RINHCEHM-RINHCEHFM-RINHBUHM-RINHHM
                            ! RATE OF CHANGE (MG/HR)
AHH=INTEG(RAAH,0.)          ! AMOUNT (MG)'
CHH=AHH/VH                  ! CONCENTRATION (MG/L)
ABH=CHH*1000000000/MWW

CHHH=CHH/PHH

!-----PARATHION IN DIAPHRAGM-----!

RAD=QD*(CA-CVD)              ! RATE OF CHANGE (MG/HR)
AD=INTEG(RAD,0.)             ! AMOUNT (MG)'
CD=AD/VD                     ! CONCENTRATION (MG/L)
!ABH=CDD*1000000000/MWW

CVD=CD/PD                    ! CONCENTRATION IN VENOUS OUTFLOW (MG/L)

!-----PARAOXON IN DIAPHRAGM-----!

RADD=(QD*(CAT-CVDD))-RINHCEDFM-RINHCEDM-RINHBUDM-RINHDM
                            ! RATE OF CHANGE (MG/HR)
ADD=INTEG(RADD,0.)          ! AMOUNT (MG)
CDD=ADD/VD                  ! CONCENTRATION (MG/L)
ABD=CVDD*1000000000/MWW
!ABD=CVDD*1000000000/MWW

CVDD=CDD/PDD                ! CONCENTRATION IN VENOUS OUTFLOW (MG/L)

!-----PARATHION IN LIVER-----!

RAL=(QL*(CA-CVL))-RAM1-RAM2+RAO+RAOO+RAOP
                            ! RATE OF CHANGE (MG/HR)
AL=INTEG(RAL,0.)            ! AMOUNT (MG)
CL=AL/VL                    ! CONCENTRATION (MG/L)

CVL=AL/(VL*PL)              ! CONCENTRATION IN VENOUS OUTFLOW (MG/L)

!-----PARATHION METABOLISM IN LIVER-----!

RAM1=(VMAX1*CVL)/(KM1+CVL)  ! RATE OF CHANGE (MG/HR)
```

```
AM1=INTEG(RAM1,0.)          ! AMOUNT (PARAOXON) (MG)
RAM2=(VMAX2*CVL)/(KM2+CVL)
AM2=INTEG(RAM2,0.)          ! AMOUNT (PNP) (MG)

!-----PARAOXON IN LIVER-----!

RALL=(QL*(CAT-CVLL))+RAM1-RAMM+raob-RINHCELM-RINHCELFM...
-RINHBULM-RINHLM!  RATE OF CHANGE (MG/HR)
ALL=INTEG(RALL,0.)          ! AMOUNT (MG)
CLL=ALL/VL                  ! CONCENTRATION (MG/L)
ABL=CVLL*1000000000/MWW
!ABL=CLL*1000000000/MWW

CVLL=ALL/(VL*PLL)           ! CONCENTRATION IN VENOUS OUTFLOW (MG/L)

!-----PARAOXON METABOLISM IN LIVER-----!

RAMM=(VMAX4*CVLL)/(KM4+CVLL)
AMM=INTEG(RAMM,0.)          ! AMOUNT (PNP) (MG)

!-----PARATHION IN BRAIN-----!

RABR=QBR*(CA-CVBR)          ! RATE OF CHANGE (MG/HR)
ABR=INTEG(RABR,0.)          ! AMOUNT (MG)
CBR=ABR/VBR                 ! CONCENTRATION (MG/L)
CVBR=ABR/(VBR*PBR)          ! CONCENTRATION IN VENOUS OUTFLOW (MG/L)

!-----PARAOXON IN BRAIN-----!

RABRR=(QBR*(CAT-CVBRR))-RINHCEBM-RINHCEBFM-RINHBUBM-RINHMc
                            ! RATE OF CHANGE (MG/HR)
ABRR=INTEG(RABRR,0.)        ! AMOUNT (MG)
CBRR=ABRR/VBR               ! CONCENTRATION (MG/L)
AB=CBRR*1000000000/MWW

CVBRR=ABRR/(VBR*PBRR)       ! CONCENTRATION IN VENOUS OUTFLOW (MG/L)

!-----PARATHION IN FAT-----!

RAF=QF*(CA-CVF)             ! RATE OF CHANGE (MG/HR)
AF=INTEG(RAF,0.)            ! AMOUNT (MG)
CF=AF/VF                    ! CONCENTRATION (MG/L)
CVF=AF/(VF*PF)              ! CONCENTRATION VENOUS OUTFLOW (MG/L)

!-----PARAOXON IN FAT-----!

RAFF=QF*(CAT-CVFF)          ! RATE OF CHANGE (MG/HR)
AFF=INTEG(RAFF,0.)          ! AMOUNT (MG)
CFF=AFF/VF                  ! CONCENTRATION (MG/L)
CVFF=AFF/(VF*PFF)           ! CONCENTRATION IN VENOUS OUTFLOW (MG/L)


!-----PARATHION IN SLOWLY PERFUSED TISSUES-----!
```

```
RAS=QS*(CA-CVS)              ! RATE OF CHANGE (MG/HR)
AS=INTEG(RAS,0.)             ! AMOUNT (MG)
CS=AS/VS                     ! CONCENTRATION (MG/L)
CVS=CS/PS                    ! CONCENTRATION IN VENOUS OUTFLOW (MG/L)

!-----PARAOXON IN SLOWLY PERFUSED TISSUES-----!

RASS=QS*(CAT-CVSS)           ! RATE OF CHANGE (MG/HR)
ASS=INTEG(RASS,0.)           ! AMOUNT (MG)
CSS=ASS/VS                   ! CONCENTRATION (MG/L)
CVSS=CSS/PSS                 ! CONCENTRATION IN VENOUS OUTFLOW (MG/L)

!-----PARATHION IN RAPIDLY PERFUSED TISSUES-----!

RAR=QR*(CA-CVR)              ! RATE OF CHANGE (MG/HR)
AR=INTEG(RAR,0.)             ! AMOUNT (MG)
CR=AR/VR                     ! CONCENTRATION (MG/L)
CVR=CR/PR                    ! CONCENTRATION IN VENOUS OUTFLOW (MG/L)

!-----PARAOXON IN RAPIDLY PERFUSED TISSUES-----!

RARR=QR*(CAT-CVRR)           ! RATE OF CHANGE (MG/HR)
ARR=INTEG(RARR,0.)           ! AMOUNT (MG)
CRR=ARR/VR                   ! CONCENTRATION (MG/L)
CVRR=CRR/PRR                 ! CONCENTRATION IN VENOUS OUTFLOW (MG/L)

!-----PHARMACODYNAMICS OF ACETYLCHOLINESTERSE-----!

RAC=K7ab-K8*AC+K5*ACA+K5*ABACa-KI*AB*AC-k1*ab*ac+k2*abac-KI2*ABAC*AB
AC=INTEG(RAC,act)
ACTIVITY=((AC+abac)/act)*100
ACTIVITYHI=ACTIVITY*1

RACA=Ki*AB*AC-K5*ACA-k6*aca     ! EQ 1
ACA=INTEG(RACA,0.)

RABAC=K1*AB*AC-k2*ABAC-Ki2*ABAC*ab+k5*abaca!-k6*abaca     ! EQ 2
ABAC=INTEG(RABAC,0.)
RABACA=ki2*ABAC*ab-K5*ABACA-K6*ABACA       ! EQ 3
ABACA=INTEG(RABACA,0.)
RABACAM=(RABACA*VBR*.0000000001)*MWW

rage=k6*aca+K5*ABACA
age=integ(rage,0.)
rreg=k5*aca+k5*abaca
reg=integ(rreg,0.)
RDEG=K8*AC
DEG=INTEG(RDEG,0.)
RINH=KI*AB*AC+KI2*AB*ABAC    ! ACHE BINDING RATE
INH=INTEG(RINH,0.)
RINHMc=(RINH*VBR*.0000000001)*MWW

!-----BRAIN-BUCHE-----!
```

```
RACABUb=Ki2b*AB*ACBUb-K5*ACABUb-K6*ACABUb  ! RATE OF CHANGE CHEMICAL
BOUND TO ACHE
ACABUb=INTEG(RACABUb,0.)
RACBUb=+K7bb-K8*ACBUb+K5*ACABUb-Ki2b*AB*ACBUb !RATE OF CHANGE CONC.
OF ACHE
ACBUb=INTEG(RACBUb,ACTBUb)
ACTIVITYBUb=(ACBUb/ACTBUb)*100    ! ACHE ACTIVITY
RDEGBUb=K8*ACBUb
DEGBUb=INTEG(RDEGBUb,0.)
RAGEBUb=K6*ACABUb                 ! ACHE AGING RATE
AGEBUb=INTEG(RAGEBUb,0.)
RINHBUb=Ki2b*AB*ACBUb             ! ACHE BINDING RATE
INHBUb=INTEG(RINHBUb,0.)
RINHBUBM=(RINHBUB*VBR*.0000000001)*MWW

!-----BRAIN CARBOXYL ESTERASE-----!

RACACEB=Ki2c*AB*ACCEB-K5*ACACEB-K6*ACACEB  ! RATE OF CHANGE CHEMICAL
BOUND TO ACHE
ACACEB=INTEG(RACACEB,0.)
RACCEB=+K7bC-K8*ACCEB+K5*ACACEB-Ki2c*AB*ACCEB  ! RATE OF CHANGE
CONC. OF ACHE
ACCEB=INTEG(RACCEB,ACTCEB)
ACTIVITYCEB=(ACCEB/ACTCEB)*100    ! ACHE ACTIVITY
RDEGCEB=K8*ACCEB
DEGCEB=INTEG(RDEGCEB,0.)
RAGECEB=K6*ACACEB                 ! ACHE AGING RATE
AGECEB=INTEG(RAGECEB,0.)
RINHCEB=Ki2c*AB*ACCEB             ! ACHE BINDING RATE
INHCEB=INTEG(RINHCEB,0.)
RINHCEBM=(RINHCEB*VBR*.0000000001)*MWW

!-----BRAIN CARBOXYL ESTERASE II-----!

RACACEBF=Ki2c*AB*ACCEBF-K5*ACACEBF-K6*ACACEBF  ! RATE OF CHANGE
CHEMICAL BOUND TO ACHE
ACACEBF=INTEG(RACACEBF,0.)
RACCEBF=+K7bd-K8*ACCEBF+K5*ACACEBF-Ki2c*AB*ACCEBF  ! RATE OF CHANGE
CONC. OF ACHE
ACCEBF=INTEG(RACCEBF,ACTCEBF)
ACTIVITYCEBF=(ACCEBF/ACTCEBF)*100   ! ACHE ACTIVITY
RDEGCEBF=K8*ACCEBF
DEGCEBF=INTEG(RDEGCEBF,0.)
RAGECEBF=K6*ACACEBF                 ! ACHE AGING RATE
AGECEBF=INTEG(RAGECEBF,0.)
RINHCEBF=Ki2c*AB*ACCEBF             ! ACHE BINDING RATE
INHCEBF=INTEG(RINHCEBF,0.)
RINHCEBFM=(RINHCEBF*VBR*.0000000001)*MWW
ACTIVITYCAB=0.5*(ACTIVITYCEB+ACTIVITYCEBF)

!-----LIVER ACHE-----!
RACl=K7al-K8*ACl+K5*ACAl+K5*ABACal-KI*ABl*ACl-k1*abl*acl+k2*abacl-
KI2*ABACl*ABl
ACl=INTEG(RACl,actl)
```

```
ACTIVITYl=((ACl+ABACl)/actl)*100
RACAl=Ki*ABl*ACl-K5*ACAl-K6*ACAL      ! EQ 1
ACAl=INTEG(RACAl,0.)
RBl=Ki*ABl*ACl+ki2*ABACl*ABl          ! EQ 1
Bl=INTEG(RBl,0.)
RABACl=K1*ABl*ACl-k2*ABACl-Ki2*ABACl*abl!+k5*abacal!-K6*ABACL ! EQ 2
ABACl=INTEG(RABACl,0.)
RABACAl=ki2*ABACl*abl-K5*ABACAl-K6*ABACAL                    ! EQ 2
ABACAl=INTEG(RABACAl,0.)
RDEGl=K8*ACl
DEGl=INTEG(RDEGl,0.)
RAGEl=K6*ACAl                         ! ACHE AGING RATE
AGEl=INTEG(RAGEl,0.)
RINHl=KI*ABl*ACl+KI2*ABl*ABACl        ! ACHE BINDING RATE
INHl=INTEG(RINHl,0.)
RINHLM=(RINHL*VL*.0000000001)*MWW

!-----LIVER-BUCHE-----!

RACABUL=Ki2b*ABL*ACBUL-K5*ACABUL-K6*ACABUL   ! RATE OF CHANGE
CHEMICAL BOUND TO ACHE
ACABUL=INTEG(RACABUL,0.)
RACBUL=+K7bl-K8*ACBUL+K5*ACABUL-Ki2b*ABL*ACBUL  ! RATE OF CHANGE
CONC. OF ACHE
ACBUL=INTEG(RACBUL,ACTBUL)
ACTIVITYBUL=(ACBUL/ACTBUL)*100     ! ACHE ACTIVITY
RDEGBUL=K8*ACBUL
DEGBUL=INTEG(RDEGBUL,0.)
RAGEBUL=K6*ACABUL                  ! ACHE AGING RATE
AGEBUL=INTEG(RAGEBUL,0.)
RINHBUL=Ki2b*ABL*ACBUL             ! ACHE BINDING RATE
INHBUL=INTEG(RINHBUL,0.)
RINHBULM=(RINHBUL*VL*.0000000001)*MWW

!-----LIVER CARBOXYL ESTERASE-----!

RACACEL=Ki2c*ABL*ACCEL-K5*ACACEL-K6*ACACEL   ! RATE OF CHANGE
CHEMICAL BOUND TO ACHE
ACACEL=INTEG(RACACEL,0.)
RACCEL=+K7lc-K8*ACCEL+K5*ACACEL-Ki2c*ABL*ACCEL    ! RATE OF CHANGE
CONC. OF ACHE
ACCEL=INTEG(RACCEL,ACTCEL)
ACTIVITYCEL=(ACCEL/ACTCEL)*100     ! ACHE ACTIVITY

RDEGCEL=K8*ACCEL
DEGCEL=INTEG(RDEGCEL,0.)

RAGECEL=K6*ACACEL                  ! ACHE AGING RATE
AGECEL=INTEG(RAGECEL,0.)

RINHCEL=Ki2c*ABL*ACCEL             ! ACHE BINDING RATE
INHCEL=INTEG(RINHCEL,0.)
```

```
RINHCELM=(RINHCEL*VL*.0000000001)*MWW

!-----LIVER CARBOXYL ESTERASE II-----!

RACACELf=Ki2c*ABL*ACCELf-K5*ACACELf-K6*ACACELf  ! RATE OF CHANGE
CHEMICAL BOUND TO ACHE
ACACELf=INTEG(RACACELf,0.)

RACCELf=+K7ld-K8*ACCELf+K5*ACACELf-Ki2c*ABL*ACCELf ! RATE OF CHANGE
CONCEN. OF ACHE
ACCELf=INTEG(RACCELf,ACTCELf)
ACTIVITYCELf=(ACCELf/ACTCELf)*100       ! ACHE ACTIVITY

RDEGCELf=K8*ACCELf
DEGCELf=INTEG(RDEGCELf,0.)

RAGECELf=K6*ACACELf                     ! ACHE AGING RATE
AGECELf=INTEG(RAGECELf,0.)

RINHCELf=Ki2c*ABL*ACCELf                ! ACHE BINDING RATE
INHCELf=INTEG(RINHCELf,0.)

RINHCELFM=(RINHCELF*VL*.0000000001)*MWW
activitycl=0.5*(activitycel+activitycelf)

!-----DIAPHRAGM ACHE-----!

RACd=K7ad-K8*ACd+K5*ACAd+K5*ABACad-KI*ABd*ACd-k1*abd*acd+k2*abacd-
KI2*ABACd*ABd
ACd=INTEG(RACd,actd)

!ACd=ACTd-ACAd-ABACd-ABACAd+K7ad-DEGd
ACTIVITYd=((ACd+ABACd)/actd)*100
RACAd=Ki*ABd*ACd-K5*ACAd-K6*ACAD         ! EQ 1
ACAd=INTEG(RACAd,0.)

RBd=Ki*ABd*ACd+ki*ABACd*ABd              ! EQ 1
Bd=INTEG(RBd,0.)

RABACd=K1*ABd*ACd-k2*ABACd-Ki2*ABACd*abd!+k5*abacad    ! EQ 2
ABACd=INTEG(RABACd,0.)

RABACAd=ki2*ABACd*abd-K5*ABACAd-K6*ABACAD             ! EQ 2
ABACAd=INTEG(RABACAd,0.)

RDEGd=K8*ACd
DEGd=INTEG(RDEGd,0.)

RAGEd=K6*ACAd                           ! ACHE AGING RATE
AGEd=INTEG(RAGEd,0.)

RINHd=KI*ABd*ACd+KI2*ABd*ABACd          ! ACHE BINDING RATE
INHd=INTEG(RINHd,0.)
```

```
RINHDM=(RINHD*VD*.0000000001)*MWW

!-----DIAPHRAGM BUCHE-----!

RACABUD=Ki2b*ABD*ACBUD-K5*ACABUD-K6*ACABUD  ! RATE OF CHANGE
CHEMICAL BOUND TO ACHE
ACABUD=INTEG(RACABUD,0.)

RACBUD=+K7db-K8*ACBUD+K5*ACABUD-Ki2b*ABD*ACBUD   ! RATE OF CHANGE
CONCEN. OF ACHE
ACBUD=INTEG(RACBUD,ACTBUD)
ACTIVITYBUD=(ACBUD/ACTBUD)*100     ! ACHE ACTIVITY

RDEGBUD=K8*ACBUD
DEGBUD=INTEG(RDEGBUD,0.)

RAGEBUD=K6*ACABUD                  ! ACHE AGING RATE
AGEBUD=INTEG(RAGEBUD,0.)

RINHBUD=Ki2b*ABD*ACBUD             ! ACHE BINDING RATE
INHBUD=INTEG(RINHBUD,0.)
RINHBUDM=(RINHBUD*VD*.0000000001)*MWW
RSYNBUD=K7*(1-ACBUD/ACTBUD)        ! ACHE SYNTHESIS RATE
SYNBUD=INTEG(RSYNBUD,0.)

!-----DIAPHRAGM CARBOXYLESTERASE-----!

RACACED=Ki2c*ABD*ACCED-K5*ACACED-K6*ACACED  ! RATE OF CHANGE
CHEMICAL BOUND TO ACHE
ACACED=INTEG(RACACED,0.)

RACCED=+K7dc-K8*ACCED+K5*ACACED-Ki2c*ABD*ACCED  ! RATE OF CHANGE
CONCEN. OF ACHE
ACCED=INTEG(RACCED,ACTCED)
ACTIVITYCED=(ACCED/ACTCED)*100    ! ACHE ACTIVITY

RDEGCED=K8*ACCED
DEGCED=INTEG(RDEGCED,0.)

RAGECED=K6*ACACED                 ! ACHE AGING RATE
AGECED=INTEG(RAGECED,0.)

RINHCED=Ki2c*ABD*ACCED            ! ACHE BINDING RATE
INHCED=INTEG(RINHCED,0.)
RINHCEDM=(RINHCED*VD*.0000000001)*MWW

!-----DIAPHRAGM CARBOXYLESTERASE II-----!

RACACEDf=Ki2c*ABD*ACCEDf-K5*ACACEDf-K6*ACACEDf  ! RATE OF CHANGE
CHEMICAL BOUND TO ACHE
ACACEDf=INTEG(RACACEDf,0.)

RACCEDf=+K7dd-K8*ACCEDf+K5*ACACEDf-Ki2c*ABD*ACCEDf  ! RATE OF CHANGE
CONC. OF ACHE
```

```
ACCEDf=INTEG(RACCEDf,ACTCEDf)
ACTIVITYCEDf=(ACCEDf/ACTCEDf)*100           ! ACHE ACTIVITY

RDEGCEDf=K8*ACCEDf
DEGCEDf=INTEG(RDEGCEDf,0.)

RAGECEDf=K6*ACACEDf                   ! ACHE AGING RATE
AGECEDf=INTEG(RAGECEDf,0.)

RINHCEDf=Ki2c*ABD*ACCEDf              ! ACHE BINDING RATE
INHCEDf=INTEG(RINHCEDf,0.)
RINHCEDFM=(RINHCEDF*VD*.0000000001)*MWW
RSYNCEDf=K7*(1-ACCEDf/ACTCEDf)        ! ACHE SYNTHESIS RATE
SYNCEDf=INTEG(RSYNCEDf,0.)

activitycd=0.5*(activityced+activitycedf)

!-----HEART ACHE-----!

RACh=K7ah-K8*ACh+K5*ACAh+K5*ABACah-KI*ABh*ACh-k1*abh*ach+k2*abach-
KI2*ABACh*ABh
ACh=INTEG(RACh,acth)
ACTIVITYh=((ACh+ABACh)/acth)*100
RACAh=Ki*ABh*ACh-K5*ACAh-K6*ACAH         ! EQ 1
ACAh=INTEG(RACAh,0.)

RBh=Ki*ABh*ACh+ki2*ABACh*ABh             ! EQ 1
Bh=INTEG(RBh,0.)

RABACh=K1*ABh*ACh-k2*ABACh-Ki2*ABACh*abh!+k5*abacah     ! EQ 2
ABACh=INTEG(RABACh,0.)

RABACAh=ki2*ABACh*abh-K5*ABACAh-K6*ABACAH               ! EQ 2
ABACAh=INTEG(RABACAh,0.)

RDEGh=K8*ACh
DEGh=INTEG(RDEGh,0.)

RAGEh=K6*ACAh                            ! ACHE AGING RATE
AGEh=INTEG(RAGEh,0.)

RINHh=KI*ABh*ACh+KI2*ABh*ABACh           ! ACHE BINDING RATE
INHh=INTEG(RINHh,0.)
RINHHM=(RINHH*VH*.0000000001)*MWW

!-----HEART BUCHE-----!

RACABUH=Ki2b*ABH*ACBUH-K5*ACABUH-K6*ACABUH ! RATE OF CHANGE CHEMICAL
BOUND TO ACHE
ACABUH=INTEG(RACABUH,0.)

RACBUH=+K7bh-K8*ACBUH+K5*ACABUH-Ki2b*ABH*ACBUH ! RATE OF CHANGE
CONC. OF ACHE
ACBUH=INTEG(RACBUH,ACTBUH)
```

```
ACTIVITYBUH=(ACBUH/ACTBUH)*100      ! ACHE ACTIVITY

RDEGBUH=K8*ACBUH
DEGBUH=INTEG(RDEGBUH,0.)

RAGEBUH=K6*ACABUH                   ! ACHE AGING RATE
AGEBUH=INTEG(RAGEBUH,0.)

RINHBUH=Ki2b*ABH*ACBUH               ! ACHE BINDING RATE
INHBUH=INTEG(RINHBUH,0.)
RINHBUHM=(RINHBUH*VH*.0000000001)*MWW

!-----HEART CARBOXYL I-----!

RACACEH=Ki2c*ABH*ACCEH-K5*ACACEH-K6*ACACEH  ! RATE OF CHANGE
CHEMICAL BOUND TO ACHE
ACACEH=INTEG(RACACEH,0.)

RACCEH=+K7hc-K8*ACCEH+K5*ACACEH-Ki2c*ABH*ACCEH  ! RATE OF CHANGE
CONC. OF ACHE
ACCEH=INTEG(RACCEH,ACTCEH)
ACTIVITYCEH=(ACCEH/ACTCEH)*100     ! ACHE ACTIVITY

RDEGCEH=K8*ACCEH
DEGCEH=INTEG(RDEGCEH,0.)

RAGECEH=K6*ACACEH                  ! ACHE AGING RATE
AGECEH=INTEG(RAGECEH,0.)

RINHCEH=Ki2c*ABH*ACCEH             ! ACHE BINDING RATE
INHCEH=INTEG(RINHCEH,0.)

RINHCEHM=(RINHCEH*VH*.0000000001)*MWW

!-----HEART CARBOXYL II-----!

RACACEHf=Ki2c*ABH*ACCEHf-K5*ACACEHf-K6*ACACEHf  ! RATE OF CHANGE
CHEMICAL BOUND TO ACHE
ACACEHf=INTEG(RACACEHf,0.)

RACCEHf=+K7hd-K8*ACCEHf+K5*ACACEHf-Ki2c*ABH*ACCEHf  !RATE OF CHANGE
CONC. OF ACHE
ACCEHf=INTEG(RACCEHf,ACTCEHf)
ACTIVITYCEHf=(ACCEHf/ACTCEHf)*100    ! ACHE ACTIVITY

RDEGCEHf=K8*ACCEHf
DEGCEHf=INTEG(RDEGCEHf,0.)

RAGECEHf=K6*ACACEHf                  ! ACHE AGING RATE
AGECEHf=INTEG(RAGECEHf,0.)

RINHCEHf=Ki2c*ABH*ACCEHf             ! ACHE BINDING RATE
INHCEHf=INTEG(RINHCEHf,0.)
RINHCEHFM=(RINHCEHF*VH*.0000000001)*MWW
```

```
activitych=0.5*(activityceh+activitycehf)

!-----ARTERIAL BLOOD ACHE-----!

RACm=K7abl-K8*ACm+K5*ACAm+K5*ABACam-KI*ABm*ACm-k1*abm*acm+k2*abacm-
KI2*ABACm*ABm
ACm=INTEG(RACm,actm)
!ACv=ACTv-ACAv-ABACv-ABACAv+K7abl-DEGv

ACTIVITYm=((ACm+ABACm)/actm)*100
RABACAm=ki2*ABACm*abm-K5*ABACAm-K6*ABACAM     ! EQ 2
ABACAm=INTEG(RABACAm,0.)

ablood=rbcsb+plasmab              ! TOTAL ACHE ELLMAN ACTIVITY BLOOD

RACAm=Ki*ABm*ACm-K5*ACAm-K6*ACAM              ! EQ 1
ACAm=INTEG(RACAm,0.)

RBm=Ki*ABm*ACm+ki2*ABACm*ABm                  ! EQ 1
Bm=INTEG(RBm,0.)

RABACm=K1*ABm*ACm-k2*ABACm-Ki2*ABACm*abm!+k5*abacam    ! EQ 2
ABACm=INTEG(RABACm,0.)

RBCS2=ABACM*140000!!!!!????
rbcs=ACM*140000  ! ACHE ACTIVITY IN RBCS OVER TIME UNINHIBIT
rbcsbAM=(rbcs+RBCS2)/(ACTM*140000)!4521380000 ! ACHE ACTIVITY IN
RBCS ELLMAN
rbcsb=((rbcs+RBCS2)/(ACTM*140000))*100!4521380000! ACHE ACTIVITY IN
RBCS ELLMAN

RACmP=K7ablP-K8*ACmP+K5*ACAmP+K5*ABACamP-KI*ABm*ACmP-k1*abm*acmP+...
k2*abacmP-KI2*ABACmP*ABm
ACmP=INTEG(RACmP,actmP)
RACAmP=Ki*ABm*ACmP-K5*ACAmP-K6*ACAMP                    ! EQ 1
ACAmP=INTEG(RACAmP,0.)
RABACmP=K1*ABm*ACmP-k2*ABACmP-Ki2*ABACmP*abm+k5*abacamP   ! EQ 2
ABACmP=INTEG(RABACmP,0.)
RABACAmP=ki2*ABACmP*abm-K5*ABACAmP-K6*ABACAMP             ! EQ 2
ABACAmP=INTEG(RABACAmP,0.)
RBCS2P=ABACMP*4800000!140000!!!!!????
rbcsP=ACMP*4800000!140000 ! ACHE ACTIVITY IN RBCS OVER TIME
UNINHIBIT rbcsbAMP=(rbcsP+RBCS2P)/(ACTMP*4800000)!4521380000 ! ACHE
ACTIVITY IN RBCS ELLMAN
rbcsbP=((rbcsP+RBCS2P)/(ACTMP*4800000))*100!4521380000 ! ACHE
ACTIVITY IN RBCS ELLMAN

RDEGm=K8*ACm
DEGm=INTEG(RDEGm,0.)

RAGEm=K6*ACAm                       ! ACHE AGING RATE
AGEm=INTEG(RAGEm,0.)
```

```
RINHm=KI*ABm*ACm+KI2*ABm*ABACm      ! ACHE BINDING RATE
INHm=INTEG(RINHm,0.)

RINHMM=(RINHM*VA*.0000000001)*MWW

!-----ARTERIAL BLOOD BUCHE-----!

RACABUM=Ki2b*ABM*ACBUM-K5*ACABUM-K6*ACABUM  ! RATE OF CHANGE
CHEMICAL BOUND TO ACHE
ACABUM=INTEG(RACABUM,0.)

RACBUM=+K7bbl-K8*ACBUM+K5*ACABUM-Ki2b*ABM*ACBUM ! RATE OF CHANGE
CONC. OF ACHE
ACBUM=INTEG(RACBUM,ACTBUM)

ACTIVITYBUM=(ACBUM/ACTBUM)*100     ! BUCHE PLASMA ACTIVITY

PLASMABU=ACBUM *2400000!ACTIVITYBUM*40000
PLASMABUT=ACTBUM *2400000!ACTIVITYBUM*40000

PLASMABUC=PLASMABU/PLASMABUT!*100  ! PLASMA BUCH/TOTAL PLASMA
ACTIVITY 0 TIME
BUCHE=(PLASMABU/PLASMABUC)*100
CHE=PLASMABUC+ABLOOD
ACHEP=rbcsP+RBCS2P      ! ACHE IN PLASMA
PLASMAACT=ACTMP*4800000
PCHE=((PLASMABU+ACHEP)/(PLASMABUCHE+PLASMAACT))*100  ! TOTAL PLASMA
CHE(ACHE+BUCHE)

RDEGBUM=K8*ACBUM
DEGBUM=INTEG(RDEGBUM,0.)

RAGEBUM=K6*ACABUM                  ! ACHE AGING RATE
AGEBUM=INTEG(RAGEBUM,0.)

RINHBUM=Ki2b*ABM*ACBUM             ! ACHE BINDING RATE
INHBUM=INTEG(RINHBUM,0.)
RINHBUMM=(RINHBUM*VA*.0000000001)*MWW
RSYNBUM=K7*(1-ACBUM/ACTBUM)        ! ACHE SYNTHESIS RATE
SYNBUM=INTEG(RSYNBUM,0.)

!-----ARTERIAL BLOOD CARBOXYL-----!

RACACEM=Ki2c*ABM*ACCEM-K5*ACACEM-K6*ACACEM  ! RATE OF CHANGE
CHEMICAL BOUND TO ACHE
ACACEM=INTEG(RACACEM,0.)

RACCEM=+K7blc-K8*ACCEM+K5*ACACEM-Ki2c*ABM*ACCEM  ! RATE OF CHANGE
CONC. OF ACHE
ACCEM=INTEG(RACCEM,ACTCEM)
ACTIVITYCEM=(ACCEM/ACTCEM)*100        ! ACHE ACTIVITY

RDEGCEM=K8*ACCEM
DEGCEM=INTEG(RDEGCEM,0.)
```

```
RAGECEM=K6*ACACEM                        ! ACHE AGING RATE
AGECEM=INTEG(RAGECEM,0.)

RINHCEM=Ki2c*ABM*ACCEM                   ! ACHE BINDING RATE
INHCEM=INTEG(RINHCEM,0.)
RINHCEMM=(RINHCEM*VA*.0000000001)*MWW

!-----ARTERIAL BLOOD CARBOXYL-----!

RACACEMf=Ki2c*ABM*ACCEMf-K5*ACACEMf-K6*ACACEMf ! RATE OF CHANGE
CHEMICAL BOUND TO ACHE
ACACEMf=INTEG(RACACEMf,0.)

RACCEMf=+K7bld-K8*ACCEMf+K5*ACACEMf-Ki2c*ABM*ACCEMf  ! RATE OF
CHANGE CONC. OF ACHE
ACCEMf=INTEG(RACCEMf,ACTCEMf)
ACTIVITYCEMf=(ACCEMf/ACTCEMf)*100    ! ACHE ACTIVITY

RDEGCEMf=K8*ACCEMf
DEGCEMf=INTEG(RDEGCEMf,0.)

RAGECEMf=K6*ACACEMf                      ! ACHE AGING RATE
AGECEMf=INTEG(RAGECEMf,0.)

RINHCEMf=Ki2c*ABM*ACCEMf                 ! ACHE BINDING RATE
INHCEMf=INTEG(RINHCEMf,0.)

RINHCEMFM=(RINHCEMF*VA*.0000000001)*MWW

activitycm=0.5*(activitycem+activitycemf)

!-----VENOUS BLOOD ACHE-----!

RACv=K7abl-K8*ACv+K5*ACAv+K5*ABACav-KI*ABv*ACv-k1*abv*acv+k2*abacv-
KI2*ABACv*ABv
ACv=INTEG(RACv,actv)
!ACv=ACTv-ACAv-ABACv-ABACAv+K7abl-DEGv

ACTIVITYv=((ACv+ABACv)/actv)*100
RACAv=Ki*ABv*ACv-K5*ACAv-K6*ACAV   ! EQ 1
ACAv=INTEG(RACAv,0.)

RBv=Ki*ABv*ACv+ki2*ABACv*ABv       ! EQ 1
Bv=INTEG(RBv,0.)

RABACv=K1*ABv*ACv-k2*ABACv-Ki2*ABACv*abv!+k5*abacav    ! EQ 2
ABACv=INTEG(RABACv,0.)

RABACAv=ki2*ABACv*abv-K5*ABACAv-K6*ABACAV              ! EQ 2
ABACAv=INTEG(RABACAv,0.)

RDEGv=K8*ACv
DEGv=INTEG(RDEGv,0.)
```

```
RAGEv=K6*ACAv                        ! ACHE AGING RATE
AGEv=INTEG(RAGEv,0.)

RINHv=KI*ABv*ACv+KI2*ABv*ABACv      ! ACHE BINDING RATE
INHv=INTEG(RINHv,0.)

RINHVM=(RINHV*VV*.0000000001)*MWW

!-----VENOUS BLOOD BUCHE-----!

RACABUV=Ki2b*ABV*ACBUV-K5*ACABUV-K6*ACABUV ! RATE OF CHANGE CHEMICAL
BOUND TO ACHE
ACABUV=INTEG(RACABUV,0.)

RACBUV=+K7bblv-K8*ACBUV+K5*ACABUV-Ki2b*ABV*ACBUV ! RATE OF CHANGE
CONC. OF ACHE
ACBUV=INTEG(RACBUV,ACTBUV)
ACTIVITYBUV=(ACBUV/ACTBUV)*100    ! ACHE ACTIVITY

RDEGBUV=K8*ACBUV
DEGBUV=INTEG(RDEGBUV,0.)

RAGEBUV=K6*ACABUV                ! ACHE AGING RATE
AGEBUV=INTEG(RAGEBUV,0.)

RINHBUV=Ki2b*ABV*ACBUV           ! ACHE BINDING RATE
INHBUV=INTEG(RINHBUV,0.)
RINHBUVM=(RINHBUV*VV*.0000000001)*MWW

!-----VENOUS BLOOD CARBOXYLESTERASE-----!

RACACEV=Ki2c*ABV*ACCEV-K5*ACACEV-K6*ACACEV ! RATE OF CHANGE CHEMICAL
BOUND TO ACHE
ACACEV=INTEG(RACACEV,0.)

RACCEV=+K7blc-K8*ACCEV+K5*ACACEV-Ki2c*ABV*ACCEV ! RATE OF CHANGE
CONC. OF ACHE
ACCEV=INTEG(RACCEV,ACTCEV)
ACTIVITYCEV=(ACCEV/ACTCEV)*100     ! ACHE ACTIVITY

RDEGCEV=K8*ACCEV
DEGCEV=INTEG(RDEGCEV,0.)

RAGECEV=K6*ACACEV                    ! ACHE AGING RATE
AGECEV=INTEG(RAGECEV,0.)

RINHCEV=Ki2c*ABV*ACCEV               ! ACHE BINDING RATE
INHCEV=INTEG(RINHCEV,0.)

RINHCEVM=(RINHCEV*VV*.0000000001)*MWW     ! ACHE SYNTHESIS RATE
SYNCEV=INTEG(RSYNCEV,0.)

!-----VENOUS BLOOD CARBOXYLESTERASE-----!
```

```
RACACEVf=Ki2c*ABV*ACCEVf-K5*ACACEVf-K6*ACACEVf ! RATE OF CHANGE
CHEMICAL BOUND TO ACHE
ACACEVf=INTEG(RACACEVf,0.)

RACCEVf=+K7bld-K8*ACCEVf+K5*ACACEVf-Ki2c*ABV*ACCEVf ! RATE OF CHANGE
CONC. OF ACHE
ACCEVf=INTEG(RACCEVf,ACTCEVf)
ACTIVITYCEVf=(ACCEVf/ACTCEVf)*100       ! ACHE ACTIVITY

RDEGCEVf=K8*ACCEVf
DEGCEVf=INTEG(RDEGCEVf,0.)

RAGECEVf=K6*ACACEVf                     ! ACHE AGING RATE
AGECEVf=INTEG(RAGECEVf,0.)

RINHCEVf=Ki2c*ABV*ACCEVf                ! ACHE BINDING RATE
INHCEVf=INTEG(RINHCEVf,0.)

RINHCEVFM=(RINHCEVF*VV*.0000000001)*MWW    ! ACHE SYNTHESIS RATE

SYNCEVf=INTEG(RSYNCEVf,0.)

activitycv=0.5*(activitycev+activitycevf)

!-----OP PARENT MASS BALANCE-----!

TMASS=AF+AL+AS+AR+AM1+AM2+ABR+MR+ASK+AH+AV+AD
! TOTAL DOSE (MG)
DOSEX=AO+IVR*TINF           ! NET AMOUNT ABSORBED (MG)

!-----OP OXON MASS BALANCE-----!

TMASSS=AFF+ALL+ASS+ARR+ABRR+ASKK+AM4+AM3+AMM+AHH+ADD! TOTAL DOSE
(MG)
DOSEXX=AOO+IVR*TINF         ! NET AMOUNT ABSORBED (MG)


END                         ! END OF DERIVATIVE
'-------------------------------------------------------------------
-'

'-------------------------------------------------------------------
--'
TERMINAL

CALL LOGD(.TRUE.)
QLC=QLC+PDL
IF(QLC.LE.PMX) GO TO L1
END

END                         ! END OF PROGRAM
```